Dissolved organic matter composition as a driver of greenhouse gas emissions in lakes

A thesis submitted to the Committee on Graduate Studies

In partial fulfilment of the requirements for Degree of Master of Science

In the Faculty of Arts and Science

Trent University

Peterborough, Ontario, Canada

Environmental and Life Sciences M.Sc. Graduate Program

September 2025

Abstract

Dissolved organic matter composition as a driver of greenhouse gas emissions in lakes

Vincent Lau

Climate-driven permafrost thaw releases microorganisms and dissolved organic matter (DOM) into northern lakes, where their interactions with microbial communities and seasonal processes shape greenhouse gas emissions. In a factorial experiment mixing DOM and microbes from thermokarst ponds and lakes, we found that both DOM and microbial identity strongly influenced degradation. Lake microbes preferentially consumed thermokarst DOM, producing 3× more CO_2 due to low growth efficiency, while thermokarst microbes altered DOM with little CO_2 release. A survey of 40 lakes across a climate gradient showed CO_2 fluxes peaking in spring from under-ice buildup and CH_4 fluxes peaking in fall after summer accumulation. Dissolved gas concentrations served as early indicators of these events, with CH_4 linked to reduced DOM and CO_2 to multiple pathways. Overall, DOM quality, microbial traits, and seasonal dynamics interact to control lake carbon cycling, emphasizing the need for year-round monitoring under climate change.

Keywords: Dissolved organic matter (DOM), Fourier-transform ion cyclotron resonance mass spectrometry (FT-ICR MS), greenhouse gases (GHGs), lakes, fluxes, thermokarst

Preface

This thesis is submitted in partial fulfillment of the requirements for the degree of Master of Science in Environmental and Life Sciences at Trent University. It represents original work conducted by the author under the supervision of Dr. Andrew Tanentzap and follows a manuscript format. Contributions from co-authors include assistance in data collection, laboratory analyses, and general supervisory guidance. Therefore, I use the pronoun "we" rather than "I" throughout the main thesis chapters.

Chapter 2 is based on an experiment designed and conducted by collaborators prior to my involvement. Optical data were collected and processed by collaborators. Greenhouse gas data were collected by collaborators but processed by me. I carried out Fourier-transform ion cyclotron resonance mass spectrometry (FT-ICR MS) sample preparation and processed the data. Flow cytometry samples were collected, DNA extracted, metagenomic sequencing performed, and bioinformatics conducted by Katherine Siket while I calculated cell growth and growth efficiency from these data. I performed all statistical analyses, synthesized the results, and wrote the manuscript.

Chapter 3 is based on a field study designed by collaborators. I contributed to field sampling alongside Dr. Sommer Starr. FT-ICR MS analyses were run on the autosampler by Dr. Starr, and I processed the FT-ICR MS output into a dataset. I performed all statistical analyses, synthesized the results, and wrote the manuscript.

Unless otherwise specified, all other data processing, statistical analysis, interpretation, and writing were performed by the author under the conceptual and editorial guidance of Dr. Andrew Tanentzap.

Acknowledgements

I would like to thank my supervisor, Dr. Andrew Tanentzap, for helping me proofread and edit all my drafts. Over the past two years, I've learned a great deal, and I hope to carry those lessons forward into my future endeavors. I'd also like to thank post-docs Dr. Jeremy Fonvielle and Dr. Sommer F. Starr for their help in proofreading and for teaching me just as much along the way, with special thanks to Sommer for all the extra work you put into getting my second chapter online. I'm also grateful to my fellow master's student, Katherine Siket, who made the journey less overwhelming by reminding me I wasn't the only one who felt out of my depth at times. These past two years have not been easy, especially with the sudden passing of my brother. I'm thankful to everyone mentioned here, as well as my friends and family, for giving me the final push I needed to finish on time.

Table of Contents:

List of figures

Chapter 2

List of tables

Chapter 2

List of abbreviations

DOM: Dissolved organic matter

FT-ICR MS: Fourier-transform ion cyclotron resonance mass spectrometry

GHGs: Greenhouse gases

CO_2: Carbon Dioxide

CH_4: Methane

H:C: hydrogen-to-carbon ratio

O:C: oxygen-to-carbon ratio

NOSC: nominal oxidation state of carbon

GFE: Gibbs Free Energy

AI_{Mod}: Modified Aromaticity Index

CDOM: chromophoric dissolved organic matter

SRNOM: Suwannee River natural organic matter

ESI: Electrospray ionization

Chapter 1 General Introduction

1.0 Thawing permafrost as a driver of inland water carbon emissions

Climate change is rapidly altering Earth's carbon balance, driving major shifts in how carbon is stored, cycled, and released across ecosystems (Schurr et al., 2015; Hugelius et al., 2020). While public attention often focuses on forests, oceans, and fossil fuels, a lesser known but critical part of the carbon cycle occurs in freshwater systems, particularly lakes and ponds (Tranvik et al., 2009; Raymond et al., 2013). Boreal and Arctic lakes cover less than 3% of Earth's land surface, yet they release an estimated 0.32–0.64 Pg C yr^{-1} as CO_2 and CH_4 to the atmosphere, comparable to about 20% of global ocean CO_2 emissions (Raymond et al., 2013; Drake et al., 2018). Even though these inland waters are small in area, their high rates of carbon processing and greenhouse gas emissions make them disproportionately important in the global carbon budget (Drake et al., 2018). They receive organic material from surrounding landscapes, process it through microbial activity, and emit greenhouse gases (GHGs) such as carbon dioxide (CO_2) and methane (CH_4) back into the atmosphere (Bastviken et al., 2011; Rosentreter et al., 2021). Improving climate projections requires a better understanding of the processes that regulate lake carbon cycling, particularly in high-latitude regions where thawing permafrost is reshaping landscapes and releasing large amounts of previously frozen carbon (Wik et al., 2016; Hugelius et al., 2013; Olefeldt et al., 2016).

Permafrost refers to ground that has remained frozen for at least two consecutive years, often for many years, and locks away vast stores of organic matter derived from ancient plant and microbial material (Schuur et al., 2015). In high-latitude regions, rising air and soil temperatures are causing permafrost to thaw, destabilizing soils and altering hydrology

(Biskaborn et al., 2019). When this frozen ground thaws, trapped organic carbon becomes accessible to microbial decomposers, which break it down and release greenhouse gases such as carbon dioxide and methane (Schuur et al., 2015; Natali et al., 2021). This “previously frozen” carbon is considered especially climate-sensitive because much of it is highly labile once thawed, creating the potential for rapid emissions that can amplify climate warming in a positive feedback loop (Schuur et al., 2015; Turetsky et al., 2020). Permafrost thaw often leads to the formation of thermokarst features, collapsed ground and newly formed wetlands or ponds, that can export organic-rich material into nearby lakes (Vonk et al., 2013; Estop-Aragonés et al., 2020). Much of this exported material is dissolved organic matter (DOM), a complex and heterogeneous mixture of compounds that strongly influences whether permafrost-derived carbon is rapidly respired or retained within aquatic systems (Spencer et al., 2008; Kellerman et al., 2014).

1.1 Dissolved Organic Matter: Composition, Lability, and Role in Aquatic Carbon Cycling

DOM encompasses a wide range of molecules, including simple sugars, amino acids, phenols, and more complex humic substances derived from plant and microbial decay (Hartnett, 2017; Kellerman et al., 2014). DOM composition, structure, size, and reactivity vary depending on its source, with thermokarst derived DOM often more aromatic, oxidized, and nitrogen rich than DOM produced within lakes (Spencer et al., 2008; Bruhn et al., 2021). The molecular composition of DOM determines its lability, which is defined as how microbes can break down DOM (LaRowe & Van Cappellen, 2011; D’Andrilli et al., 2015). Low molecular weight, structurally simple, and carbon-rich compounds (e.g., aliphatics, simple carbohydrates, amino acids) are generally more bioavailable because they require less enzymatic and energetic

investment to degrade. In contrast, high molecular weight, aromatic-rich, and well oxidized compounds (e.g., lignin derivatives, condensed aromatics) are more resistant to microbial degradation and therefore more recalcitrant (LaRowe & Van Cappellen, 2011; D'Andrilli et al., 2015; Mostovaya et al., 2017). Microbes use DOM both for biomass growth and as an energy source, breaking it down through extracellular enzymes and metabolic pathways that release CO_2 and CH_4 as by-products of respiration, much like how humans exhale CO_2 when breathing. More labile DOM is rapidly metabolized, often triggering bursts of microbial activity and gas production, whereas less labile DOM can persist in the water column for longer periods (Fasching et al., 2014; Vonk et al., 2013).

The ability of microbes to utilize DOM also depends on their physiological traits and adaptation to local conditions (Hu et al., 2022; Guillemette et al., 2016). Microbial communities often exhibit adaptations to the type of DOM that dominates their local environment (Fierer et al., 2009; Gholz et al., 2000). For example, a microbial community can develop enzyme systems and metabolic pathways optimized for breaking down specific molecular structures they encounter most frequently. As a result, they can efficiently degrade familiar DOM but may struggle to process novel inputs with unfamiliar chemical bonds or complex structures, such as the highly aromatic, oxidized compounds often found in thermokarst DOM (Starr et al., 2025). The process by which microbes adapt to degrading certain compounds is like the concept of niches in ecology, where an animal adapts to a specific prey. If there is a microbial–DOM mismatch, DOM decomposition rates may slow, and the fate of carbon may change, such as being respired out as CO_2 rather than used for energy or biomass production (Guillemette et al., 2011). Beyond serving as a food source for heterotrophic microbes, DOM also acts as a vehicle for transporting carbon across ecosystem boundaries, moving organic matter from terrestrial

landscapes into aquatic systems through runoff, groundwater flow, and erosion, and in turn from lakes and rivers to downstream waters and ultimately the ocean (Drake et al., 2018; Tranvik et al., 2009). Along this journey, DOM is chemically and biologically transformed, linking carbon cycles across terrestrial, freshwater, and marine ecosystems (Aufdenkampe et al., 2011; Battin et al., 2008; Tranvik et al., 2009). These properties make DOM a central component of aquatic carbon cycling, functioning both as a food source for heterotrophic microbes and as a mode for transporting carbon across ecosystem boundaries (Drake et al., 2018; Tranvik et al., 2009). By understanding DOM sources, composition, and its reactivity, we can better predict how changes in surrounding landscapes due to climate change will affect carbon cycling. However, the fate of DOM material is not determined by its characteristics alone but also on the physical characteristics of the system and a range of abiotic processes.

1.2 Lake morphology and non-biological processes influencing DOM fate

The physical structure of a lake plays a major role in determining whether carbon is emitted to the atmosphere or stored long-term in sediments. Shallow, nutrient-rich systems often receive larger organic matter inputs, experience greater light penetration to sediments at the bottom of the lake, and undergo more frequent mixing, conditions that can enhance CO_2 and CH_4 emissions (DelSontro et al., 2016; Geng et al., 2025; Wik et al., 2016). In contrast, deeper, colder, or oligotrophic lakes tend to have lower amounts of organic matter and stronger stratification, which can promote long-term carbon burial in sediments (DelSontro et al., 2016; Valiente et al., 2022). These physical attributes can also determine the environmental conditions under which non-biological processes can operate such as photodegradation, flocculation, and sorption onto sediments which can modify or remove DOM from the water column (Ward et al.,

2017; Helms et al., 2008). The balance among these pathways, microbial processing, photochemical alteration, and physical removal, ultimately determines whether DOM is retained in aquatic systems or released to the atmosphere, shaping its role in the carbon cycle (Tranvik et al., 2009; Raymond et al., 2013). In permafrost regions, disturbances such as thermokarst formation can disrupt this balance by delivering large pulses of reactive DOM and nutrients, altering light penetration, oxygen dynamics, and particle settling rates (Vonk et al., 2013; Estop-Aragonés et al., 2020). These morphological and abiotic controls interact strongly with temperature, which regulates the rates of both biological and non-biological processes.

1.3 Temperature effects on greenhouse gases and its relation to DOM

Temperature is a key driver of microbial metabolism, which governs the breakdown of DOM and, in turn, the rates of GHG production (Yvon-Durocher et al., 2014; Chen et al., 2021). Warmer conditions typically enhance microbial activity which accelerates the enzymatic degradation of DOM thus increasing the production of GHGs (Winder et al., 2023; DelSontro et al., 2016). Conversely, colder temperatures can suppress microbial respiration, resulting in the accumulation of DOM in waters (O'Donnell et al., 2016). However, this relationship is not always linear or uniform across systems. In northern environments with strong seasonal variation, winter and shoulder seasons like fall can exhibit unexpectedly high CH_4 emissions due to seasonal shifts in physical and biogeochemical conditions (DelSontro et al., 2016; Kuhn et al., 2021; Valiente et al., 2022). During ice cover, oxygen replenishment from the atmosphere is cut off, and continued microbial decomposition of organic matter depletes what oxygen is available, creating anoxic conditions that favor methanogenesis in sediments and the hypolimnion (Tranvik et al., 2009; Wik et al., 2016). In fall, overturn events mix the water column, bringing CH_4-rich

bottom waters to the surface where it can be rapidly emitted to the atmosphere before being oxidized (Wik et al., 2016). Changes in temperature and light over the seasons can also alter DOM availability and composition, influencing the balance between methanogenesis and methane oxidation (DelSontro et al., 2016).

These dynamics show the importance of considering temporal variation when assessing GHG fluxes, particularly in the context of climate change which is expected to lengthen the ice-free season and increase DOM bioavailability (Wik et al., 2016; Kuhn et al., 2021). Longer ice-free periods enhance photodegradation of high–molecular weight compounds, converting them into smaller, more labile molecules, while warmer water temperatures accelerate microbial enzyme activity that can break down complex DOM (Ward & Cory, 2016). Thawing permafrost and greater terrestrial runoff can also deliver a supply of reactive DOM to lakes, increasing the amount of carbon that microbes can metabolize (Vonk et al., 2013; Abbott et al., 2014). Temperature influences DOM quality and lake morphology to regulate the balance between carbon storage and greenhouse gas release, with these interactions varying seasonally.

1.4 Analyzing DOM through Fourier-transform ion cyclotron resonance mass spectrometry (FT-ICR MS)

Because DOM is chemically complex, its ecological role cannot be fully understood without detailed molecular characterization (Hertkorn et al., 2008; Kellerman et al., 2014). Conventional bulk metrics often mask important differences in reactivity (Fellman et al., 2010), so advanced analytical tools are needed to link composition to carbon cycling outcomes. For example, Fellman et al. (2010) used fluorescence spectroscopy to distinguish humic-like

compounds from terrestrial inputs versus protein-like fluorophores from microbial or algal sources, finding much higher humification index values in peat bog waters than in lakes which is evidence of more aromatic, recalcitrant DOM in terrestrial systems. Such differences would be hard to detect if only concentrations of total dissolved organic carbon were measured. Fourier-transform ion cyclotron resonance mass spectrometry (FT-ICR MS) offers ultra-high-resolution analysis capable of detecting thousands of distinct molecular formulas in a single sample (Koch et al., 2006; Kujawinski et al., 2009). Formulae obtained by FT-ICR MS can also be used to annotate into operational groups such as lipids, proteins, or condensed aromatics that differ in bioavailability and degradation pathways. This allows researchers to determine whether DOM is enriched in labile aliphatic compounds likely to fuel microbial growth, or in aromatic structures resistant to degradation (D'Andrilli et al., 2015, 2023).

In this thesis, FT-ICR MS is used as a bridge between molecular chemistry and ecosystem function by connecting the identity and abundance of specific molecular compounds to microbial metabolism, carbon transformation, and greenhouse gas emissions in lakes. By pairing FT-ICR MS data with microbial growth rates, GHG measurements, and seasonal flux observations, we can link molecular traits such as aromaticity, oxidation state, and nitrogen content to patterns of rapid degradation versus long-term persistence (D'Andrilli et al., 2015, 2023; Mostovaya et al., 2017; Ward et al., 2017). Metrics like hydrogen-to-carbon (H:C) and oxygen-to-carbon (O:C) ratios or the nominal oxidation state of carbon (NOSC) help infer lability, energy potential, and resistance to breakdown (LaRowe & Van Cappellen, 2011; Riedel & Dittmar, 2014). This molecular perspective strengthens process-based carbon models and improves predictions of how climate-driven changes in DOM inputs and lake conditions will influence carbon storage and emissions.

Thesis aims

This thesis addresses key knowledge gaps in how climate change alters DOM composition and influences carbon fate. Using FT-ICR MS alongside large-scale spatial and temporal lake water sampling, we investigate four main questions, organized into two chapters:

2.1. How does the composition of DOM differ between thermokarst and lake sources (Chapter 2)?

2.2. How do microbial communities from lake and thermokarst environments respond to DOM of different origins (Chapter 2)?

2.3. How do greenhouse gas fluxes and dissolved gas concentrations vary across seasons and temperature regimes (Chapter 3)?

2.4. How does the amount and type of GHGs relate to DOM composition (Chapter 3)?

More specifically, Chapter 2 examines how mixing DOM and microbial communities from contrasting environments influences DOM transformation and carbon processing. We conducted a controlled factorial incubation experiment pairing DOM from thermokarst and lake sources with microbial inocula from each environment and a sterile control. This design disentangled the individual and interactive effects of DOM chemistry and microbial community identity. DOM compositional changes were assessed using UV–visible spectrophotometry and FT-ICR MS, microbial growth was tracked with flow cytometry, and CO_2 and CH_4 production was quantified through dissolved gas concentrations. This chapter evaluates how efficiently carbon from different DOM sources is incorporated into microbial biomass versus lost as greenhouse gases. Chapter 3 builds on these findings by quantifying CO_2 and CH_4 fluxes, as well as dissolved gas concentrations, across a broad spatial gradient seasonally over one year. Emphasis is placed on underrepresented periods such as fall and winter to capture seasonal and regional variability in

greenhouse gas emissions. DOM composition, analyzed by FT-ICR MS, was then correlated with gas flux measurements and dissolved gas concentrations to directly link molecular characteristics of DOM to carbon emissions from inland waters. Finally, Chapter 4 synthesizes the key findings of this thesis and outlines future research directions.

References

Abbott, B. W., Larouche, J. R., Jones, J. B., Bowden, W. B., & Balser, A. W. (2014). Elevated dissolved organic carbon biodegradability from thawing and collapsing permafrost. *Journal of Geophysical Research: Biogeosciences*, *119*(10), 2049–2063. https://doi.org/10.1002/2014JG002678

Aufdenkampe, A. K., Mayorga, E., Raymond, P. A., Melack, J. M., Doney, S. C., Alin, S. R., Aalto, R. E., & Yoo, K. (2011). Riverine coupling of biogeochemical cycles between land, oceans, and atmosphere. *Frontiers in Ecology and the Environment*, *9*(1), 53–60. https://doi.org/10.1890/100014

Bastviken, D., Tranvik, L. J., Downing, J. A., Crill, P. M., & Enrich-Prast, A. (2011). Freshwater methane emissions offset the continental carbon sink. *Science*, 331(6013), 50–50. https://doi.org/10.1126/science.1196808

Battin, T. J., Kaplan, L. A., Findlay, S., Hopkinson, C. S., Marti, E., Packman, A. I., Newbold, J. D., & Sabater, F. (2008). Biophysical controls on organic carbon fluxes in fluvial networks. *Nature Geoscience*, 1(2), 95–100. https://doi.org/10.1038/ngeo101

Biskaborn, B. K., et al. (2019). Permafrost is warming at a global scale. *Nature Communications*, 10, 264. https://doi.org/10.1038/s41467-018-08240-4

Boye, K., Noël, V., Tfaily, M. M., Bone, S. E., Williams, K. H., Bargar, J. R., & Fendorf, S. (2017). Thermodynamically controlled preservation of organic carbon in floodplains. *Nature Geoscience*, *10*(6), 415–419. https://doi.org/10.1038/ngeo2940

Bruhn, A. D., Stedmon, C. A., Comte, J., Matsuoka, A., Speetjens, N. J., Tanski, G., Vonk, J. E., & Sjöstedt, J. (2021). Terrestrial dissolved organic matter mobilized from eroding permafrost controls microbial community composition and growth in arctic coastal zones. *Frontiers in Earth Science*, 9. https://doi.org/10.3389/feart.2021.640580

Crump, B. C., Kling, G. W., Bahr, M., & Hobbie, J. E. (2003). Bacterioplankton community shifts in an arctic lake correlate with seasonal changes in organic matter source. *Applied and Environmental Microbiology*, *69*(4), 2253–2268. https://doi.org/10.1128/AEM.69.4.2253-2268.2003

Danczak, R. E., Chu, R. K., Fansler, S. J., Goldman, A. E., Graham, E. B., Tfaily, M. M., Toyoda, J., & Stegen, J. C. (2020). Using metacommunity ecology to understand environmental metabolomes. *Nature Communications*, *11*(1), 6369. https://doi.org/10.1038/s41467-020-19989-y

D'Andrilli, J., Cooper, W. T., Foreman, C. M., & Marshall, A. G. (2015). An ultrahigh-resolution mass spectrometry index to estimate natural organic matter lability. *Rapid*

Communications in Mass Spectrometry, 29(24), 2385–2401. https://doi.org/10.1002/rcm.7400=

D'Andrilli, J., Romero, C. M., Zito, P., Podgorski, D. C., Payn, R. A., Sebestyen, S. D., Zimmerman, A. R., & Rosario-Ortiz, F. L. (2023). Advancing chemical lability assessments of organic matter using a synthesis of FT-ICR MS data across diverse environments and experiments. *Organic Geochemistry*, 184, 104667. https://doi.org/10.1016/j.orggeochem.2023.104667

Drake, T. W., Raymond, P. A., & Spencer, R. G. M. (2018). Terrestrial carbon inputs to in land waters: A current synthesis of estimates and uncertainty. *Limnology and Oceanography | Letters*, 3(3), 132–142. https://doi.org/10.1002/lol2.10055

DelSontro, T., Boutet, L., St-Pierre, A., Del Giorgio, P. A., & Prairie, Y. T. (2016). Methane ebullition and diffusion from northern ponds and lakes regulated by the interaction between temperature and system productivity. *Limnology and Oceanography*, *61*(S1). https://doi.org/10.1002/lno.10335

Estop-Aragonés, C., Olefeldt, D., Abbott, B. W., Chanton, J. P., Czimczik, C. I., Dean, J. F., Egan, J. E., Gandois, L., Garnett, M. H., Hartley, I. P., Hoyt, A., Lupascu, M., Natali, S. M., O'Donnell, J. A., Raymond, P. A., Tanentzap, A. J., Tank, S. E., Schuur, E. A. G., Turetsky, M., & Anthony, K. W. (2020). Assessing the potential for mobilization of old soil carbon after permafrost thaw: A synthesis of14 c measurements from the northern permafrost region. *Global Biogeochemical Cycles*, 34(9), e2020GB006672. https://doi.org/10.1029/2020GB006672

Fasching, C., Ulseth, A. J., Schelker, J., Steniczka, G., & Battin, T. J. (2016). Hydrology controls dissolved organic matter export and composition in an Alpine stream and its hyporheic zone. *Limnology and Oceanography*, *61*(2), 558–571. https://doi.org/10.1002/lno.10232

Fierer, N., Strickland, M. S., Liptzin, D., Bradford, M. A., & Cleveland, C. C. (2009). Global patterns in belowground communities. *Ecology Letters*, *12*(11), 1238–1249. https://doi.org/10.1111/j.1461-0248.2009.01360.x

Geng, Y., Yu, R., Lu, X., Li, X., Wang, X., Zhao, Y., Liu, Q., Sun, H., & Wang, R. (2025). Aquatic plants govern CH4 and CO2 production and flux partitioning in lake emission pathways. *Ecological Indicators*, *178*, 113864. https://doi.org/10.1016/j.ecolind.2025.113864

Hartnett, H. E. (2017). Dissolved organic matter (DOM). In W. M. White (Ed.), *Encyclopedia of Geochemistry: A Comprehensive Reference Source on the Chemistry of the Earth* (pp. 1–3). *Springer International Publishing*. https://doi.org/10.1007/978-3-319-39193-9_155-1

Helms, J. R., Stubbins, A., Ritchie, J. D., Minor, E. C., Kieber, D. J., & Mopper, K. (2008). Absorption spectral slopes and slope ratios as indicators of molecular weight, source, and photobleaching of chromophoric dissolved organic matter. *Limnology and Oceanography*, 53(3), 955–969. https://doi.org/10.4319/lo.2008.53.3.0955

Hertkorn, N., Frommberger, M., Witt, M., Koch, B. P., Schmitt-Kopplin, Ph., & Perdue, E. M. (2008). Natural organic matter and the event horizon of mass spectrometry. *Analytical Chemistry*, *80*(23), 8908–8919. https://doi.org/10.1021/ac800464g

Hu, A., Jang, K.-S., Meng, F., Stegen, J., Tanentzap, A. J., Choi, M., Lennon, J. T., Soininen, J., & Wang, J. (2022). Microbial and environmental processes shape the link between organic matter functional traits and composition. *Environmental Science & Technology*, 56(14), 10504–10516. https://doi.org/10.1021/acs.est.2c01432

Hugelius, G., Loisel, J., Chadburn, S., Jackson, R. B., Jones, M., MacDonald, G., Marushchak, M., Olefeldt, D., Packalen, M., Siewert, M. B., Treat, C., Turetsk M., Voigt, C., & Yu, Z. (2020). Large stocks of peatland carbon and nitrogen are vulnerable to permafrost thaw. *Proceedings of the National Academy of Sciences* 117(34), 2043820446. https://doi.org/10.1073/pnas.1916387117

Gholz, H. L., Wedin, D. A., Smitherman, S. M., Harmon, M. E., & Parton, W. J. (2000). Long-term dynamics of pine and hardwood litter in contrasting environments: Toward a global model of decomposition. *Global Change Biology*, *6*(7), 751–765. https://doi.org/10.1046/j.1365-2486.2000.00349.x

Guillemette, F., & Del Giorgio, P. A. (2011). Reconstructing the various facets of dissolved organic carbon bioavailability in freshwater ecosystems. *Limnology and Oceanography*, *56*(2), 734–748. https://doi.org/10.4319/lo.2011.56.2.0734

Guillemette, F., Leigh McCallister, S., & del Giorgio, P. A. (2016). Selective consumption and metabolic allocation of terrestrial and algal carbon determine allochthony in lake bacteria. *The ISME Journal*, 10(6), 1373–1382. https://doi.org/10.1038/ismej.2015.215

Kellerman, A. M., Dittmar, T., Kothawala, D. N., & Tranvik, L. J. (2014). Chemodiversity of dissolved organic matter in lakes driven by climate and hydrology. *Nature Communications*, 5(1). https://doi.org/10.1038/ncomms4804

Koch, B. P., & Dittmar, T. (2006). From mass to structure: An aromaticity index for high-resolution mass data of natural organic matter. *Rapid Communications in Mass Spectrometry*, 20(5), 926–932. https://doi.org/10.1002/rcm.2386

Kujawinski, E. B., Longnecker, K., Blough, N. V., Vecchio, R. D., Finlay, L., Kitner, J. B., & Giovannoni, S. J. (2009). Identification of possible source markers in marine dissolved

organic matter using ultrahigh resolution mass spectrometry. *Geochimica et Cosmochimica Acta*, *73*(15), 4384–4399. https://doi.org/10.1016/j.gca.2009.04.033

Kuhn, M. K. A., Thompson, L. M., Winder, J. C., Braga, L. P., Tanentzap, A. J., Bastviken, D., & Olefeldt, D (2021). Opposing effects of climate and permafrost thaw on CH_4 and CO_2 emissions from Northern Lakes. *AGU Advances*, 2(4). https://doi.org/10.1029/2021av000515

LaRowe, D. E., & Van Cappellen, P. (2011). Degradation of natural organic matter: A thermodynamic analysis. *Geochimica et Cosmochimica Acta*, 75(8), 2030–2042. https://doi.org/10.1016/j.gca.2011.01.020

Mostovaya, A., Hawkes, J. A., Koehler, B., Dittmar, T., & Tranvik, L. J. (2017). Emergence of the reactivity continuum of organic matter from kinetics of a multitude of individual molecular constituents. *Environmental Science & Technology*, *51*(20), 11571–11579. https://doi.org/10.1021/acs.est.7b02876

Natali, S. M., et al. (2021). Permafrost carbon feedbacks threaten global climate goals. *Proceedings of the National Academy of Sciences*, 118(21), e2100163118. https://doi.org/10.1073/pnas.2100163118

Olefeldt, D., Goswami, S., Grosse, G., Hayes, D., Hugelius, G., Kuhry, P., McGuire, A. D., Romanovsky, V. E., Sannel, A. B. K., Schuur, E. a. G., & Turetsky, M. R. (2016). Circumpolar distribution and carbon storage of thermokarst landscapes. *Nature Communications*, *7*(1), 13043. https://doi.org/10.1038/ncomms1304

Raymond, P. A., Hartmann, J., Lauerwald, R., Sobek, S., McDonald, C., Hoover, M., Butman, D., Striegl, R., Mayorga, E., Humborg, C., Kortelainen, P., Dürr, H., Meybeck, M., Ciais, P., & Guth, P. (2013). Global carbon dioxide emissions from inland waters. *Nature*, *503*(7476), 355–359. https://doi.org/10.1038/nature12760

Rosentreter, J. A., Borges, A. V., Deemer, B. R., Holgerson, M. A., Liu, S., Song, C., Melack, J., Raymond, P. A., Duarte, C. M., Allen, G. H., Olefeldt, D., Poulter, B., Battin, T. I., & Eyre, B. D. (2021). Half of global methane emissions come from highly variable aquatic ecosystem sources. *Nature Geoscience*, *14*(4), 225–230. https://doi.org/10.1038/s41561-021-00715-2

Schuur, E. A. G., et al. (2015). Climate change and the permafrost carbon feedback. *Nature*, 520, 171–179. https://doi.org/10.1038/nature14338

Segers, R. (1998). Methane production and methane consumption: A review of processes underlying wetland methane fluxes. *Biogeochemistry*, *41*(1), 23–51. https://doi.org/10.1023/A:1005929032764\

Spencer, R. G. M., Aiken, G. R., Wickland, K. P., Striegl, R. G., & Hernes, P. J. (2008). Seasonal and spatial variability in dissolved organic matter quantity and composition from the Yukon River basin, Alaska. *Global Biogeochemical Cycles*,22(4), 2008GB003231. https://doi.org/10.1029/2008GB003231

Starr, S. F., Wickland, K. P., Kellerman, A. M., McKenna, A. M., Kurek, M. R., Miller, A., Katsaras, A., Douglas, T. A., Mackelprang, R., Shade, A. L., & Spencer, R. G. M. (2025). Organic matter composition versus microbial source: Controls on carbon loss from fen wetland and permafrost soils. *Journal of Geophysical Research: Biogeosciences*, 130(5), e2024JG008445. https://doi.org/10.1029/2024JG008445

Tranvik, L. J., Downing, J. A., Cotner, J. B., Loiselle, S. A., Striegl, R. G., Ballatore, T. J., Dillon, P., Finlay, K., Fortino, K., Knoll, L. B., Kortelainen, P. L., Kutser, T., Larsen, Soren., Laurion, I., Leech, D. M., McCallister, S. L., McKnight, D. M., Melack, J. M., Overholt, E., Porter, J. A., Prairie, Y., Renwick, W. H., Roland, F., Sherman, B. S., Sobek, S., Tremblay, A., Vanni, M. J., Verschoor, A. M., Von Wachenfeldt, E., Weyhenmeyer, G. A. (2009). Lakes and reservoirs as regulators of carbon cycling and climate. *Limnology and Oceanography*, *54*(6part2), 2298–2314. https://doi.org/10.4319/lo.2009.54.6_part_2.2298

Turetsky, M. R., et al. (2020). Carbon release through abrupt permafrost thaw. *Nature Geoscience*, 13, 138–143. https://doi.org/10.1038/s41561-019-0526-0

Valiente, N., Eiler, A., Allesson, L., Andersen, T., Clayer, F., Crapart, C., Dörsch, P., Fontaine, L., Heuschele, J., Vogt, R. D., Wei, J., De Wit, H. A., & Hessen, D. O. (2022). Catchment properties as predictors of greenhouse gas concentrations across a gradient of boreal lakes. *Frontiers in Environmental Science*, *10*, 880619. https://doi.org/10.3389/fenvs.2022.880619

Vonk, J. E., Tank, S. E., Mann, P. J., Spencer, R. G. M., Treat, C. C., Striegl, R. G., Abbott, B. W., & Wickland, K. P. (2015). Biodegradability of dissolved organic carbon in permafrost soils and aquatic systems: A meta-analysis. *Biogeosciences*, *12*(23), 6915–6930. https://doi.org/10.5194/bg-12-6915-2015

Ward, C. P., & Cory, R. M. (2016). Complete and partial photo-oxidation of dissolved organic matter draining permafrost soils. *Environmental Science & Technology*, 50(7), 3545–3553. https://doi.org/10.1021/acs.est.5b05354

Ward, C. P., Nalven, S. G., Crump, B. C., Kling, G. W., & Cory, R. M. (2017). Photochemical alteration of organic carbon draining permafrost soils shifts microbial metabolic pathways and stimulates respiration. *Nature Communications*, 8(1), 772. https://doi.org/10.1038/s41467-017-00759-2

Wik, M., Varner, R. K., Anthony, K. W., MacIntyre, S., & Bastviken, D. (2016). Climate-sensitive northern lakes and ponds are critical components of methane release. *Nature Geoscience*, 9(2), 99–105. https://doi.org/10.1038/ngeo2578

Chapter 2

Mismatch Between Microbes and DOM Drives Inefficient Carbon Use in Ponds Impacted by Permafrost Thaw

Abstract

Climate-driven permafrost thaw is releasing microorganisms and dissolved organic matter (DOM) into freshwaters that would otherwise persist in frozen soils. If this DOM is returned to the atmosphere by microbial respiration, especially methane, it can act as a positive feedback to climate change, but its fate depends on its composition and that of microbial communities. We tested how the molecular composition of DOM and microbial communities interact to influence the short-term persistence of DOM in freshwaters impacted by permafrost thaw. We used a fully factorial experiment mixing DOM and microbial communities from thermokarst ponds and adjacent lakes in northern Canada. We quantified changes in DOM composition via optical and ultrahigh-resolution mass spectrometry and assessed microbial responses through cell counts and greenhouse gas emissions over 72 hours. We found that DOM and microbial community composition exerted equal and interactive control over DOM degradation. Lake microbes preferentially degraded thermokarst DOM, releasing 3× more CO_2 because of low carbon use efficiency. In contrast, thermokarst microbes grew similarly across DOM sources but altered DOM composition with minimal CO_2 production, consistent with a more conservative metabolic strategy. This study highlights a mechanism by which mismatches between microbial communities and DOM arising from environmental change can elevate terrestrial carbon losses. More broadly, our study identifies the importance of integrating

microbial functional traits and DOM chemistry into biogeochemical models to predict the fate of permafrost carbon under future climate scenarios.

Keywords: Dissolved Organic Matter (DOM), Microbial Communities, Permafrost Thaw, Thermokarst Lakes, Carbon Use, Fourier-transform ion cyclotron resonance mass spectrometry (FT-ICR MS)

Introduction

Perennially frozen ground, termed permafrost, is thawing because of climate change with the potential for large but unknown consequences for the global carbon cycle (Hugelius et al., 2020). Permafrost soils store approximately 1,500 Pg of organic carbon, twice the amount of carbon in the atmosphere (Hugelius et al., 2013; Schuur et al., 2015). Depending on how this permafrost formed, such as if it coincided with organic matter accumulation, the carbon that was sequestered in frozen soils can remain highly bioavailable when thawed (Estop-Aragonés et al., 2020; Hugelius et al., 2014; Maines et al., 2021; Schuur et al., 2008; Vonk et al., 2013). By contrast, in many boreal peatlands, organic matter may have accumulated for millennia before freezing, during which it was exposed to microbial activity (Manies et al., 2021). This organic matter may be more microbially processed and less likely to be mineralized (Shur & Jorgenson, 2007). Thawing permafrost also releases microorganisms that have remained active but isolated from modern microbiomes over millennia (Graham et al., 2012; Jansson & Taş 2014; Mackelprang et al., 2017). These microbes can quickly become metabolically active upon thaw, even under low oxygen or anaerobic conditions (Burkert et al., 2019). As permafrost thaws it causes the rapid formation of permanent waterbodies through land subsidence, a process known as thermokarst (Olefeldt et al., 2016) that increases the hydrological connectivity (Connon et al., 2014) to both permafrost-derived organic matter and microorganisms that can be released into freshwaters. The extent to which these newly released microbes and molecules stabilize or amplify carbon cycling alongside present-day microbiomes and metabolomes remains poorly known in northern lakes and ponds that are major greenhouse gas sources (Graham et al., 2012; Mackelprang et al., 2017; Wik et al., 2016; Woodcroft et al., 2018).

The composition of organic matter released by thawing permafrost into lakes and ponds can differ from material available in present-day habitats (Jansson & Taş, 2014; Mackelprang et al., 2017; Vonk et al., 2013). Most of the biologically active organic matter released into freshwaters is available in dissolved form (Battin et al., 2008; Ward & Cory, 2016). This dissolved organic matter (DOM) can be rich in low molecular weight and oxygenated compounds, making it more labile, but it can also contain aromatic moieties derived from ancient plant material, which are less biologically reactive (Mann et al., 2015; O'Donnell et al., 2016; Spencer et al., 2015). Consequently, labile fractions may be rapidly mineralized to CO_2 and CH_4, while others could be allocated to microbial biomass (Drake et al., 2018; Guillemette et al., 2015; Mayumi et al., 2016; Starr et al., 2023, 2024, 2025). In contrast, present-day DOM is often more nitrogen-rich and aliphatic, traits associated with higher microbial bioavailability (Fellman & Spencer, 2010). However, this material can also be more prone to microbial reworking, reflecting ongoing decomposition (Fasching et al., 2014; Guillemette et al., 2016; Kellerman et al., 2014, 2015). Therefore, depending on its precise molecular composition, concentration, and microbial community (Arrieta et al., 2015; Bruhn et al., 2021; Ward et al., 2017), DOM from thawing permafrost can stimulate microbial respiration and act as positive feedback to climate change or fuel heterotrophic productivity. Resolving the responses of microbes to permafrost-derived DOM should be a key priority to improve predictions of future climate change.

Like DOM composition, the microbial communities released by thawing permafrost into lakes and ponds can differ from those in present-day environments (Graham et al., 2012; Jansson & Taş, 2014; Mackelprang et al., 2017). These communities include anaerobic fermenters, syntrophs, hydrogenotrophic and acetoclastic methanogens, and cold-adapted decomposers, many of which are rare or absent in present-day surface waters (Coolen & Orsi, 2015; Woodcroft

et al., 2018). For example, Methanobacteriales and Methanosarcinales, commonly found in thawed permafrost layers, are key players in methane production but are underrepresented in oxic lake surface microbiomes (Winder et al., 2023). These compositional shifts, favoring anaerobic metabolism and high-efficiency carbon mineralizers, may alter methane cycling in receiving waters and contribute to nonlinear increases in CH_4 and CO_2 emissions under warming scenarios (Graham et al., 2012; Kuhn et al., 2021; Schuur et al., 2015).

To investigate how permafrost thaw may reshape carbon cycling in northern ecosystems, we conducted a factorial incubation experiment using dissolved organic matter (DOM) and microbial communities collected from thermokarst ponds and their downstream lakes in subarctic Quebec, Canada. By manipulating the source of DOM (thermokarst versus lake) and microbial inoculum (control, lake, or thermokarst), we tested how novel combinations between lake and thermokarst waters may affect DOM transformation, greenhouse gas production, and metabolism. We asked: (1) how do thermokarst microbes transform DOM versus lake microbes? and (2) What are the consequences of these mixtures for carbon cycling, specifically microbial growth versus respiration? To answer these questions, we used optical spectrophotometry and Fourier-transform ion cyclotron resonance mass spectrometry (FT-ICR MS) to assess changes in the molecular composition of DOM and link these to measurements of greenhouse gas production, microbial growth rates, and microbial growth efficiency inferred with flow cytometry. Because thermokarst microbes are adapted to degrading complex DOM (Woodcroft et al., 2018), which may be less suitable for assimilation into biomass (Bruhn et al., 2021; D'Andrilli et al., 2023; Guillemette et al., 2016), we predicted that they would increase greenhouse gas emissions when grown on more complex substrates (Guillemette et al., 2016; Judd et al., 2006).

Methods

Sampling sites

During September 2023, we collected water from two thermokarst ponds, and the lakes they drained into, near James Bay, Quebec, Canada above the northern limit of sporadic permafrost (Tremblay et al., 2014). The first pond (53.50296°N, 77.69901°W) was located near Lake Duncan (53.48006°N, 77.93327°W). Tremblay et al (2014) previously characterized this site as a thermokarst pond in a *Sphagnum*-dominated peatland. The downstream lake, Lake Duncan, is a natural oligotrophic lake with clear water (Tremblay et al., 1996). Detailed limnological data on Lake Duncan are not publicly available. The second pond (53.74534°N, 77.58816°W) was located near La Grande Reservoir (53.684733°N, 77.106318°W) in a similar peatland to the first site. The reservoir has a surface area of 2835 km^2, a max depth of 137 m, and a mean depth of 21.8 m, and was also an oligotrophic lake with clear water like Lake Duncan (Tremblay et al., 1996).

DOM and microbial inoculum

At each of the four sites, we collected 5 L of water from the shoreline into polyethylene terephthalate bottles. Prior to sampling, we rinsed the bottles three times with deionized water and three times with sample water. We obtained the DOM and microbial inoculum by passing 1 L of water through two 0.2 μm cartridge filters (Sterivex, Millipore, USA). The filtrate was collected into a pre-combusted (450 °C for 4 h) amber glass bottle and used as the DOM inoculum. Then, we back-flushed the filter with 20 mL of mineral water to obtain the microbial

inoculum. We used mineral water to ensure cells would not burst due to differences in osmotic pressure. We passed an additional 1 L of water from each site through a 0.2 μm cartridge filter (Sterivex, Millipore) and stored the filter at -20°C until it was used to characterize initial microbial community composition.

We diluted the DOM and microbial inoculum to ensure all experimental treatments had comparable initial concentrations. DOM concentrations were estimated based on optical properties, following Helms et al. (2008). We recorded UV-visible absorbance spectra (190–800 nm) using a Flame spectrophotometer (OceanOptics, USA; see below for further details) and used absorbance at 420nm (A_{420}) as a proxy for DOM concentration. Absorbance at this wavelength corresponds to a region of strong chromophoric dissolved organic matter (CDOM) absorbance and is commonly used as an indicator of DOM concentration in humic-rich systems like ours (Peacock et al., 2015; Zhang et al., 2020), supporting its use for standardization of DOM inoculum across treatments.

We estimated the abundance of microbes in each inoculum after staining RNA using acridine orange (Francisco et al., 1973). Briefly, we prepared a dilution series of each microbial inoculum (10×, 100×, and 1000×) using sterile mineral water. Each dilution was stained with acridine orange at a final concentration of 0.01%, incubated in the dark for 30 minutes, and then measured for fluorescence at 680 nm emission and 450 nm excitation using a portable fluorometer (BBE Moldaenke, Germany). We then fit a linear calibration curve to the fluorescence intensity of each inoculum with the dilution level as a predictor and proxy for relative cell abundance. We used these equations to estimate the cell concentration of the undiluted inoculum. Based on these estimates, all inocula were diluted using mineral water to

match the abundance of the lowest concentration inoculum, approximately 6.0×10^4 cells mL^{-1}, as later verified by flow cytometry.

Experimental design

We used a fully factorial design to test how novel DOM sources or microbial communities impact carbon cycling in permafrost environments. The experiment consisted of 2 DOM sources (lake and thermokarst) and 3 microbial communities (control with no microbes, lake, and thermokarst). We generated all possible combinations of these treatments within each of two sites Lake Duncan and La Grande Reservoir, resulting in 6 treatments per site. Each treatment was replicated 6 times resulting in 36 samples per site and 72 across both sites. For each treatment, we added 1 mL of the corresponding microbial inoculum and 114 mL of DOM inoculum into pre-combusted clear 120 mL glass serum bottles. For microbial controls, we added 1 mL of deionized water filtered at 0.5 μm as a baseline measurement. All bottles were crimped gas-tight with no headspace and sealed with rubber septa, with one replicate from each treatment per site removed at the start of the experiment (T_0) and processed immediately. The remaining 60 were incubated at room temperature (~22°C) for 3 days.

To sample each bottle, we pierced its septa with two sterile needles and 30 mL of water was removed by one needle while injecting the same volume of atmospheric air with the other to create a headspace for greenhouse gas measurements. 1 mL of sample water was immediately dispatched into a quartz cuvette to measure optical properties and 4 mL were placed in a cryotube for flow cytometry with 1 mL of 25% glutaraldehyde that was incubated for 30 min in the dark before storing at -20°C. We then measured greenhouse gases from the headspace (see below), before adding 1 mL of 37% HCl to the remaining 85 mL of water in the sample bottle to

preserve the sample for FT-ICR MS. Cryotubes were frozen at -20°C while the remaining samples were stored at 4°C until measurement.

Molecular composition of DOM

We extracted DOM from 60 mL in each bottle using solid phase extraction according to Dittmar et al (2008). We cleaned and activated 3 mL styrene-divinylbenzene polymer cartridges (Bond Elut PPL, Agilent, Santa Clara, USA) by filling them with HPLC-grade methanol and letting them soak overnight. Cartridges were then rinsed with one volume of ultrapure water, methanol, and ultrapure water acidified to pH 2 with 1M HCl acid. We then passed 60 mL of sample through each cartridge and dried them with N_2 gas. The extracts were eluted into pre-combusted amber borosilicate vials with 4 mL of methanol and stored at -20°C until measurement.

We analyzed the samples on a 7T Fourier transform ion-cyclotron resonance mass spectrometer (FT-ICR MS, SolariX XR, Bruker, Germany) at Trent University's Water Quality Center. The system was equipped with an electrospray ionization source applied in negative ionization mode. We diluted the samples to a volume of 300 µL at a carbon concentration of 5 ppm in a 50:50 methanol:water mixture, assuming an extraction efficiency of 60%, before injecting 150 µL into the FT-ICR MS. Our mass spectrometry method had the following settings: 8-magnetron mode, 250 scans, and ~0.3 ms accumulation time to keep the total ion counts in between 0.8×10^9 and 1×10^9, and used a mass range of *m/z* 100-1000, where *m/z* is mass to charge ratio. We calibrated the instrument daily according to manufacturer instructions and a solution of 0.1 mg mL^{-1} sodium trifluoroacetate methanol. Before running the samples, we analyzed a blank

(300 µL of 50:50 methanol and Milli-Q water) and a Suwannee River natural organic matter (SRNOM, International Humic Acid Substances Society batch SR101N) reference standard for quality control. The SRNOM standard, with its well-characterized molecular formula distribution, was used to assess instrument performance by evaluating peak shape, intensity range, and spectral reproducibility against expected profiles (Koch & Dittmar, 2006). Spectra were also visually inspected to confirm a normal distribution of peaks and appropriate signal intensity relative to other samples (e.g. Figure A1). If deviations in spectral quality or signal intensity were observed, samples were re-run at adjusted dilution concentrations and/or additional blanks were analyzed until instrument performance stabilized.

Raw spectra were calibrated using the Bruker Compass Data Analysis software (Bruker, Billerica, USA) with a custom method file configured for negative electrospray ionization (ESI) mode and a mass range of *m/z* 100–1000 . Calibration involved iterative removal of extreme error calibrants until the mass accuracy dropped below 0.2 ppm. Molecular formulae were assigned to the calibrated spectra using the ICBM-OCEAN online tool (Merder et al., 2020). Default method detection levels were used; outlier removal and single mass shift selection were not applied. Formula assignment used a 1 ppm tolerance and allowed elements were restricted to carbon ($C \leq 100$), hydrogen ($H \leq 200$), oxygen ($O \leq 70$), nitrogen ($N \leq 4$), sulfur ($S \leq 1$), and phosphorus ($P \leq 1$). The N, S, P rule was enabled, following recommendations for DOM (Riedel & Dittmar, 2014). We removed single-instance peaks (“singlets”), activated isotope verification using mean and second ^{13}C settings, and enabled homologous series network analysis for CH_2 and CO_2. To align molecular assignments between samples, we then performed a sample junction with a 2 ppm sample tolerance using the Fast Join method.

Using the ftmsRanalysis package v1.1.0 (Bramer et al., 2025), we summarized the molecular composition of each sample. We calculated the Gibbs Free Energy (GFE), the modified aromaticity index (AI_{Mod}), nominal oxidative state of carbon (NOSC), oxygen to carbon ratio (O:C), and hydrogen to carbon ratio (H:C). GFE in this context is not directly measured but rather estimated by NOSC following a linear relationship proposed by LaRowe and Van Cappellen (2011). It provides a thermodynamic proxy for the energy potentially available to microbes during the oxidation of a compound where more negative values indicate compounds that can yield energy, while positive values suggest that energy input may be required for microbial processing (LaRowe & Van Cappellen, 2011). AI_{Mod} estimates molecular aromaticity and stability, with higher values indicating more aromatic and structurally stable compounds (Koch & Dittmar, 2006). NOSC reflects the oxidative state of carbon within organic molecules; with higher NOSC values indicating more oxidized compounds (LaRowe & Van Cappellen, 2011). The O:C ratio is another indicator of oxidation, with higher ratios reflecting more oxidized molecules, but unlike with NOSC, higher O:C can indicate a higher amount of oxygen atoms bound to elements other than carbon (e.g. N, P, S). The H:C ratio is commonly used as a general indicator for molecular characteristics. Higher H:C values suggest more aliphatic and bioavailable compounds, while lower values imply more complex condensed structures, which often contribute to chemical stability and resistance to degradation (Kim et al., 2003). All metrics were calculated as intensity-weighted averages per sample.

We also classified molecular formulae according to their atomic composition (D'Andrill et al., 2015). Formulae were assigned to seven putative compound classes: lipid-like, protein-like, amino sugar-like, carbohydrate-like, lignin-like, tannin-like, and condensed hydrocarbon-like. For each sample, we then summed the intensities of all formulae within each class and

calculated their contribution to total molecular intensity. We used independent two-sample t-tests to compare the total intensities of each compound class between initial DOM treatments (lake versus thermokarst).

DOM optical properties

We recorded the UV-visible spectra of each DOM sample using a Flame spectrophotometer (OceanView, USA), scanning absorbance from 250 to 655 nm at ~1 nm intervals. A Milli-Q water blank was measured before each sample to establish a baseline for absorbance, correct for background signal, and detect any instrument drift or contamination in the system. From the optical spectra, we quantified four complementary indices to assess DOM composition and degradation (Zhang et al., 2020). These included the Helms slope ratio, which compares the absorbance spectra between 275–295 nm relative to 350–400 nm. A higher ratio indicates a dominance of lower molecular weight compounds and greater degradation (Helms et al., 2008). In addition, we calculated the E2:E3 ratio (absorbance at 254 nm relative to 365 nm) and the E4:E6 ratio (absorbance at 465 nm relative to 665 nm). These ratios are proxies for DOM molecular weight and aromaticity, respectively (De Haan & De Boer, 1987; Chen et al., 1977). Finally, we quantified chromophoric dissolved organic matter (CDOM), defined as the fraction of DOM that absorbs UV-visible light between 200 to 400 nm. Higher CDOM typically represents high molecular weight and more aromatic compounds, and its reduction is often used to signal microbial or photochemical breakdown of DOM (Ha et al., 2010; Helms et al., 2008). We calculated changes in each index from the initial time point (T_0) to the final time point (T_f) to evaluate shifts in DOM composition over the course of the incubation

DNA extraction

To obtain genetic material from the microbial community retained on 0.2 μm cartridge filters (Sterivex, Millipore), we placed filters from each sample in separate 2 mL microcentrifuge tubes. We added 600 μL of Phenol:Chloroform:Isoamyl Alcohol (25:24:1, Sigma-Aldrich P3803) to each tube and vortexed at maximum speed for 15 minutes. Samples were centrifuged at 15,000 rpm (4°C) for 10 minutes, after which the resulting supernatant was transferred to clean 2 mL tubes and stored at 4°C overnight.

DNA was extracted from the supernatant using the DNEasy PowerSoil Pro Kit (Qiagen, Aarhus, Denmark) and automated with a QIAcube Connect (Qiagen, Aarhus, Denmark), following manufacturer's protocols. A negative control, consisting of molecular-grade nuclease-free water, was processed alongside the samples. DNA concentration was initially quantified using a High Sensitivity dsDNA Kit with a Qubit 3.0 Fluorometer (ThermoFisher Scientific, Waltham, USA). Due to low DNA yield (< 0.01 ng μL^{-1}), we re-extracted the Sterivex filters by adding a bead-beating step with PowerBeads (Qiagen, Aarhus, Denmark) to lyse cells trapped within the filter. The first and second extractions were pooled for each sample. Final DNA concentrations were re-quantified with the Qubit 3.0, and fragment size distributions were evaluated using a Bioanalyzer HS DNA chip (Agilent, Santa Clara, CA) at The Centre for Applied Genomics, Toronto, Canada to ensure the DNA was not degraded for a total DNA yield of 2.48 ng μL^{-1} after re-extraction.

Metagenomic sequencing and bioinformatics

Shotgun metagenomic libraries were prepared using a total of 2.4 ng of DNA and the Ligation Sequencing gDNA Native Barcoding Kit 24 V14 (SQK-NBD114.24 Oxford Nanopore Technologies, UK). Sequencing was performed on an Oxford Nanopore Technologies PromethION 2 flow cell (R.10.4.1) using MinKNOW™ with live base-calling at ultra-high resolution enabled (Median read lengths: Duncan - lake and thermokarst DOM, 238 bp; La Grande Reservoir - lake DOM, 237 bp; La Grande Reservoir - thermokarst DOM, 257 bp). Simplex data were collected with a minimum Q-score threshold of 9 to maximize sequencing depth at the detriment of accuracy. Taxonomic classification of sequences was performed using the BugSeq metagenomic pipeline, which incorporates quality control and species-level annotation using the BugRef database (Fan et al., 2021). To further minimize contamination and spurious hits, we post-processed the BugSeq outputs. Specifically, species detected in the negative control at ≥10% relative abundance were removed from all samples, and we filtered taxonomic assignments to retain only those with a minimum identity threshold ≥80%. We retrieved the proportion of methanotrophs by comparing our taxonomic assignment to a previously established database (Webster et al., 2022). To visualize similarities in microbial community composition across environments and sites, we created a species-level co-occurrence network using Cytoscape v3.10.3 (Shannon et al., 2003). This allowed us to assess both shared and unique taxa across lake and thermokarst habitats.

Greenhouse gases concentrations

Carbon dioxide (CO_2) and methane (CH_4) concentrations in the headspace of each bottle were measured using an infrared gas analyzer based on off-axis integrated cavity output spectroscopy (ultraportable greenhouse gas analyzer 915, Los Gatos Research, Mountain View,

USA). Bottles were shaken for one minute to equilibrate gases between the air and water phases. Gas concentrations in the headspace were measured by inserting two needles through the septum and running the bottle in a closed-loop system for approximately two minutes. First, the amount of gas in the headspace was converted into moles using the Ideal Gas Law. Next, Henry's Law was used to calculate how much gas was dissolved in the water prior to equilibration, using Henry's constant for CO_2 or CH_4 at 20°C. We then summed the gas in the headspace and water phases to determine total CO_2 and CH_4 in each bottle. However, because the headspace was created using atmospheric air, a portion of this gas was not biologically produced. Therefore, we repeated the Ideal Gas Law calculation for CO_2 and CH_4 based on ambient room concentrations measured by the gas analyzer. We then subtracted the ambient values from the total CO_2 and CH_4 in each bottle to estimate the net gas concentrations attributable to DOM degradation and microbial activity.

Flow cytometry for microbial abundance

We quantified microbial abundance using flow cytometry. Each sample was stained with SYBR-Green I at a final 100× concentration and incubated in the dark for 30 minutes at room temperature. Samples were run in 96-well U-bottom plates on an Attune NxT flow cytometer equipped with a CytKick Autosampler (ThermoFisher Scientific, Waltham, USA). Particle counts were acquired for both stained and unstained replicates, with unstained controls providing background signal information for gating. Each sample was measured at a flow rate of 12.5 µL min^{-1}, with a total volume of 50 µL analyzed per replicate. Fluorescence data were processed using the Floreada.io web tool (https://floreada.io/). Electronic gating was applied to both green fluorescence and side scatter channels using a threshold of 0.2 × 1000 to distinguish microbial

cells from background particles. Gates were standardized across all replicates within each treatment group to ensure comparability in downstream analyses.

Cell growth and growth efficiency

Microbial cell growth and growth efficiency were calculated based on flow cytometry and greenhouse gas measurements. We began by isolating microbial growth not attributable to the experimental treatments by subtracting the mean cell abundance measured in the no microbe control treatments from individual cell counts in the lake and thermokarst microbe treatments. Changes in cell abundance over the incubation period (i.e. between T_0 to T_f) were then normalized to incubation duration (72 hours) to derive microbial growth rates in cells mL^{-1} hr^{-1}. To estimate growth efficiency, we first estimated microbial respiration rates from the difference in headspace CO_2 concentrations measured at the end versus the start of the incubation. CO_2 concentrations were converted to mol L^{-1} and normalized by the incubation period to yield respiration rates in mol of C L^{-1} hr^{-1}. Microbial growth efficiency was calculated as the proportion of carbon allocated to biomass production relative to total carbon, i.e. the sum of cell growth and respiration. To express growth and respiration in comparable units, we converted changes in cell abundance into moles of carbon using an average cellular carbon content of 280 femtograms per microbial cell, based on published estimates for aquatic bacteria (Fagerbakke et al., 1996).

Statistical analyses

We tested if the molecular composition of DOM initially differed between thermokarst and lake samples in the microbial control treatments. We fitted linear models to the FT-ICR MS metrics with DOM source and site (Lake Duncan or La Grande Reservoir) as predictors, allowing for a statistical interaction between source and site. The models were fitted with the lm function in R version 4.3.2 (R Core Team, 2023). We then estimated marginal means among DOM treatments across sites using the emmeans R package (Lenth, 2024). P-values were adjusted for multiple comparisons using Tukey's Honest Significant Difference.

We then tested how the molecular and optical properties of DOM, greenhouse gas emissions, and microbial growth changed in our experiment using linear models. Non-normally distributed responses were log-transformed prior to analysis. The model predictors always were DOM source (lake or thermokarst), microbial community (control, lake, thermokarst), and site (Lake Duncan or La Grande Reservoir), allowing for interactions between DOM source and microbial community. All models included an interaction between DOM source (comparing the microbial treatments), and within microbial treatments (comparing the DOM sources). To interpret these effects, we calculated estimated marginal means using the emmeans package. P-values were adjusted for multiple comparisons using Tukey's Honest Significant Difference. Because initial T_0 measurements were only available for optical properties, all other response variables: greenhouse gas emissions, molecular composition, microbial growth, and growth efficiency, were calculated relative to sterile controls. We compared each microbial addition to the corresponding control within the same DOM source. This design minimizes confounding effects from baseline differences in DOM characteristics between lake and thermokarst sources, allowing us to isolate microbial effects.

Results

Initial differences in DOM and microbial composition among treatments

The molecular composition of DOM differed between thermokarst ponds and lakes in the absence of microbes (Figure 1), with these differences being more consistent than those between sites (Table 1). Both thermokarst and lake DOM were dominated by lignin-like compounds, suggesting predominantly plant-derived inputs (Figure 1a). However, lake DOM contained a higher relative abundance of bioavailable lipid-like compounds across both sites ($t = 3.02$, $df = 18.6$, $p = 0.007$), whereas condensed hydrocarbons were more prevalent in thermokarst DOM reflecting increased aromaticity and unsaturation ($t = –2.61$, $df = 22.0$, $p = 0.016$). Labile formulae comprised 7.6% of all 6,266 molecular formulae detected across the four DOM sources, with 342 of these occurring in lake DOM versus 259 in thermokarst DOM (Figure 1b, 1c). Together, these formulae reached a higher total relative intensity in lake compared to thermokarst DOM ($t = 2.52$, $df = 6.43$, $p = 0.042$).

FT-ICR MS-derived metrics revealed that lake DOM was more saturated and reduced, while thermokarst DOM was more oxidized and structurally complex (Table 1). DOM from lake sources had a higher H:C ratio compared to thermokarst DOM at both Lake Duncan ($t = 5.33$, $df = 8$, $p < 0.001$) and La Grande Reservoir ($t = 5.33$, $df = 8$, $p = 0.011$). In contrast, the O:C ratio was higher in thermokarst DOM at La Grande Reservoir ($t = -2.93$, $df = 8$, $p = 0.019$), but not at Lake Duncan (Table 1). Aromaticity, as indicated by AI_{Mod}, showed the reverse pattern of being higher in thermokarst than lake DOM at Lake Duncan ($t = –3.04$, $df = 8$, $p = 0.0160$), but with no difference at La Grande Reservoir, thereby highlighting the variability between sites. However, NOSC was higher in thermokarst DOM at both Lake Duncan ($t = 3.34$, $df = 8$, $p = 0.010$) and La Grande Reservoir ($t = 3.34$, $df = 8$, $p = 0.010$). As GFE is derived from NOSC, the observed

increases in NOSC of thermokarst DOM translated directly into lower GFE in thermokarst DOM at both sites (Table 1).

Table 1: Pairwise comparisons of molecular and elemental traits between lake and thermokarst DOM in the absence of microbes, i.e. control treatments. Differences were estimated separately for each site based on linear models. Positive t-ratios indicate higher values in lake DOM shown in the Result column. Statistically significant comparisons ($p < 0.05$) are bolded. For all, degrees of freedom = 8.

Metric	Site	*t*-ratio	*p*-value	Result
O:C	Duncan	-0.93	0.3816	Lake < Thermokarst
O:C	**La Grande**	**-2.93**	**0.019**	**Lake < Thermokarst**
H:C	**Duncan**	**5.33**	**<0.001**	**Lake > Thermokarst**
H:C	**La Grande**	**3.33**	**0.0105**	**Lake > Thermokarst**
AI_{Mod}	**Duncan**	**-3.04**	**0.016**	**Lake < Thermokarst**
AI_{Mod}	La Grande	-<0.01	0.9984	Lake < Thermokarst
NOSC	**Duncan**	**-2.80**	**0.0231**	**Lake < Thermokarst**
NOSC	**La Grande**	**-3.34**	**0.0103**	**Lake < Thermokarst**
GFE	**Duncan**	**2.80**	**0.0231**	**Lake > Thermokarst**
GFE	**La Grande**	**3.34**	**0.0103**	**Lake > Thermokarst**

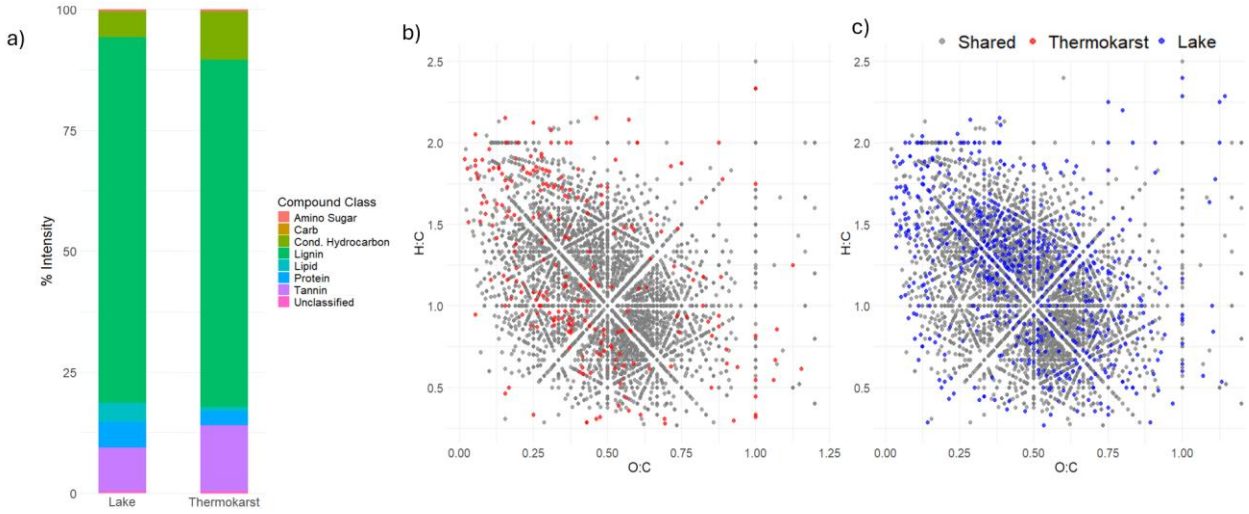

Figure 1: Molecular composition of DOM derived from lake and thermokarst sources under control microbial conditions. (a) Stacked bar plot showing the percent intensity of putative compound classes for each DOM source averaged across sites (n =8 samples per treatment). Van Krevelen diagrams depicting the number of unique molecular formulae detected in (b) thermokarst DOM (total n = 4184) and (c) lake DOM (total n = 5208) across both sites.

Microbial communities, bacteria only, no archaeal sequences detected, also initially differed between habitats and between sites despite 35% of the 925 microbial species identified in our study being found at all sites. We retrieved 61,190 to 135,259 reads per site that could be classified at least to a microbial Family. The most dominant bacteria were species endemic to permafrost environments, with the general chemoheterotrophs *Granulicella sibirica*, the nitrite oxidiser Candidatus *Nitrotoga arctica*, and sulfur oxidising *Sulfuriferula plumbiphila* accounting for 3.6, 3.3, and 2.2% of the total reads in the dataset, respectively (Table A1, A2). There was also evidence of microbes involved in methane cycling, with between 5 to 7 methanotroph species collectively accounting for 0.38% to 0.63% of all the reads in a site with no methanogens detected. Generally, the two thermokarst samples were as like each other as they were to lakes in the same site (Figure 2). Lake Duncan thermokarst shared 35 species with La Grande Reservoir thermokarst and each shared 40 and 21 species with Lake Duncan and La Grande Reservoir, respectively (Figure 2; Table A1). By contrast, Lake Duncan and La Grande Reservoir only shared 11 species (Figure 2; Table A1). All species-level read counts (≥80% ID, negative control removed) and their associated families are provided in Supplementary Data 1.

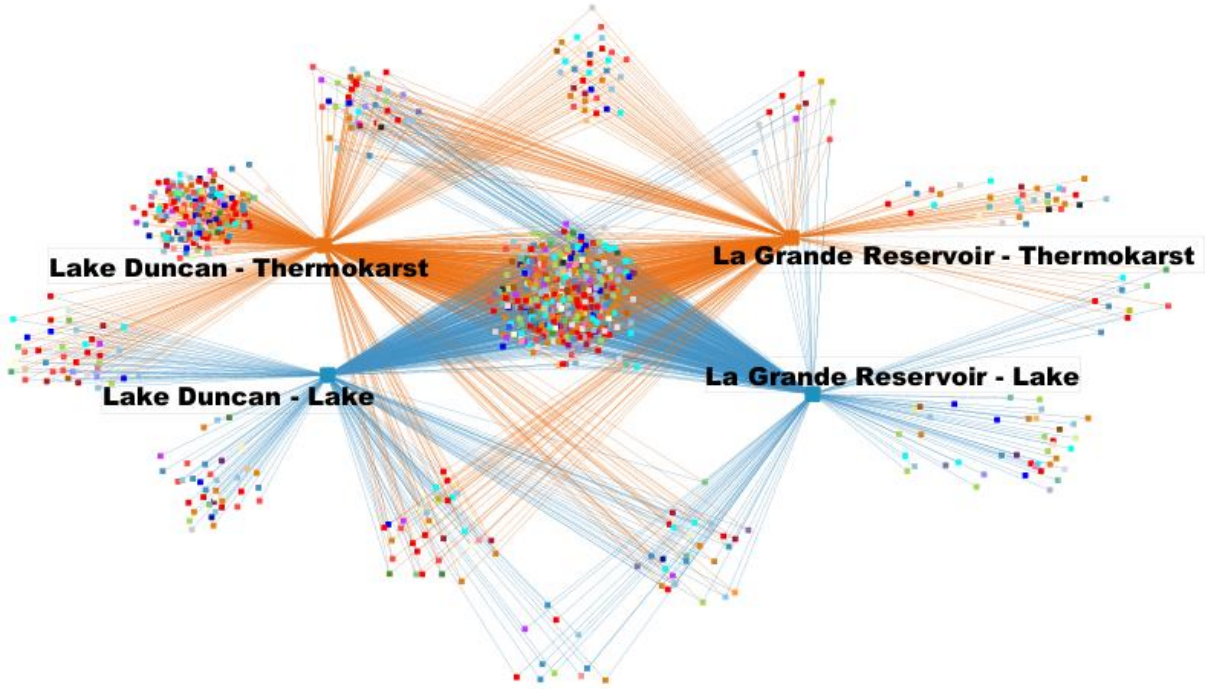

Figure 2: Habitats and sites share similar microbial composition. Nodes are individual microbial Families (N = 349 families) colored by Class. Lines indicate occurrence in either thermokarst (orange) or lake (blue) sites.

Microbes consumption of DOM suggests greater degradation potential of lake microbes

Microbes transformed both DOM sources to be more oxidized, unsaturated, and energetically depleted regardless of origin. Relative to the controls, both lake and thermokarst microbial communities caused consistent decreases in H:C towards more unsaturated or aromatic compounds. With lake DOM, the lake and thermokarst microbial treatments reduced H:C, on average, by 7.2% ($t = 3.51$, $df = 29$, $p = 0.004$) and 5.3% ($t = 2.99$, $df = 29$, $p = 0.015$), respectively (Figure 3a). The same pattern was observed under thermokarst DOM, where the H:C ratio declined, on average, by 4.9% with lake microbes ($t = 2.63$, $df = 29$, $p = 0.035$) and 5.9% with thermokarst microbes ($t = 3.05$, $df = 29$, $p = 0.013$) relative to the control. For O:C, only the more energetically favorable thermokarst DOM, as indicated by its lower GFE (Table

2), became even more oxidised during the incubation (Figure 3b). However, this effect only arose with the lake but not thermokarst microbial inoculum (Table 2).

The shifts in elemental composition were accompanied by changes in thermodynamic favourability (Figures 4c, d). The NOSC values of lake DOM exposed to lake and thermokarst microbes were, on average, 100% ($t = -2.81$, $df = 29$, $p = 0.023$) and 88% ($t = -2.63$, $df = 29$, $p = 0.035$) higher than the control, respectively. On thermokarst DOM exposed to lake and thermokarst microbes, NOSC was elevated by 191% ($t = -3.03$, $df = 29$, $p = 0.014$) and 222% ($t = -2.63$, $df = 29$, $p = 0.035$) respectively. GFE mirrored NOSC, showing an equal change in the opposite direction (Figure 3d). No other comparisons were statistically significant (Table 2).

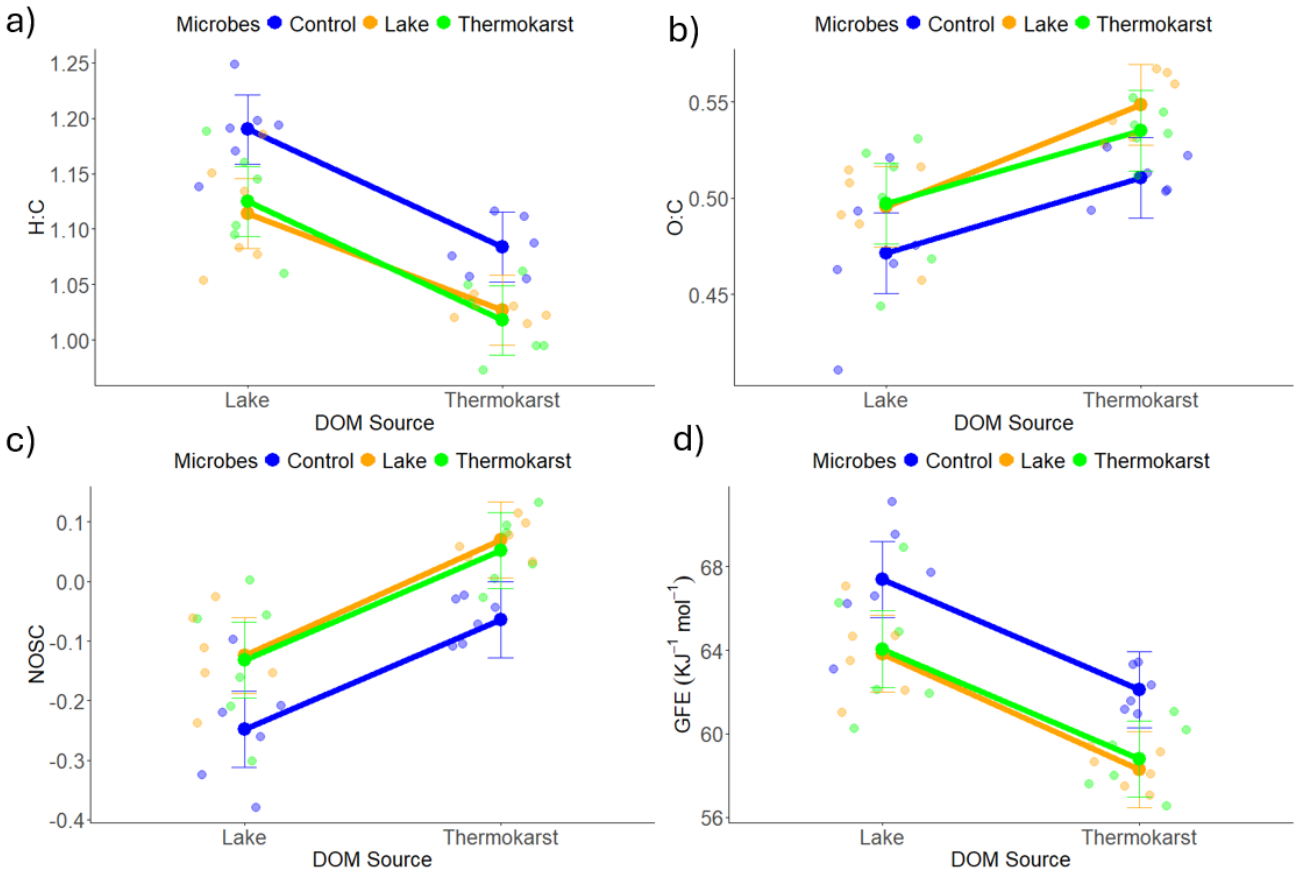

Figure 3: DOM became less bioavailable and more oxidized after biodegradation irrespective of both its origin and that of microbial communities. We measured the (a) hydrogen-to-carbon ratio (H:C), (b) oxygen-to-carbon ratio (O:C), (c) nominal oxidation state of carbon (NOSC), and (d) Gibbs Free Energy (GFE) in N = 36 bottles. Solid points are marginal means averaged across sites ± 95% confidence intervals estimated using the emmeans package in R. Lines indicate changes in means of each microbial treatment between the two DOM sources. Pairwise statistical comparisons were performed within each DOM source (see Table 2).

Table 2: Pairwise comparisons of changes in molecular properties among microbial treatments within DOM sources. Comparisons were averaged over the two sites (Lake Duncan and La Grande Reservoir) with marginal means estimated from a linear model. P-values were corrected for multiple differences with Tukey's honest significant differences. The Results column highlights which microbe treatment (control, lake, or thermokarst) had a higher value. Statistically significant differences ($p < 0.05$) were bolded. For all, degrees of freedom = 29.

Metric	DOM Source	Results	*t*-ratio	*p*-value
H:C	**Lake**	**Control > Lake**	**3.51**	**0.004**
H:C	**Lake**	**Control > Thermokarst**	**2.99**	**0.015**
H:C	Lake	Lake < Thermokarst	-0.51	0.865
H:C	**Thermokarst**	**Control > Lake**	**2.63**	**0.035**
H:C	**Thermokarst**	**Control > Thermokarst**	**3.05**	**0.013**
H:C	Thermokarst	Lake > Thermokarst	0.42	0.908
O:C	Lake	Control < Lake	-1.67	0.232
O:C	Lake	Control < Thermokarst	-1.77	0.196
O:C	Lake	Lake < Thermokarst	-0.10	0.995
O:C	**Thermokarst**	**Control < Lake**	**-2.64**	**0.035**
O:C	Thermokarst	Control < Thermokarst	-1.71	0.220
O:C	Thermokarst	Lake > Thermokarst	0.93	0.626
NOSC	**Lake**	**Control < Lake**	**-2.81**	**0.023**
NOSC	**Lake**	**Control < Thermokarst**	**-2.63**	**0.035**
NOSC	Lake	Lake > Thermokarst	0.17	0.983
NOSC	**Thermokarst**	**Control < Lake**	**-3.03**	**0.014**
NOSC	**Thermokarst**	**Control < Thermokarst**	**-2.63**	**0.035**
NOSC	Thermokarst	Lake > Thermokarst	0.41	0.914
GFE	**Lake**	**Control > Lake**	**2.81**	**0.023**
GFE	**Lake**	**Control > Thermokarst**	**2.63**	**0.035**
GFE	Lake	Lake < Thermokarst	-0.17	0.983
GFE	**Thermokarst**	**Control > Lake**	**3.03**	**0.014**
GFE	**Thermokarst**	**Control > Thermokarst**	**2.63**	**0.035**
GFE	Thermokarst	Lake < Thermokarst	-0.41	0.914

AI_{Mod}	Lake	Control < Lake	-1.45	0.329
AI_{Mod}	Lake	Control < Thermokarst	-1.26	0.426
AI_{Mod}	Lake	Lake > Thermokarst	0.19	0.981
AI_{Mod}	Thermokarst	Control > Lake	0.59	0.828
AI_{Mod}	Thermokarst	Control < Thermokarst	-0.65	0.795
AI_{Mod}	Thermokarst	Lake < Thermokarst	-1.24	0.442

Changes in optical properties were only observed when lake microbes were exposed to thermokarst DOM (Table 3). CDOM absorbance decreased by 3480%, on average, when thermokarst DOM was incubated with lake microbes compared to the no microbe control treatment ($t = 4.40$, $df = 53$, $p < 0.001$). Additionally, lake microbes showed, on average, a 316% decrease compared to the thermokarst microbes ($t = –3.44$, $df = 53$, $p = 0.003$) (Figure 4a). Similarly, the SR_{Helms} of thermokarst DOM increased by 128%, on average, when exposed to lake microbes compared to the control treatment ($t = -2.96$, $df = 53$, $p = 0.013$) indicating a shift towards more microbial-processed DOM. The CDOM of lake microbe treatments also showed, on average, a 111% increase compared to the of thermokarst microbes ($t = 2.78$, $df = 53$, $p = 0.021$) (Figure 4b). No other treatments had statistically significant effects (Table 3).

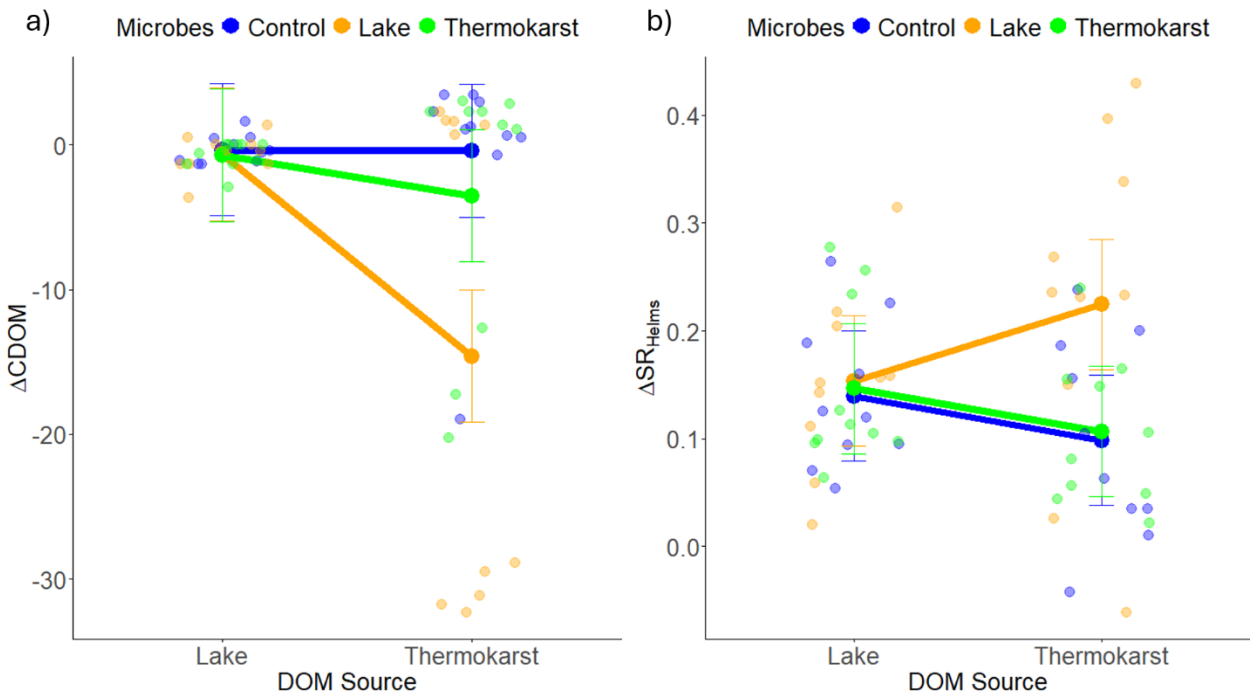

Figure 4: Lake microbial communities changed the optical properties of thermokarst DOM. We calculated changes in (a) chromophoric dissolved organic matter (CDOM) and (b) the Helms slope ratio (SR_{Helms}) between the start and end of a three-day incubation. Points represent N = 30 replicates per site. Solid points are marginal means ± 95% confidence intervals averaged across sites and estimated using the emmeans package in R. Lines indicate changes in means of each microbial treatment between the two DOM sources. Pairwise statistical comparisons were performed within each DOM source (see Table 3).

Table 3: Pairwise comparisons of changes in DOM optical properties among microbial treatments within DOM sources. Comparisons were averaged over the two sites (Lake Duncan and La Grande Reservoir) with marginal means estimated from a linear model. P-values were corrected for multiple comparisons with Tukey's honest significant differences. Results column highlights which microbe type (control, lake, or thermokarst) had a higher value. Statistically significant differences ($p < 0.05$) were bolded. For all, degrees of freedom = 53.

Metric	DOM source	Results	*t-ratio*	*p-value*
CDOM	Lake	Control < Lake	0.10	0.994
CDOM	Lake	Control < Thermokarst	0.12	0.992
CDOM	Lake	Lake < Thermokarst	0.02	0.999
CDOM	**Thermokarst**	**Control < Lake**	**4.40**	**<0.001**
CDOM	Thermokarst	Control < Thermokarst	0.96	0.605
CDOM	**Thermokarst**	**Lake > Thermokarst**	**-3.44**	**0.003**

Helms	Lake	Control > Lake	-0.33	0.944
Helms	Lake	Control > Thermokarst	-0.17	0.985
Helms	Lake	Lake > Thermokarst	-0.16	0.986
Helms	**Thermokarst**	**Control > Lake**	**-2.96**	**0.013**
Helms	Thermokarst	Control > Thermokarst	-0.19	0.981
Helms	**Thermokarst**	**Lake < Thermokarst**	**2.78**	**0.021**

Thermokarst DOM results in higher carbon emissions when exposed to novel microbes

Only microbial additions to thermokarst DOM influenced greenhouse gas emissions. Within thermokarst DOM, lake microbes increased CO_2 emissions by 184%, on average, compared to the control treatment ($t = -3.25$, $df = 51$, $p = 0.006$, Figure 5a), consistent with the degradation of the labile DOM (Figure 3). By contrast, CH_4 emissions decreased by 90%, on average, with lake microbes relative to the control treatment ($t = 3.55$, $df = 51$, $p = 0.002$), consistent with the higher proportion of methanotrophic bacteria in Lake Duncan compared to Lake Duncan thermokarst (0.63 and 0.38%, respectively). There were no other differences in greenhouse gas emissions between treatments (Table 4). CO_2 findings, coupled with DOM composition and optical properties analysis indicate that while thermokarst DOM may be more oxidized and energetically favorable (LaRowe & Van Cappellen, 2011). Thermokarst DOM is poorly assimilated by non-native microbial communities, and even native communities degrade it inefficiently, resulting in elevated CO_2 emissions and low carbon use efficiency. By contrast, thermokarst microbes responded more modestly when incubated with thermokarst DOM. They showed some CO_2 respiration but to a lesser extent compared to lake DOM.

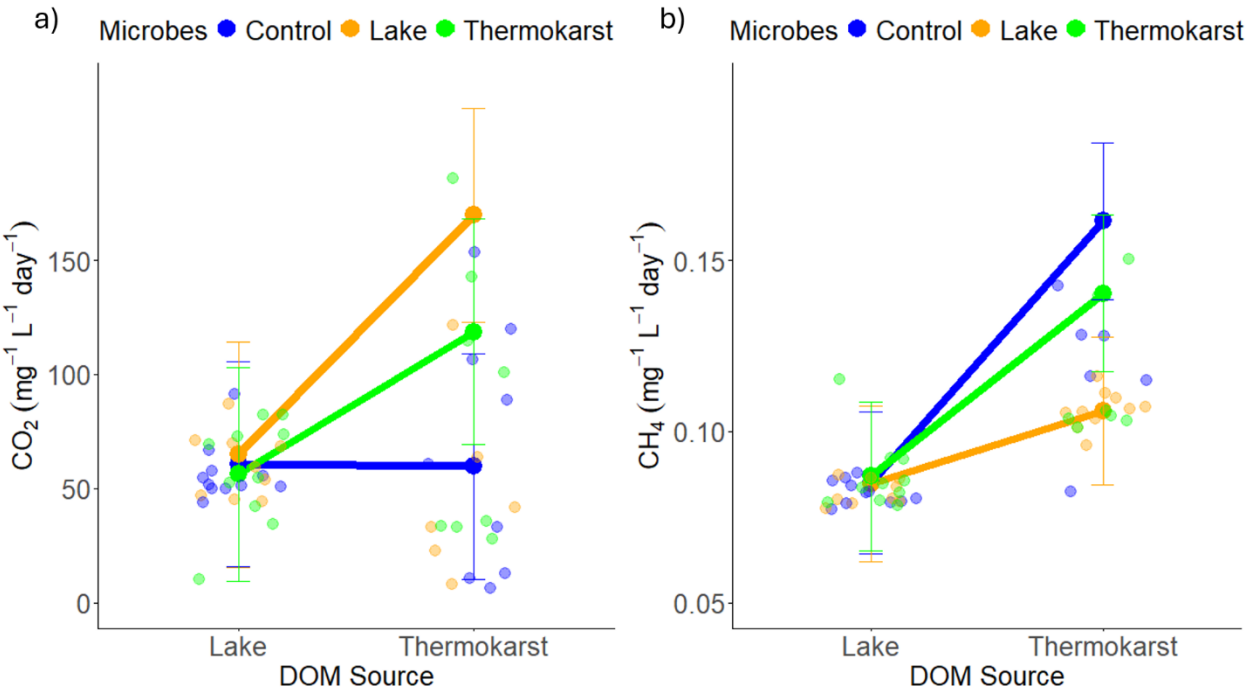

Figure 5*:* Lake microbes change greenhouse gas emissions when exposed to thermokarst DOM. We measured (a) CO_2 and (b) CH_4 production rates (mg L^{-1} day^{-1}). Points represent N = 59 replicates per site. Solid points are marginal means ± 95% confidence intervals averaged across sites estimated using the emmeans package in R. Lines indicate changes in means of each microbial treatment between the two DOM sources. Pairwise statistical comparisons were performed within each DOM source (see Table 4).

Table 4: Pairwise comparisons of CO_2 and CH_4 among microbial treatments within DOM sources. Comparisons were averaged over the two sites (Lake Duncan and La Grande Reservoir) with marginal means estimated from a linear model. P-values were corrected for multiple comparisons with Tukey's honest significant differences. Results column highlights which microbe type (control, lake, or thermokarst) had a higher value. Statistically significant differences ($p < 0.05$) were bolded. For all, degrees of freedom = 51.

Gas	DOM source	Results	t-ratio	p-value
CO_2	Lake	Control < Lake	-0.12	0.992
CO_2	Lake	Control > Thermokarst	0.14	0.999
CO_2	Lake	Lake > Thermokarst	0.25	0.966
CO_2	**Thermokarst**	**Control < Lake**	**-3.25**	**0.006**
CO_2	Thermokarst	Control < Thermokarst	-1.69	0.217
CO_2	Thermokarst	Lake > Thermokarst	1.51	0.296
CH_4	Lake	Control > Lake	0.02	0.999
CH_4	Lake	Control < Thermokarst	-0.13	0.991

CH_4	Lake	Lake < Thermokarst	-0.14	0.989
CH_4	**Thermokarst**	**Control > Lake**	**3.55**	**0.002**
CH_4	Thermokarst	Control > Thermokarst	1.31	0.395
CH_4	Thermokarst	Lake < Thermokarst	-2.20	0.081

As expected, given differences in DOM composition, lake microbes respired more when exposed to thermokarst DOM. This increased respiration is unlikely to be solely driven by methanotrophy, as our results only showed higher methanotroph abundance, not activity. Instead, we found that lake microbes inefficiently utilized thermokarst DOM (Figure 5a, b). In the control treatments with no microbes, cell abundance was a mean ± standard error of 643.3 ± 159.6 cells mL^{-1} at the end of the experiment across all treatments, confirming that we managed to remove most particles through filtration. By contrast, cell abundances were 81,097 ± 35,326 mL^{-1} and 51,094 ± 14,499 cells mL^{-1} in the treatments with lake and thermokarst microbes, respectively. However, lake microbes grew, on average, 42% more slowly compared to the communities remaining in the control ($t = 4.71$, $df = 41$, $p < 0.001$). Cell growth was also 52% lower, on average, in lake microbes compared to thermokarst microbes when incubated with thermokarst DOM ($t = –3.16$, $df = 41$, $p = 0.008$). In comparison, growth efficiency in lake microbes decreased ($t = -2.79$, $df = 41$, $p = 0021$) (Figure 5b). Thermokarst microbes did not change in cell abundance, which, together with the CO_2 findings, suggests they may follow a more specialized strategy compared to lake microbes. Aside from the statistically significant differences noted above, other comparisons were not statistically significant (Table 5).

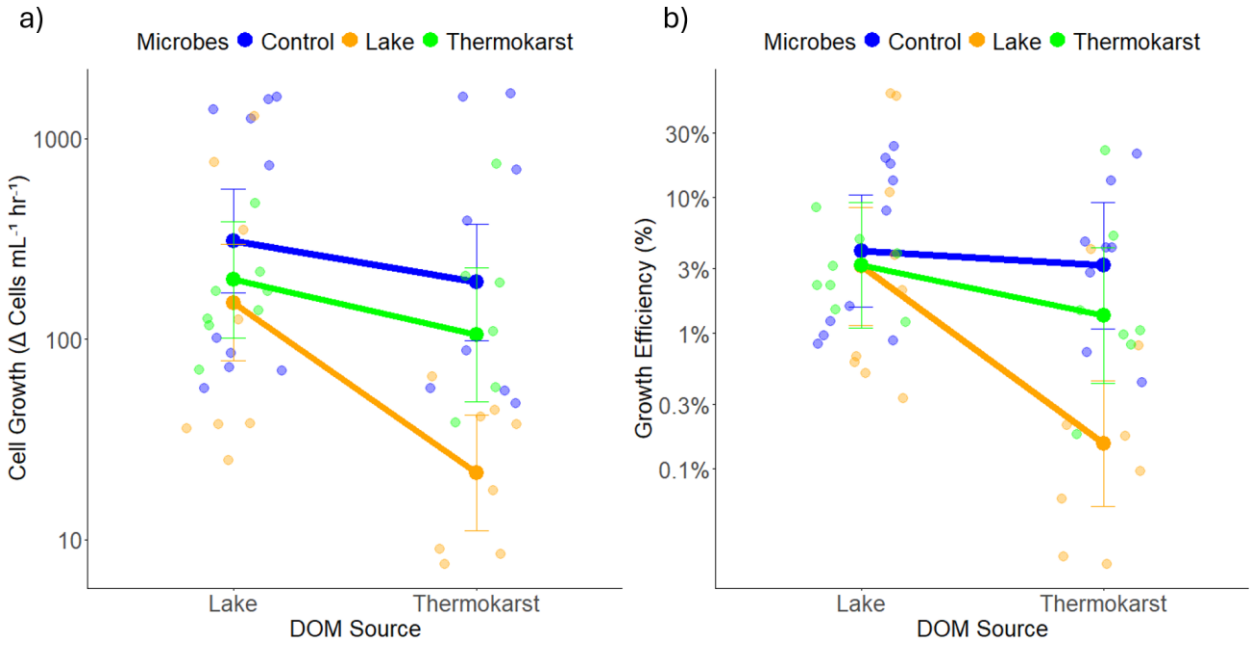

Figure 6: Lake microbes poorly utilize thermokarst DOM. (a) Cell growth shown as changes in cell number over the incubation period. (b) Growth efficiency expressed in terms of carbon used for biomass growth relative to the sum of carbon allocated to the sum of biomass and respiration. Points represent N = 30 replicates per site. Solid points are marginal means ± 95% confidence intervals averaged across sites estimated using the emmeans package in R. Lines indicate changes in means of each microbial treatment between the two DOM sources. Pairwise statistical comparisons were performed within each DOM source (see Table 5).

Table 5: Pairwise comparisons of cell growth and microbial growth efficiency between microbial treatments within each DOM source. Comparisons are averaged over the two sites (Lake Duncan and La Grande Reservoir) based on marginal means estimated from a linear model. P-values were corrected for multiple comparisons using Tukey's honest significant differences. Results column highlights which microbial treatment had a higher value. Statistically significant differences ($p < 0.05$) were bolded. For all, degrees of freedom = 41.

Metric	DOM source	Results	t-ratio	p-value
Cell Growth	Lake	Control > Lake	1.60	0.256
Cell Growth	Lake	Control > Thermokarst	1.01	0.576
Cell Growth	Lake	Lake < Thermokarst	-0.56	0.840
Cell Growth	**Thermokarst**	**Control > Lake**	**4.71**	<0.001
Cell Growth	Thermokarst	Control > Thermokarst	1.20	0.458
Cell Growth	**Thermokarst**	**Lake < Thermokarst**	**-3.16**	0.008
Growth Efficiency	Lake	Control > Lake	0.38	0.923
Growth Efficiency	Lake	Control > Thermokarst	0.35	0.934

Growth Efficiency	Lake	Lake < Thermokarst	-0.01	0.999
Growth Efficiency	**Thermokarst**	**Control > Lake**	**4.04**	<0.001
Growth Efficiency	Thermokarst	Control > Thermokarst	1.10	0.5176
Growth Efficiency	**Thermokarst**	**Lake < Thermokarst**	**-2.79**	0.021

Discussion

Our results show that mismatches between microbial metabolic capabilities and the molecular properties of thermokarst DOM can lead to inefficient carbon use, elevating CO_2 emissions without corresponding to microbial growth (LaRowe & Van Cappellen, 2011; Ward et al., 2017; Winder et al., 2023). When exposed to thermokarst DOM, lake microbes were unable to grow and were inefficient at using the available DOM. In general, thermokarst DOM contains compounds that can provide energy to microbes, but those compounds are often hard to access (Abbott et al., 2014; Vonk et al., 2015). Our results found that lake microbes inefficiently extracted usable energy from thermokarst DOM, highlighted by the 3× higher CO_2 emission in thermokarst DOM than in lake DOM and the lower growth efficiency (Guillemette et al., 2016). By contrast in lake DOM, thermokarst microbes did not emit more CO_2 than the control, suggesting they were unable to oxidize or use lake DOM as an energy source. These contrasting responses highlight how mismatches between DOM quality and microbial traits can amplify CO_2 emissions from thawing permafrost carbon, with implications for carbon cycling in northern lakes.

Both lake and thermokarst microbes altered DOM composition but their responses depended on the DOM source. Lake microbes emitted more CO_2 and degraded more CDOM than thermokarst microbes, but at the cost of low growth efficiency. This pattern may reflect how lake microbes experience diverse and dynamic DOM inputs from multiple sources (Amelia et al.,

2018; Hu et al., 2022; Hu et al., 2023; Ruben et al., 2024), equipping them with broad enzymatic repertoires that enable them to degrade unfamiliar substrates. On the other hand, thermokarst microbes, which originate from permafrost environments, are adapted to a consistent and a relatively small pool of complex DOM (Bruhn et al., Starr et al., 2025). Thermokarst microbes showed no statistically significant change in cell abundance across DOM sources and emitted less CO_2 than lake microbes. These patterns are consistent with a more limited metabolic response to the DOM sources tested, which may reflect specialization for a narrower range of substrates (Mackelprang et al., 2011, 2017; Woodcroft et al., 2018). Thermokarst DOM is typically enriched in complex, aromatic, and highly oxidized compounds that provide limited accessible energy, favoring microbial communities adapted to metabolize a narrower suite of substrates (Abbott et al., 2014; Vonk et al., 2015). These patterns suggest that differences in the capacity of lake and thermokarst microbes to adapt to unfamiliar DOM sources may influence how organic matter is degraded in thawed permafrost ecosystems.

The scope of our experiment was constrained by both the short incubation duration and the use of warm, oxic conditions, which differ from the cold, anoxic environments typical of thermokarst systems, potentially biasing our observations toward faster, aerobic processes and underrepresenting the slower, anaerobic carbon pathways that dominate in situ. Thermokarst ponds occur in permafrost regions where short summers, continuous meltwater inputs from thawing ice, and low solar heating keep water temperatures freezing for much of the year. In such environments, high organic matter inputs and stratification frequently lead to anoxia, while low temperatures slow metabolic rates and select for cold-adapted microbial taxa that may respond differently to DOM inputs (Coolen & Orsi, 2015; Mackelprang et al., 2017). This difference may have suppressed the activity of cold-adapted thermokarst microbial taxa, meaning

our incubations may underestimate their potential for DOM transformation and associated CO_2 or CH_4 emissions (Waldrop et al., 2023, 2024). Our three-day incubation also may not have fully captured early-phase metabolic responses from slow-growing microbes, particularly those adapted to low-resource, anaerobic conditions typical of thermokarst environments (Mackelprang et al., 2011). Previous studies suggest that incubations extending from two to six weeks are often required to capture the full spectrum of microbial responses to permafrost DOM, particularly the slower activation of anaerobic and resource-limited taxa (Abbott et al., 2014; Vonk et al., 2015). However, while longer incubations can reveal broader microbial dynamics such as syntrophy and methanogenesis (del Giorgio, 2008; Schink & Stams, 2013; Conrad, 2020), they also increase the risk of artificial shifts in community composition over time, i.e., bottle effects (Hammes et al., 2010). Thus, our relatively short incubation aimed to balance detection of microbial activity with minimization of these artifacts, though it likely underrepresents slower carbon processing pathways (Mach et al., 2015; Kevorkian et al., 2022). Lastly, the lack of DOC measurements limits our ability to identify the functional drivers of DOM degradation and track the full fate of carbon. These limitations highlight the need for better, more comprehensive measurements in the future.

Our study highlights an underappreciated mechanism by which greenhouse gases can be released: the low efficiency of microbes when exposed to novel, relatively recalcitrant DOM sources. Such mismatches between microbial metabolic capabilities and their organic substrates, arising from climate change, can elevate CO_2 release without corresponding microbial growth. In our experiment, thermokarst DOM was more oxidized and aromatic, traits associated with low lability and poor microbial growth efficiency (Kellerman et al., 2014, 2015; Guillemette et al., 2016), yet microbes still oxidized substantial amounts to CO_2. These characteristics, typical of

DOM from *Sphagnum*-dominated peatlands common in northern Canada (D'Andrilli et al., 2010; Saarela et al., 2022), help explain why respiration remained high despite limited biomass production. Complex aromatic compounds can be metabolized, but often via energy-intensive pathways that yield little biomass, leading to high respiration and low growth efficiency (Guillemette et al., 2016; Mostovaya et al., 2017). This effect has been observed elsewhere, with more labile DOM generally supporting greater microbial carbon use efficiency (D'Andrilli et al., 2023). Our findings underscore the need to move beyond bulk carbon inventories and account for microbial community composition and efficiency in carbon cycling models. Identifying which microbial communities promote carbon retention versus loss will improve predictions of permafrost-driven GHG emissions and inform climate mitigation strategies.

Appendix A

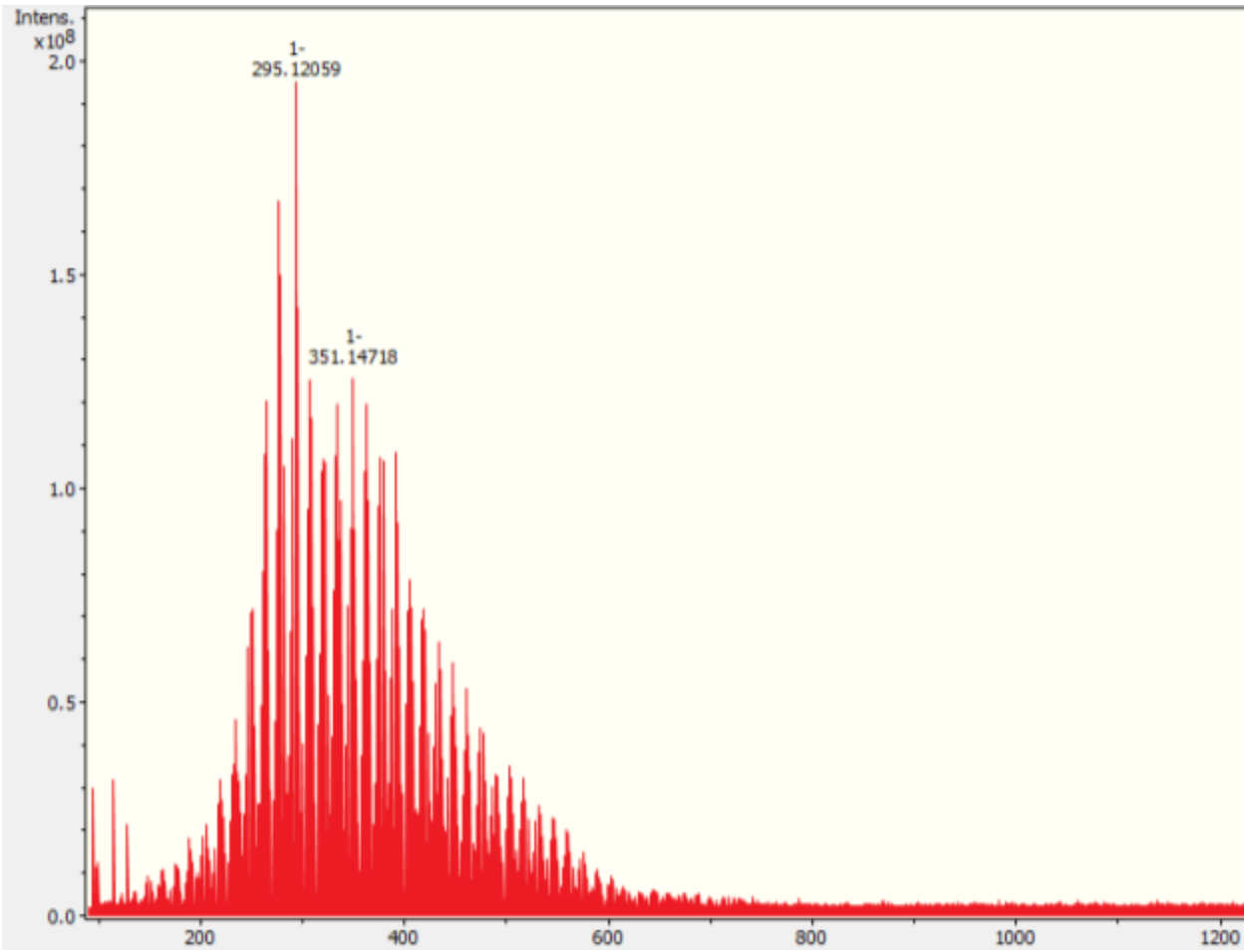

Figure A1: Example FT-ICR MS mass spectrum illustrating a peak distribution across the 100–1200 *m/z* range (example spectrum shown for illustrative purposes only).

Table A1: Microbial species common to both thermokarst ponds but absent from lakes.

Species	Family
Alterococcus agarolyticus	Alterococcaceae
Arenimonas maotaiensis	Lysobacteraceae
Argonema antarcticum	Oscillatoriaceae
Eubacterium yurii	Filifactoraceae
Euryhalinema mangrovii	Nodosilineaceae
Fundidesulfovibrio butyratiphilus	Desulfovibrionaceae
Geoalkalibacter subterraneus	Geoalkalibacteraceae
Gloeocapsopsis dulcis	Chroococcaceae
Glutamicibacter uratoxydans	Micrococcaceae
Haliangium ochraceum	Kofleriaceae
Haliplanktos anthonyquinnii	Chroococcidiopsidaceae
Halorhodospira halophila	Ectothiorhodospiraceae
Hansschlegelia zhihuaiae	Methylopilaceae
Horticoccus luteus	Opitutaceae
Howardella ureilytica	Eubacteriales incertae sedis
Hyphomicrobium album	Hyphomicrobiaceae
Micromonospora coerulea	Micromonosporaceae
Mycoplasma iguanae	Mycoplasmataceae
Niameybacter massiliensis	Lachnospiraceae
Oligosphaera ethanolica	Oligosphaeraceae
Paludibacterium denitrificans	Chromobacteriaceae
Pelotomaculum isophthalicicum	Desulfotomaculaceae
Peribacillus frigoritolerans	Bacillaceae
Rhodanobacter koreensis	Rhodanobacteraceae
Roseiarcus fermentans	Roseiarcaceae
Rubritepida flocculans	Roseomonadaceae
Ructibacterium gallinarum	Oscillospiraceae

Saccharopolyspora rectivirgula	Pseudonocardiaceae
Soehngenia saccharolytica	Tissierellaceae
Streptomyces dysideae	Streptomycetaceae
Sulfuriferula nivalis	Sulfuricellaceae
Symmachiella macrocystis	Planctomycetaceae
Thermodesulfobium narugense	Thermodesulfobiaceae
Thermogemmatispora foliorum	Thermogemmatisporaceae
Thioalkalivibrio halophilus	Ectothiorhodospiraceae

Table A2: Microbial species common to both lakes but absent from thermokarst ponds.

Species	Family
Anaerobacterium chartisolvens	Oscillospiraceae
Clostridium pasteurianum	Clostridiaceae
Geobacter sulfurreducens	Geobacteraceae
Helicovermis profundi	Clostridia incertae sedis
Herbaspirillum seropedicae	Oxalobacteraceae
Hyphomicrobium aestuarii	Hyphomicrobiaceae
Paraburkholderia oxyphila	Burkholderiaceae
Piscinibacter aquaticus	Sphaerotilaceae
Symmachiella dynata	Planctomycetaceae
Thiohalorhabdus denitrificans	Thiohalorhabdaceae
Tistrella bauzanensis	Geminicoccaceae

Supplementary Data 1: Species read counts (≥80% ID, negative control removed) with associated families. Available as Supplementary_Data_1_All_Species_Reads_80_families.csv.

References

Abbott, B. W., Larouche, J. R., Jones, J. B., Bowden, W. B., & Balser, A. W. (2014). Elevated dissolved organic carbon biodegradability from thawing and collapsing permafrost. *Journal of Geophysical Research: Biogeosciences*, *119*(10), 2049–2063. https://doi.org/10.1002/2014JG002678

Arrieta, J. M., Mayol, E., Hansman, R. L., Herndl, G. J., Dittmar, T., & Duarte, C. M. (2015). Dilution limits dissolved organic carbon utilization in the deep ocean. *Science*, 348(6232), 331–333. https://doi.org/10.1126/science.1258955

Battin, T. J., Kaplan, L. A., Findlay, S., Hopkinson, C. S., Marti, E., Packman, A. I., Newbold, J. D., & Sabater, F. (2008). Biophysical controls on organic carbon fluxes in fluvial networks. *Nature Geoscience*, 1(2), 95–100. https://doi.org/10.1038/ngeo101

Bramer, L., White, A., Thompson, A., & McCue, L. A. (2025). Introduction to ftmsRanalysis. https://emsl-computing.github.io/ftmsRanalysis/articles/ftmsRanalysis.html

Bruhn, A. D., Stedmon, C. A., Comte, J., Matsuoka, A., Speetjens, N. J., Tanski, G., Vonk, J. E., & Sjöstedt, J. (2021). Terrestrial dissolved organic matter mobilized from eroding permafrost controls microbial community composition and growth in arctic coastal zones. *Frontiers in Earth Science*, 9. https://doi.org/10.3389/feart.2021.640580

Burkert, A., Douglas, T. A., Waldrop, M. P., & Mackelprang, R. (2019). Changes in the active, dead, and dormant microbial community structure across a pleistocene permafrost chronosequence. *Applied and Environmental Microbiology*, 85(7), e02646-18. https://doi.org/10.1128/AEM.02646-18

Chen, Y., Senesi, N., & Schnitzer, M. (1977). Information provided on humic substances by e4/e6 ratios. *Soil Science Society of America Journal*, 41(2), 352–358. https://doi.org/10.2136/sssaj1977.03615995004100020037x

Connon, R. F., Quinton, W. L., Craig, J. R., & Hayashi, M. (2014). Changing hydrologic connectivity due to permafrost thaw in the lower Liard River valley, NWT, Canada. *Hydrological Processes*, 28(14), 4163–4178. https://doi.org/10.1002/hyp.10206

Conrad, R. (2020). Methane production in soil environments—Anaerobic biogeochemistry and microbial life between flooding and desiccation. *Microorganisms*, *8*(6), 881. https://doi.org/10.3390/microorganisms8060881

Coolen, M. J., & Orsi, W. D. (2015). The transcriptional response of microbial communities in thawing Alaskan permafrost soils. *Frontiers in Microbiology*, 6, 197.

D'Andrilli, J., Chanton, J. P., Glaser, P. H., & Cooper, W. T. (2010). Characterization of dissolved organic matter in northern peatland soil porewaters by ultra high-resolution mass

spectrometry. *Organic Geochemistry*, *41*(8), 791–799. https://doi.org/10.1016/j.orggeochem.2010.05.009

D'Andrilli, J., Cooper, W. T., Foreman, C. M., & Marshall, A. G. (2015). An ultrahigh-resolution mass spectrometry index to estimate natural organic matter lability. *Rapid Communications in Mass Spectrometry*, 29(24), 2385–2401. https://doi.org/10.1002/rcm.7400=

D'Andrilli, J., Romero, C. M., Zito, P., Podgorski, D. C., Payn, R. A., Sebestyen, S. D., Zimmerman, A. R., & Rosario-Ortiz, F. L. (2023). Advancing chemical lability assessments of organic matter using a synthesis of FT-ICR MS data across diverse environments and experiments. *Organic Geochemistry*, 184, 104667. https://doi.org/10.1016/j.orggeochem.2023.104667

De Haan, H., & De Boer, T. (1987). Applicability of light absorbance and fluorescence as measures of concentration and molecular size of dissolved organic carbon in humic Lake Tjeukemeer. *Water Research*, 21(6), 731–734. https://doi.org/10.1016/0043-1354(87)90086-8

Del Giorgio, P. A., & Gasol, J. M. (2008). Physiological structure and single-cell activity in marine bacterioplankton. *Microbial Ecology of the Oceans*, 243-298.

Dittmar, T., Koch, B., Hertkorn, N., & Kattner, G. (2008). A simple and efficient method for the solid-phase extraction of dissolved organic matter (Spe-dom) from seawater. *Limnology and Oceanography: Methods*, *6*(6), 230–235. https://doi.org/10.4319/lom.2008.6.230

Drake, T. W., Raymond, P. A., & Spencer, R. G. M. (2018). Terrestrial carbon inputs to in land waters: A current synthesis of estimates and uncertainty. *Limnology and Oceanography* | Letters, 3(3), 132–142. https://doi.org/10.1002/lol2.10055

Dumont, M. G., & Murrell, J. C. (2005). Community-level analysis: Key genes of aerobic methane oxidation. In *Methods in Enzymology* (Vol. 397, pp. 413–427). Academic Press. https://doi.org/10.1016/S0076-6879(05)97025-0

Estop-Aragonés, C., Olefeldt, D., Abbott, B. W., Chanton, J. P., Czimczik, C. I., Dean, J. F., Egan, J. E., Gandois, L., Garnett, M. H., Hartley, I. P., Hoyt, A., Lupascu, M., Natali, S. M., O'Donnell, J. A., Raymond, P. A., Tanentzap, A. J., Tank, S. E., Schuur, E. A. G., Turetsky, M., & Anthony, K. W. (2020). Assessing the potential for mobilization of old soil carbon after permafrost thaw: A synthesis of14 c measurements from the northern permafrost region. *Global Biogeochemical Cycles*, 34(9), e2020GB006672. https://doi.org/10.1029/2020GB006672

Fasching, C., Behounek, B., Singer, G. A., & Battin, T. J. (2014). Microbial degradation of terrigenous dissolved organic matter and potential consequences for carbon

cycling in brown-water streams. *Scientific Reports*, 4(1), 4981. https://doi.org/10.1038/srep04981

Fagerbakke, K., Heldal, M., & Norland, S. (1996). Content of carbon, nitrogen, oxygen, sulfur and phosphorus in native aquatic and cultured bacteria. *Aquatic Microbial Ecology*, 10, 15–27. https://doi.org/10.3354/ame010015

Fellman, J. B., Hood, E., & Spencer, R. G. M. (2010). Fluorescence spectroscopy opens new windows into dissolved organic matter dynamics in freshwater ecosystems: A review. *Limnology and Oceanography*, 55(6), 2452–2462. https://doi.org/10.4319/lo.2010.55.6.2452

Francisco, D. E., Mah, R. A., & Rabin, A. C. (1973). Acridine orange-epifluorescence technique for counting bacteria in natural waters. *Transactions of the American Microscopical Society*, *92*(3), 416. https://doi.org/10.2307/3225245

Graham, D. E., Wallenstein, M. D., Vishnivetskaya, T. A., Waldrop, M. P., Phelps, T. J., Pfiffner, S. M., Onstott, T. C., Whyte, L. G., Rivkina, E. M., Gilichinsky, D. A., Elias, D. A., Mackelprang, R., VerBerkmoes, N. C., Hettich, R. L., Wagner, D. Wullschleger, S. D., & Jansson, J. K. (2012). Microbes in thawing permafrost: The unknown variable in the climate change equation. *The ISME Journal,* 6(4), 709–712. https://doi.org/10.1038/ismej.2011.163

Guillemette, F., & Del Giorgio, P. A. (2011). Reconstructing the various facets of dissolved organic carbon bioavailability in freshwater ecosystems. *Limnology and Oceanography*, *56*(2), 734–748. https://doi.org/10.4319/lo.2011.56.2.0734

Guillemette, F., Leigh McCallister, S., & del Giorgio, P. A. (2016). Selective consumption and metabolic allocation of terrestrial and algal carbon determine allochthony in lake bacteria. *The ISME Journal*, 10(6), 1373–1382. https://doi.org/10.1038/ismej.2015.215

Hammes, F., Vital, M., & Egli, T. (2010). Critical evaluation of the volumetric "bottle effect" on microbial batch growth. *Applied and Environmental Microbiology*, *76*(4), 1278–1281. https://doi.org/10.1128/AEM.01914-09

Helms, J. R., Stubbins, A., Ritchie, J. D., Minor, E. C., Kieber, D. J., & Mopper, K. (2008). Absorption spectral slopes and slope ratios as indicators of molecular weight, source, and photobleaching of chromophoric dissolved organic matter. *Limnology and Oceanography*, 53(3), 955–969. https://doi.org/10.4319/lo.2008.53.3.0955

Hu, A., Jang, K.-S., Meng, F., Stegen, J., Tanentzap, A. J., Choi, M., Lennon, J. T., Soininen, J., & Wang, J. (2022). Microbial and environmental processes shape the link between organic matter functional traits and composition. *Environmental*

Science & Technology, 56(14), 10504–10516. https://doi.org/10.1021/acs.est.2c01432

Hu, J., Kang, L., Li, Z., Feng, X., Liang, C., Wu, Z., Zhou, W., Liu, X., Yang, Y., & Chen, L. (2023). Photo-produced aromatic compounds stimulate microbial degradation of dissolved organic carbon in thermokarst lakes. *Nature Communications*, 14(1), 3681. https://doi.org/10.1038/s41467-023-39432-2

Hugelius, G., Bockheim, J. G., Camill, P., Elberling, B., Grosse, G., Harden, J. W., Johnson, K., Jorgenson, T., Koven, C. D., Kuhry, P., Michaelson, G., Mishra, U., Palmtag, J., Ping, C.-L., O'Donnell, J., Schirrmeister, L., Schuur, E. A. G., Sheng, Y., Smith, L. C., … Yu,Z. (2013). A new data set for estimating organic carbon storage to 3 m depth in soils of the northern circumpolar permafrost region. *Earth System Science Data*, 5(2), 393–402. https://doi.org/10.5194/essd-5-393-2013

Hugelius, G., Strauss, J., Zubrzycki, S., Harden, J. W., Schuur, E. a. G., Ping, C.-L., Schirrmeister, L., Grosse, G., Michaelson, G. J., Koven, C. D., O'Donnell, J. A., Elberling, B., Mishra, U., Camill, P., Yu, Z., Palmtag, J., & Kuhry, P. (2014). Estimated stocks of circumpolar permafrost carbon with quantified uncertainty ranges and identified data gaps. *Biogeosciences*, *11*(23), 6573–6593. https://doi.org/10.5194/bg-11-6573-2014

Hugelius, G., Loisel, J., Chadburn, S., Jackson, R. B., Jones, M., MacDonald, G., Marushchak, M., Olefeldt, D., Packalen, M., Siewert, M. B., Treat, C., Turetsk M., Voigt, C., & Yu, Z. (2020). Large stocks of peatland carbon and nitrogen are vulnerable to permafrost thaw. *Proceedings of the National Academy of Sciences* 117(34), 2043820446. https://doi.org/10.1073/pnas.1916387117

Judd, K. E., Crump, B. C., & Kling, G. W. (2006). Variation in dissolved organic matter controls bacterial production and community composition. Ecology, 87(8), 2068 –2079. https://doi.org/10.1890/0012-9658(2006)87[2068:VIDOMC]2.0.CO;2

Kellerman, A. M., Kothawala, D. N., Dittmar, T., & Tranvik, L. J. (2015). Molecular dissolved organic matter composition in lakes across Sweden as relative intensities of FT-ICR MS peaks and PARAFAC components and optical indices. 2 datasets. https://doi.org/10.1594/PANGAEA.844884

Kellerman, A. M., Dittmar, T., Kothawala, D. N., & Tranvik, L. J. (2014). Chemodiversity of dissolved organic matter in lakes driven by climate and Hydrology. *Nature Communications*, 5(1). https://doi.org/10.1038/ncomms4804

Kevorkian, R. T., Sipes, K., Winstead, R., Paul, R., & Lloyd, K. G. (2022). Cryptic methane-cycling by methanogens during multi-year incubation of estuarine sediment. *Frontiers in Microbiology*, *13*, 847563. https://doi.org/10.3389/fmicb.2022.847563

Kim, S., Kramer, R. W., & Hatcher, P. G. (2003). Graphical method for analysis of ultrahigh-resolution broadband mass spectra of natural organic matter, the van krevelen diagram. *Analytical Chemistry*, 75(20), 5336–5344. https://doi.org/10.1021/ac034415p

Koch, B. P., & Dittmar, T. (2006). From mass to structure: An aromaticity index for high-resolution mass data of natural organic matter. *Rapid Communications in Mass Spectrometry*, 20(5), 926–932. https://doi.org/10.1002/rcm.2386

Kuhn, M. K. A., Thompson, L. M., Winder, J. C., Braga, L. P., Tanentzap, A. J., Bastviken, D., & Olefeldt, D (2021). Opposing effects of climate and permafrost thaw on CH_4 and CO_2 emissions from Northern Lakes. *AGU Advances*, 2(4). https://doi.org/10.1029/2021av000515

LaRowe, D. E., & Van Cappellen, P. (2011). Degradation of natural organic matter: A thermodynamic analysis. *Geochimica et Cosmochimica Acta*, 75(8), 2030–2042. https://doi.org/10.1016/j.gca.2011.01.020

Lenth, R. V. (2024). emmeans: Estimated Marginal Means, aka Least-Squares Means. R package version 1.10.4. https://CRAN.R-project.org/package=emmeans

Mach, V., Blaser, M. B., Claus, P., Chaudhary, P. P., & RulÃk, M. (2015). Methane production potentials, pathways, and communities of methanogens in vertical sediment profiles of river Sitka. *Frontiers in Microbiology*, *6*. https://doi.org/10.3389/fmicb.2015.00506

Mackelprang, R., Waldrop, M. P., DeAngelis, K. M., David, M. M., Chavarria, K. L., Blazewicz, S. J., Rubin, E. M., & Jansson, J. K. (2011). Metagenomic analysis of a permafrost microbial community reveals a rapid response to thaw. *Nature*, 480 (7377), 368–371. https://doi.org/10.1038/nature10576

Mackelprang, R., Burkert, A., Haw, M., Mahendrarajah, T., Conaway, C. H., Douglas, T.A., & Waldrop, M. P. (2017). Microbial survival strategies in ancient permafrost: Insights from metagenomics. *The ISME Journa*l, 11(10), 2305–2318. https://doi.org/10.1038/ismej.2017.93

Manies, K. L., Jones, M. C., Waldrop, M. P., Leewis, M., Fuller, C., Cornman, R. S., & Hoefke, K. (2021). Influence of permafrost type and site history on losses of permafrost carbon after thaw. *Journal of Geophysical Research*: Biogeosciences, 126(11), e2021JG006396. https://doi.org/10.1029/2021JG006396

Mayumi, D., Mochimaru, H., Tamaki, H., Yamamoto, K., Yoshioka, H., Suzuki, Y., Kamagata, Y., & Sakata, S. (2016). Methane production from coal by a single methanogen. *Science*, 354(6309), 222–225. https://doi.org/10.1126/science.aaf8821

Merder, J., Freund, J. A., Feudel, U., Hansen, C. T., Hawkes, J. A., Jacob, B., Klaproth, K., Niggemann, J., Noriega-Ortega, B. E., Osterholz, H., Rossel, P. E., Seidel, M.,

Singer, G., Stubbins, A., Waska, H., & Dittmar, T. (2020). ICBM-ocean: Processing ultrahigh-resolution mass spectrometry data of complex molecular mixtures. *Analytical Chemistry*, 92(10), 6832–6838. https://doi.org/10.1021/acs.analchem.9b05659

Mostovaya, A., Hawkes, J. A., Koehler, B., Dittmar, T., & Tranvik, L. J. (2017). Emergence of the reactivity continuum of organic matter from kinetics of a multitude of individual molecular constituents. *Environmental Science & Technology*, *51*(20), 11571–11579. https://doi.org/10.1021/acs.est.7b02876

O'Donnell, J. A., Aiken, G. R., Butler, K. D., Guillemette, F., Podgorski, D. C., & Spencer, R. G. (2016). DOM composition and transformation in boreal forest soils: The effects of temperature and organic-horizon decomposition state. Journal of Geophysical Research: *Biogeosciences*, 121(10), 2727–2744. https://doi.org/10.1002/2016jg003431

Olefeldt, D., Goswami, S., Grosse, G., Hayes, D., Hugelius, G., Kuhry, P., McGuire, A. D., Romanovsky, V. E., Sannel, A. B. K., Schuur, E. a. G., & Turetsky, M. R. (2016). Circumpolar distribution and carbon storage of thermokarst landscapes. *Nature Communications*, *7*(1), 13043. https://doi.org/10.1038/ncomms1304

Peacock, M., Freeman, C., Gauci, V., Lebron, I., & Evans, C. D. (2015). Investigations of freezing and cold storage for the analysis of peatland dissolved organic carbon (Doc) and absorbance properties. *Environmental Science: Processes & Impacts*, 17(7), 1290–1301. https://doi.org/10.1039/C5EM00126A

Ruben, M., Marchant, H., Wietz, M., Gentz, T., Strauss, J., Koch, B. P., & Mollenhauer, G. (2024). Microbial communities degrade ancient permafrost -derived organic matter in arctic seawater. *Journal of Geophysical Research: Biogeosciences*, 129(7), e2023JG007936. https://doi.org/10.1029/2023JG007936

Saarela, T., Zhu, X., Jäntti, H., Ohashi, M., Ide, J., Siljanen, H., Pesonen, A., Aaltonen, H., Ojala, A., Nishimura, H., Kekäläinen, T., Jänis, J., Berninger, F., & Pumpanen, J. (2022). Dissolved organic matter composition regulates microbial degradation and carbon dioxide production in pristine subarctic rivers. *Biogeosciences,* https://doi.org/10.5194/bg-2022-225

Schink, B., & Stams, A. J. M. (2013). Syntrophism among prokaryotes. In *The Prokaryotes* (pp. 471–493). Springer, Berlin, Heidelberg. https://doi.org/10.1007/978-3-642-30123-0_59

Schuur, E. a. G., McGuire, A. D., Schädel, C., Grosse, G., Harden, J. W., Hayes, D. J., Hugelius,G., Koven, C. D., Kuhry, P., Lawrence, D. M., Natali, S. M., Olefeldt, D., Romanovsky, V. E., Schaefer, K., Turetsky, M. R., Treat, C. C., & Vonk, J. E.

(2015). Climate change and the permafrost carbon feedback. *Nature*, 520(7546), 171–179. https://doi.org/10.1038/nature14338

Shannon, P., Markiel, A., Ozier, O., Baliga, N. S., Wang, J. T., Ramage, D., Amin, N., Schwikowski, B., & Ideker, T. (2003). Cytoscape: A software environment for integrated models of biomolecular interaction networks. *Genome Research*, *13*(11), 2498–2504. https://doi.org/10.1101/gr.1239303

Starr, S. (2024). Carbon dynamics in a changing arctic landscape: Characterizing dissolved organic matter across multiple scales - proquest. Carbon Dynamics in a Changing Arctic Landscape: Characterizing Dissolved Organic Matter Across Multiple Scales – ProQuest

Starr, S. F., Wickland, K. P., Kellerman, A. M., McKenna, A. M., Kurek, M. R., Miller, A., Katsaras, A., Douglas, T. A., Mackelprang, R., Shade, A. L., & Spencer, R. G. M. (2025). Organic matter composition versus microbial source: Controls on carbon loss from fen wetland and permafrost soils. *Journal of Geophysical Research: Biogeosciences*, 130(5), e2024JG008445. https://doi.org/10.1029/2024JG008445

Starr, S. F., Frey, K. E., Smith, L. C., Kellerman, A. M., McKenna, A. M., & Spencer, R. G. M. (2024). Peatlands versus permafrost: Landscape features as drivers of dissolved organic matter composition in west siberian rivers. Journal of Geophysical Research: Biogeosciences, 129(2), e2023JG007797. https://doi.org/10.1029/2023JG007797

Starr, S., Johnston, S. E., Sobolev, N., Perminova, I., Kellerman, A., Fiske, G., Bulygina,E., Shiklomanov, A., McKenna, A., & Spencer, R. G. M. (2023). Characterizing uncertainty in pan-arctic land-ocean dissolved organic carbon flux: Insights from the Onega River, Russia. *Journal of Geophysical Research: Biogeosciences*, 128(5), e2022JG007073. https://doi.org/10.1029/2022JG007073

Stenson, A. C., Marshall, A. G., & Cooper, W. T. (2003). Exact masses and chemical formulas of individual Suwannee River fulvic acids from ultrahigh resolution electrospray ionization Fourier transform ion cyclotron resonance mass spectra. *Analytical Chemistry*, 75(6), 1275–1284. https://doi.org/10.1021/ac026106p

Shur, Y. L., & Jorgenson, M. T. (2007). Patterns of permafrost formation and degradation in relation to climate and ecosystems. *Permafrost and Periglacial Processes*, 18(1), 7–19. https://doi.org/10.1002/ppp.582

Tranvik, L. J., Downing, J. A., Cotner, J. B., Loiselle, S. A., Striegl, R. G., Ballatore, T. J., Dillon, P., Finlay, K., Fortino, K., Knoll, L. B., Kortelainen, P. L., Kutser, T., Larsen, Soren., Laurion, I., Leech, D. M., McCallister, S. L., McKnight, D. M., Melack, J. M., Overholt, E., Porter, J. A., Prairie, Y., Renwick, W. H., Roland, F., Sherman, B. S., Sobek, S., Tremblay, A., Vanni, M. J., Verschoor, A. M., Von Wachenfeldt, E., Weyhenmeyer, G. A.

(2009). Lakes and reservoirs as regulators of carbon cycling and climate. *Limnology and Oceanography*, *54*(6part2), 2298–2314. https://doi.org/10.4319/lo.2009.54.6_part_2.2298

Tremblay, A., Lucotte, M., & Rheault, I. (1996). Methylmercury in a benthic food web of two hydroelectric reservoirs and a natural lake of Northern Québec (Canada). Water, Air, and *Soil Pollution*, 91(3), 255–269. https://doi.org/10.1007/BF00666262

Tremblay, S., Bhiry, N., & Lavoie, M. (2014). Long-term dynamics of a palsa in the sporadic permafrost zone of northwestern Quebec (Canada). *Canadian Journal of Earth Sciences*, 51(5), 500–509. https://doi.org/10.1139/cjes-2013-0123

Vonk, J. E., Mann, P. J., Davydov, S., Davydova, A., Spencer, R. G. M., Schade, J., Sobczak, W.V., Zimov, N., Zimov, S., Bulygina, E., Eglinton, T. I., & Holmes, R. M. (2013). High biolability of ancient permafrost carbon upon thaw. *Geophysical Research Letters*, 40(11), 2689–2693. https://doi.org/10.1002/grl.50348

Vonk, J. E., Tank, S. E., Mann, P. J., Spencer, R. G. M., Treat, C. C., Striegl, R. G., Abbott, B. W., & Wickland, K. P. (2015). Biodegradability of dissolved organic carbon in permafrost soils and aquatic systems: A meta-analysis. *Biogeosciences*, *12*(23), 6915–6930. https://doi.org/10.5194/bg-12-6915-2015

Waldrop, M. P., Chabot, C. L., Liebner, S., Holm, S., Snyder, M. W., Dillon, M., Dudgeon, S. R., Douglas, T. A., Leewis, M.-C., Walter Anthony, K. M., McFarland, J. W., Arp, C. D., Bondurant, A. C., Taş, N., & Mackelprang, R. (2023). Permafrost microbial communities and functional genes are structured by latitudinal and soil geochemical gradients. *The ISME Journal*, 17(8), 1224-1235. https://doi.org/10.1038/s41396-023-01429-6

Waldrop, M. P., Ernakovich, J. G., Vishnivetskaya, T. A., Schaefer, S. R., Mackelprang, R., Barta, J., O′Brien, J. M., Winkel, M., Barbato, R. A., Heffernan, L., Leewis, M., Hewitt, R. E., Hultman, J., Sun, Y., Biasi, C., Bradley, J. A., Liebner, S., Ricketts, M. P., Muscarella, M. E., … Onstott, T. C. (2025). Microbial ecology of permafrost soils: Populations, processes, and perspectives. *Permafrost and Periglacial Processes*, 36(2), 245–258. https://doi.org/10.1002/ppp.2264

Ward, C. P., & Cory, R. M. (2016). Complete and partial photo-oxidation of dissolved organic matter draining permafrost soils. *Environmental Science & Technology*, 50(7), 3545–3553. https://doi.org/10.1021/acs.est.5b05354

Ward, C. P., Nalven, S. G., Crump, B. C., Kling, G. W., & Cory, R. M. (2017). Photochemical alteration of organic carbon draining permafrost soils shifts microbial metabolic pathways and stimulates respiration. *Nature Communications*, 8(1), 772. https://doi.org/10.1038/s41467-017-00759-2

Webster, K. D., Schimmelmann, A., Drobniak, A., Mastalerz, M., Rosales Lagarde, L., Boston, P. J., & Lennon, J. T. (2022). Diversity and composition of methanotroph communities in caves. *Microbiology Spectrum*, 10(4), e01566-21. https://doi.org/10.1128/spectrum.01566-21

Wik, M., Varner, R. K., Anthony, K. W., MacIntyre, S., & Bastviken, D. (2016). Climate-sensitive northern lakes and ponds are critical components of methane release. *Nature Geoscience*, 9(2), 99–105. https://doi.org/10.1038/ngeo2578

Winder, J. C., Braga, L. P. P., Kuhn, M. A., Thompson, L. M., Olefeldt, D., & Tanentzap, A. J. (2023). Climate warming has direct and indirect effects on microbes associated with carbon cycling in northern lakes. *Global Change Biology*, 29(11), 3039–3053. https://doi.org/10.1111/gcb.16655

Woodcroft, B. J., Singleton, C. M., Boyd, J. A., Evans, P. N., Emerson, J. B., Zayed, A. A. F., Hoelzle, R. D., Lamberton, T. O., McCalley, C. K., Hodgkins, S. B., Wilson, R. M., Purvine, S. O., Nicora, C. D., Li, C., Frolking, S., Chanton, J. P., Crill, P. M., Saleska, S. R., Rich, V. I., & Tyson, G. W. (2018). Genome-centric view of carbon processing in thawing permafrost. *Nature*, 560(7716), 49–54. https://doi.org/10.1038/s41586-018-0338-1

Zhang, Y., Zhou, L., Zhou, Y., Zhang, L., Yao, X., Shi, K., Jeppesen, E., Yu, Q., & Zhu, W. (2021). Chromophoric dissolved organic matter in inland waters: Present knowledge and future challenges. *Science of The Total Environment*, 759, 143550. https://doi.org/10.1016/j.scitotenv.2020.143550

Chapter 3

Predicting Seasonal and Regional Variability in CO_2 and CH_4 Dynamics in Lakes from DOM Composition

Abstract

Dissolved organic matter (DOM) plays a critical role in the carbon cycle. DOM composition, how it's processed by microbes, and the environmental and thermal factors that affect these processes can determine the amount of greenhouse gas emitted in aquatic ecosystems. Here we examined how dissolved organic matter composition relates to seasonal GHG dynamics in 40 lakes spanning a space-for-time gradient for future warming scenarios, integrating high-resolution molecular data and seasonal dissolved gas and flux measurements. Contrary to the expected summer peak, CO_2 fluxes were highest in spring, linked to under-ice gas buildup, while CH_4 fluxes peaked in fall following hypolimnetic accumulation during summer stratification. Dissolved gas concentrations provided early indicators of these seasonal flux events as dissolved gas concentrations were the highest in the season leading up to those peak flux events. For example, CO_2 dissolved gas concentration was their highest in winter because of under-ice build up which was rapidly released in spring. The same is true with CH_4 concentrations where they were their highest in summer due to CH_4 build up in the hypolimnion in the stratified lake. CH_4 was then rapidly released during the fall turnover. Molecular analyses revealed strong positive associations between CH_4 and reduced, low O:C DOM, consistent with methanogenesis from labile precursors, while CO_2 showed weaker and more diffuse molecular correlations, reflecting multiple production and input pathways. These results demonstrate that

seasonal dissolved gas buildup and DOM quality jointly shape emission patterns, highlighting the need for year-round measurements to accurately capture lake carbon budgets.

Keywords: Greenhouse gas (GHG), Dissolved Organic Matter (DOM), Flux, Ebullition, Lake Carbon Cycling, Fourier-transform ion cyclotron resonance mass spectrometry (FT-ICR MS)

Introduction

Lakes and ponds are important sources of greenhouse gases (GHGs), particularly carbon dioxide (CO_2) and methane (CH_4), which contribute to global climate change (Tranvik et al., 2009; Bastviken et al., 2011). Inland waters emit roughly 2.1 Pg C yr^{-1} of CO_2 to the atmosphere (Raymond et al., 2013; Tranvik et al., 2009). They are also a major natural source of methane, contributing ~45% of global natural CH_4 emissions (Rosentreter et al., 2021), with lakes responsible for a disproportionately large amount, estimated at 9 to 19% of global CH_4 emissions (Bastviken et al., 2004; Wik et al., 2016). Understanding the factors that regulate GHG production from lakes is critical to improving climate models (Raymond et al., 2013; DelSontro et al., 2018). However, current climate models often fail to capture how microbial degradation of DOM, and its interaction with lake physical processes, regulates CO_2 and CH_4 emissions, leaving a major source of uncertainty in global carbon budgets (Guillemette & del Giorgio, 2011; Kuhn et al., 2021).

Microbial degradation of dissolved organic matter (DOM) is the main pathway by which CO_2 and CH_4 are produced in lakes. DOM is a chemically diverse mixture of compounds derived from terrestrial inputs and aquatic production and its composition influences how microbes process it (Hartnett, 2017; Tanentzap et al., 2019). Some DOM molecules, such as simple sugars, amino acids, and low-molecular-weight organic acids (e.g., acetate, formate), are easily degraded and used for energy or biomass, while others are more chemically complex and resistant to breakdown. Certain microbial groups specialize in processing specific DOM types, such as methanogens that produce methane under oxygen-limited conditions using simple labile substrates. These substrates are small, low-molecular weight compounds like methanol, acetate, formate, and hydrogen which can be directly metabolised without extensive enzymatic

breakdown (Mayumi et al., 2016; Woodcroft et al., 2018; Bogard et al., 2014). In contrast, aerobic heterotrophs may oxidize more aromatic DOM, such as lignin-derived phenols, tannins, and other polyphenolic compounds, into CO_2 through oxidative enzymatic pathways (e.g., peroxidases, laccases). Such compounds are typically derived from terrestrial plant material and require specialized enzyme systems to break their stable aromatic rings (Berggren et al., 2010; Kellerman et al., 2014; Mostovaya et al., 2017; Tanentzap et al., 2019). Consequently, the molecular traits of DOM such as its lability, aromaticity, and oxidation state, can shape both microbial community structure and GHG production pathways (Kellerman et al., 2014; Tanentzap et al., 2019).

The relationship between DOM and microbes are shaped by environmental factors such as temperature, sunlight, and stratification, which together regulate whether DOM is transformed, buried, or emitted as greenhouse gases (Raymond et al., 2013; Valiente et al., 2022). These environmental controls are strongly seasonal: long summer days bring warmer temperatures and higher light availability, while fall overturn and winter ice cover reset mixing regimes and oxygen supply. Warmer conditions tend to accelerate microbial metabolism, enhancing the breakdown of labile DOM into CO_2 and CH_4 (Yvon-Durocher et al., 2012; Gudasz et al., 2010), while cooler temperatures in deep or seasonally ice-covered waters slow microbial activity and promote DOM preservation (Tranvik et al., 2009). Sunlight can photodegrade DOM into smaller, more bioavailable molecules (Moran & Zepp, 1997; Cory et al., 2014), stimulating heterotrophic uptake or mineralizing it directly to CO_2 (Koehler et al., 2014). In shallow, well-mixed systems, high light penetration and oxygen replenishment favor aerobic processing, whereas strong stratification in deeper lakes fosters anoxic bottom waters that promote anaerobic pathways such as methanogenesis (Bastviken et al., 2004; DelSontro et al., 2016). Because

dissolved gas pools capture both biological production and gases accumulated through physical processes (Raymond et al., 2013), their seasonal buildup can shape DOM correlations in ways that may differ from flux measurements. Understanding these dynamics requires attention to how gas production and accumulation vary across seasons, with winter remaining one of the least researched periods (Denfeld et al., 2018; Hampton et al., 2017; Powers & Hampton, 2016; Karlsson et al., 2013).

Under ice cover, reduced light, physical isolation from the atmosphere, and low temperatures alter microbial metabolism, slow gas exchange, and shift redox conditions (Denfeld et al., 2018; Karlsson et al., 2013; Powers & Hampton, 2016; Hampton et al., 2017). This can lead to wintertime "storage fluxes," where CO_2 accumulates under ice and is released during spring turnover, while CH_4 production continues in anoxic sediments, allowing for substantial buildup until mixing events or ice-off (Walter et al., 2007; Sepulveda-Jauregui et al., 2015; Jansen et al., 2020). These dynamics are especially important in northern lakes, where climate change is shortening ice cover duration and altering the timing of freeze–thaw cycles (Sharma et al., 2021). A shorter ice season can reduce the period of CO_2 and CH_4 buildup under ice but increase the frequency of flux events in the fall and spring, while also modifying DOM inputs through changing runoff and permafrost thaw (Spencer et al., 2008; O'Donnell et al., 2016; Ward & Cory, 2020; Hu et al., 2022; Winder et al., 2023).

To address these knowledge gaps, we asked: (1) how do greenhouse gas fluxes and dissolved gas concentrations vary across seasons and temperature regimes, and (2) how does the amount and type of GHGs relate to DOM composition. Using a space-for-time approach, we sampled lakes for GHGs spanning a natural temperature gradient over the course of a year to capture both spatial and seasonal variability. This design allowed us to explore how current

temperature differences may serve as analogs for future climate warming scenarios (Kuhn et al., 2021; Winder et al., 2023). We then quantified DOM characteristics using Fourier-transform ion cyclotron resonance mass spectrometry (FT-ICR MS), a high-resolution technique that provides molecular insight into DOM composition (Kellerman et al., 2014). We hypothesized that warmer lakes would emit more CO_2 and CH_4 because their DOM would be more chemically reactive and accessible to microbial degradation (Zhou et al., 2019).

Methods

Sampling sites

Between August 2024 and August 2025, we conducted seasonal water and gas flux measurements across 10 lakes in each of four regions: northern Michigan (45.3893 N, -84.6817 W; mean annual temperature (MAT) ~7.2 °C), central Ontario (45.1819 N, -78.9772 W; MAT ~5.2°C), central Quebec (48.4757 N, -78.9529 W; MAT ~2.4 °C), northern Quebec (53.6468 N, -77.7941 W; MAT ~ -1.8 °C) (Figure 1; Figure B1a, b, c, d). Regions were chosen to represent a space-for-time gradient, where each successive region is approximately 1.5–2.5 °C warmer than the one to its north. This design allows present-day temperature differences to serve as analogs for future climate warming scenarios, enabling us to assess how lake greenhouse gas emissions and DOM characteristics may respond to projected temperature increases. Lakes were selected based on ease of road and boat access, availability of bathymetric data to identify representative sampling locations, and a diverse span of lake areas within each region. Across the four regions sampled, lakes ranged from 0.13 km^2 to 67.66 km^2 with mean depths between 3 m and 34 m (Table B1). Most lakes were surrounded by forest and grass cover with some Ontario and

Michigan lakes surrounded by greater recreational land use based on visual observations. At each lake, sampling points were selected where the water depth approximated the mean depth of each lake. Two additional points were selected along a transect from the sampling point to the shoreline for GHG sampling replicates.

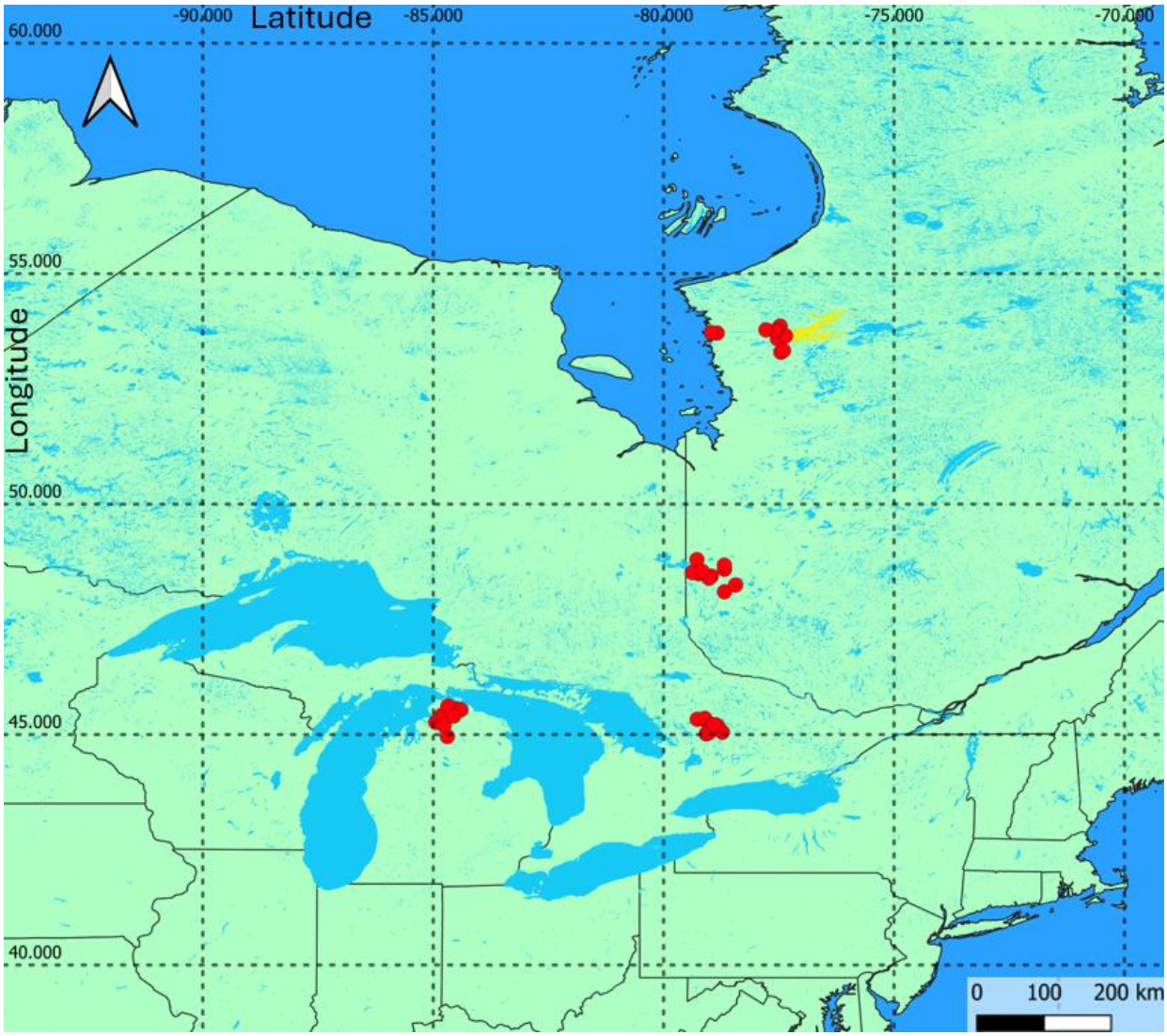

Figure 1: Locations of sampled lakes across a latitudinal gradient. Red points indicate individual sampling coordinates. Selected lakes are shown in yellow and water bodies are in blue. The map was generated in QGIS using HydroLAKES data (Messager et al., 2016).

Sampling design

In each of the four study regions, ten lakes were sampled seasonally over one year. Sampling occurred between July and August of 2024 (summer), October and November 2024 before ice-on (fall), January to March of 2025 when lakes were frozen (winter), and May to June 2025 when lakes thawed (spring). During each sampling event, we took two types of GHG measurements: fluxes from the lake surface and dissolved gas measurements in surface lake water, with additional hypolimnion samples during the summer. Water samples to characterise the molecular composition of DOM were also collected from the lake surface and the hypolimnion in summer only. Water used for DOM analysis was filtered through pre-combusted glass fibre filters (0.45 μm pore size) and collected into pre-muffled (450 °C for 4 hours) 40 mL glass amber vials, with no headspace and acidified with ~0.4 mL of 1M HCl to a pH of 2. The bottles were stored at 4 °C for up to 30 days before analysis.

Flux measurements

We estimated GHG fluxes (CO_2 and CH_4) from the surface of every lake using a floating chamber (Bastviken et al., 2004). The chamber was approximately 9.45 L in volume, 0.0418 m^2 surface area, and was wrapped in aluminium tape to reduce internal heating (Gålfalk et al., 2013). The chamber was connected to an infrared gas analyzer using off-axis integrated cavity output spectroscopy (ultraportable greenhouse gas analyzer 915, Los Gatos Research, Mountain View, USA) in a closed loop. Three replicate measurements consisting of 15-minute intervals were conducted at three sampling points per lake for concentrations of CO_2 and CH_4. In the winter, when lake surfaces were frozen, we placed the chamber directly on top of the ice and packed it with snow around the base to seal the chamber better and prevent gas leakage into the atmosphere.

Due to unexpected equipment failure, Ontario winter and Michigan spring greenhouse gas flux measurements were collected using N_2-flushed 12 mL glass vials (Extetainer®, Labco, Labeled, Flat Bottom, DW Cap, UK). The vials were attached in a closed loop to the floating chamber in 1-minute increments at 5-minute intervals from 0 min to 15 min. This collection was repeated twice per lake. The exetainers were then wrapped in sealable film and stored upside down in a thin layer of water at 4°C until analysis (Davidson et al., 2006). In the lab, the exetainers were run within 3 months in a closed-loop system through the gas analyzer to characterise CO_2 and CH_4 concentrations.

GHG fluxes were quantified using a custom R Shiny application, where users manually selected time intervals corresponding to: (1) diffusive flux which is characterized by steady, linear increases in headspace gas concentration from water-to-air diffusion and (2) ebullition events which is identified by sudden, non-linear increases in gas concentration due to bubble release from sediments (Tanentzap et al., 2025). For both types of fluxes, linear regression was separately applied within each recorded time interval to model CO_2 or CH_4 concentration (ppm) as a function of elapsed time (s) using the lm() function in R (R Core Team, 2024). The linear model, gas concentration = $\beta_0 + \beta_1 \times$ Time, provided a slope (β_1) representing the gas accumulation rate (ppm s^{-1}).

These rates were converted to area-specific fluxes (μmol m^{-2} s^{-1}) using the Ideal Gas Law, chamber volume, chamber footprint area, and measurements of headspace temperature (°C) and pressure (torr) recorded by the gas analyzer, which were converted to Kelvin and Pascals, respectively, prior to calculation. For diffusive fluxes, slopes were calculated from linear intervals representing steady accumulation. Coefficients of determination (R^2) were extracted from the models to quantify the goodness of fit for quality control where only samples with an R^2

> 0.8 were retained (DelSontro et al., 2016). For winter samples specifically, a $R^2 > 0.5$ was accepted following the suggestions of a recent paper (Sø et al., 2024). This threshold balances quality control with data retention, particularly in winter when low flux magnitudes and small concentration changes are at the limit of what our gas analyzer can measure which can affect the R^2. A stricter cutoff could exclude valid low flux measurements. Ebullition events were manually identified in the Shiny application by selecting time intervals that exhibited a sharp, step-like or non-linear increase in gas concentration, with a magnitude visibly exceeding the underlying diffusive trend. Only the rising phase of each event was selected, and linear regressions were fitted to these intervals to calculate fluxes using the Ideal Gas Law and chamber measurements. Ebullitive fluxes within each replicate measurement were averaged, weighted by the duration of each event. Total gas flux (μmol m^{-2} s^{-1}) was then calculated as the weighted average of diffusive and ebullition fluxes within each measurement. Potential outliers for the total flux were removed using the interquartile range (IQR) method, applied separately for each gas (CO_2, CH_4) within each region and season (Tukey, 1977; Zurr et al., 2007). This method involved excluding observations falling more than 1.5×IQR below the first quartile or above the third quartile.

Quantifying the fluxes collected in the exetainers involved the usage of a Shiny application that followed a similar analytical framework as the one used for chamber measurements. Within each measurement interval, the mean gas concentration, pressure, and air temperature were calculated over two-minutes. We calculated flux as the slope of a line fitted through four exetainer concentration measurements, taken at 5-minute intervals starting at minute 0 for each sample. The resulting slope (ppm s^{-1}) was then converted to an area-specific flux (μmol m^{-2} s^{-1}) by applying the Ideal Gas Law with the same chamber volume and footprint area. Because measurements for the exetainers were conducted indoors, room temperature and

atmospheric pressure were used in the calculations instead of the temperature and pressure values recorded by the gas analyzer.

Dissolved gas measurements

Dissolved gas measurements were collected from surface water in all seasons and from the hypolimnion in summer only. Water from the hypolimnion was collected with a Van Dorn sampler lowered to just above the lake bottom and was not collected during spring and fall because the lakes were mixed. During the winter, when lakes were frozen, we had to use an auger to drill a hole to collect water. Dimensions of the drilled hole were roughly double the size of the flux chamber. We then filled 120 mL clear glass serum bottles with water and no headspace and sealed them with gas-tight crimp caps. A headspace was created in each bottle by inserting a syringe through the rubber septum and forcibly withdrawing 10 mL of water, creating a near vacuum. Each bottle was shaken vigorously by hand for 90 seconds to equilibrate the water and headspace. After shaking, two needles attached to the same gas analyzer that was used for flux measurements were inserted through the rubber septum in a closed-loop and headspace gas concentrations were measured for approximately two minutes.

Using a custom R Shiny application like the one used for flux measurements, we quantified headspace CH_4 and CO_2 concentrations from equilibrated water samples. For each sample, users manually selected time intervals corresponding to dissolved gas measurements. Within each interval, the mean gas concentration and pressure were recorded, along with the mean atmospheric concentration. Dissolved gas concentrations in water were then estimated by applying Henry's Law and the Ideal Gas Law using water temperature collected simultaneously

with a ProDSS Multiparameter Digital Water Quality Meter (YSI Inc., USA). Measured headspace concentrations (ppm) were then converted to partial pressures and used to back-calculate the original dissolved concentration in water, accounting for headspace-to-water volume ratios, water temperature, pressure, and gas-specific Henry's constants (μmol L^{-1}). The same IQR method used for fluxes was also used here to remove potential outliers separately for each gas.

Dissolved organic matter (DOM) concentration and composition

In the lab, DOM concentration was measured as dissolved organic carbon (DOC) on a Shimadzu TOC-L analyzer within 30 days of collection. For DOM composition, only summer measurements were analysed due to time and resource limitations. Samples for compositional analyses were first subjected to solid phase extraction with styrene-divinylbenzene polymer cartridge (PPL) following Dittmar et al., 2008. 3 mL PPL cartridges (Bond Elut PPL, Agilent, Santa Clara, USA) were soaked with HPLC-grade methanol overnight, rinsed with Milli-Q water and acidified pH 2 Milli-Q water, and kept wet with acidified Milli-Q until use. Utilizing measured DOC concentrations, a volume of water equal to a target of 50 μg C^{-1} was passed over each cartridge to ensure consistent spectra intensity assuming an extraction efficiency of 60%. The cartridges were then desalinized with deionized water, dried under inert N_2 gas, and eluted with 1 mL of methanol into pre-weighed, muffled (450 °C for 4 hours) glass vials. Extracts were stored at -20 °C for up to 90 days until analysis. For analysis, extracts were transferred to muffled 2 mL autosampler vials with 300 μL glass inserts.

Samples were analyzed on a 7T Bruker Solarix FT-ICR MS at the Trent University Water Quality Centre using negative electrospray ionization (ESI) and an autosampler coupled with an UHPLC pump (Elute Plus, Bruker, Germany). Extracts were injected into the instrument at a flow rate of 0.01 mL min^{-1} at pressure between 25 and 35 psi until all 300 µL was injected into the FT-ICR MS. The method used 150 scans at 8M resolution with 0.010 s accumulation time. A methanol blank was run every 10 samples to verify visually there was no carry-over between samples. Acquired spectra were calibrated with the Compass DataAnalysis software (Bruker, USA) with a custom method file configured for negative ESI, which involved the iterative removal of extreme error calibrants until the standard deviation of the spectra dropped below 0.2 ppm. Molecular formulae were assigned using the ICBM-OCEAN online tool (Merder et al., 2020) with 1 ppm tolerance and constraints of C≤100, H≤200, O≤70, N≤4, S≤1, and P≤1, using the N, S, P rule (Riedel & Dittmar, 2014). Assignments included isotopic filtering and homologous series detection (CH_2 and CO_2), and formulae were aligned across samples using Fast Join (2 ppm tolerance). We filtered out formulae with chemically implausible H:C and O:C ratios, retaining only those within the ranges of 0.3–2.5 for H:C and 0–1.0 for O:C (Koch & Dittmar, 2006; Sleighter et al., 2008).

Using the ftmsRanalysis package v1.1.0 (Bramer et al., 2025), we characterized the molecular composition of each sample by calculating five intensity-weighted molecular metrics: hydrogen-to-carbon ratio (H:C), oxygen-to-carbon ratio (O:C), nominal oxidation state of carbon (NOSC), modified aromaticity index (AI_{Mod}), and Gibbs Free Energy (GFE). These metrics provide insight into the biochemical lability and oxidation state of DOM. H:C serves as a general indicator of aliphatic content and bioavailability, with higher values suggesting more saturated and labile compounds (Kim et al., 2003). O:C reflects oxygenation, with higher values indicating

more oxidized molecules, though this may include oxygen bound to heteroatoms such as nitrogen, phosphorus, or sulfur (Kellerman et al., 2014). NOSC quantifies the oxidative state of carbon atoms in a molecule, with more positive values representing increasingly oxidized compounds (LaRowe & Van Cappellen, 2011). AI_{Mod} estimates aromaticity and structural stability, where higher values denote more condensed and refractory molecules (Koch & Dittmar, 2006). GFE, estimated from NOSC via a linear relationship (LaRowe & Van Cappellen, 2011), serves as a proxy for the thermodynamic favourability of microbial oxidation; more negative values represent compounds that yield energy upon oxidation, whereas positive values may require energy investment for microbial transformation.

Statistical analyses

To evaluate how GHGs varied across regions and seasons, we fitted linear mixed-effects models (LMMs) using the lmer() function from the lme4 package (Bates et al., 2015) in R version 4.3.2. Separate models were constructed for CO_2 and CH_4, with either total flux (μmol m^{-2} s^{-1}) or surface dissolved gas concentration (μmol L^{-1}), as the response variable. Season and region were included as fixed effects, and lake was specified as a random effect to account for repeated measurements across seasons. To assess the overall effects of season and region, we performed Type III analysis of variance (ANOVA) using the lmerTest package (Kuznetsova et al., 2017), which applies Satterthwaite's method to estimate *p*-values. Degrees of freedom and 95% confidence intervals were calculated using the Kenward–Roger approximation, and pairwise comparisons between levels of each fixed effect were performed using the emmeans package (Lenth, 2024), with Tukey's Honestly Significant Difference (HSD) method applied to adjust for multiple comparisons (Kenward & Roger, 1997; Tukey, 1949). Model performance

was evaluated using marginal (R^2_m) and conditional (R^2_c) coefficients of determination, which quantify the proportion of variance explained by the fixed effects alone (R^2_m) and by both fixed and random effects combined (R^2_c) (Nakagawa & Schielzeth, 2013). Values were computed using the performance package in R (Lüdecke et al., 2025).

We also evaluated vertical differences in dissolved CH_4 and CO_2 concentrations between surface and hypolimnion waters during the summer. Separate linear models were fit for each gas, with dissolved concentration (μmol L^{-1}) as the response variable. Depth (surface or hypolimnion), region, and their interactions were specified as fixed effects. Region and Depth interaction were kept to account for the possibility that depth effects may differ among regions. A Type II ANOVA was used to assess the significance of fixed effects Depth and Region. Pairwise comparisons were not conducted for depth effects as the factor included only two levels (surface and hypolimnion), and the significance of the main effect was directly assessed using ANOVA.

To assess spatial variation in DOM composition, we tested for differences across regions using a Type III ANOVA. Each DOM metric (H:C, O:C, AI_{Mod}, NOSC, and GFE) was analyzed separately as a response variable and region (central Ontario, central Quebec, northern Quebec, and northern Michigan) as a fixed effect. Post-hoc comparisons among regions were performed using Tukey's HSD test to identify pairwise differences among regions.

We also assessed relationships between molecular composition and dissolved greenhouse gas concentrations (CH_4 and CO_2) by calculating Spearman's rank correlations between each DOM metric (GFE, AI_{Mod}, NOSC, H:C, and O:C) and concentrations (μmol L^{-1}) of each GHG. Dissolved CH_4 and CO_2 concentrations were used to assess relationships with DOM composition over fluxes because these values provide a more direct reflection of in situ microbial activity than gas fluxes (Bastviken et al., 2004; Wik et al., 2016). Gas fluxes were also unbalanced

spatially and seasonally meaning that measurements may not capture peak emission periods and could bias annual or regional estimates. We further investigated molecular-level patterns by calculating Spearman's rank correlations between the intensity of each molecular formula and dissolved gas concentrations. All correlations were computed separately for each region.

Results

Seasonal and regional differences in greenhouse gas fluxes

Seasonal patterns in greenhouse gas fluxes did not follow the typical expectation of peak emissions in summer, instead showing highest CO_2 fluxes in spring and highest CH_4 fluxes in fall when averaged across sites. Mean ± standard error (SE) CO_2 flux was highest in spring, averaging 81.3 ± 13.5 μmol m^{-2} s^{-1} (N = 26), followed by winter (66.6 ± 69.6 μmol m^{-2} s^{-1} N = 4), fall (48.7 ± 7.0 μmol m^{-2} s^{-1}, N = 41), and then summer (23.0 ± 10.5 μmol m^{-2} s^{-1}, N = 20) (ANOVA: $F_{(3, 84.07)} = 6.24$, $p < 0.001$; Figure 2a). Pairwise comparisons confirmed that spring fluxes were larger than in fall ($t = -2.81$, df = 83.1, $p = 0.031$) and in summer ($t = 3.83$, df = 85.6, $p = 0.001$), with other comparisons not statistically significant ($p > 0.074$). For CH_4, fluxes were highest, on average, in fall at 4.3 ± 0.8 μmol m^{-2} s^{-1} (N = 44), followed by summer (1.3 ± 0.4 μmol m^{-2} s^{-1}, N = 50), spring (0.7 ± 0.2 μmol m^{-2} s^{-1}, N = 22), and winter (0.020 ± 0.008 μmol m^{-2} s^{-1}, N = 4) (ANOVA: $F_{(3, 110.92)} = 3.97$, $p = 0.009$; Figure 2b). Pairwise comparisons identified fall CH_4 fluxes were larger than spring ($t = 2.71$, df = 113, $p = 0.038$), and winter ($t = 2.68$, df = 108, $p = 0.042$), with no other statistically significant difference ($p > 0.058$).

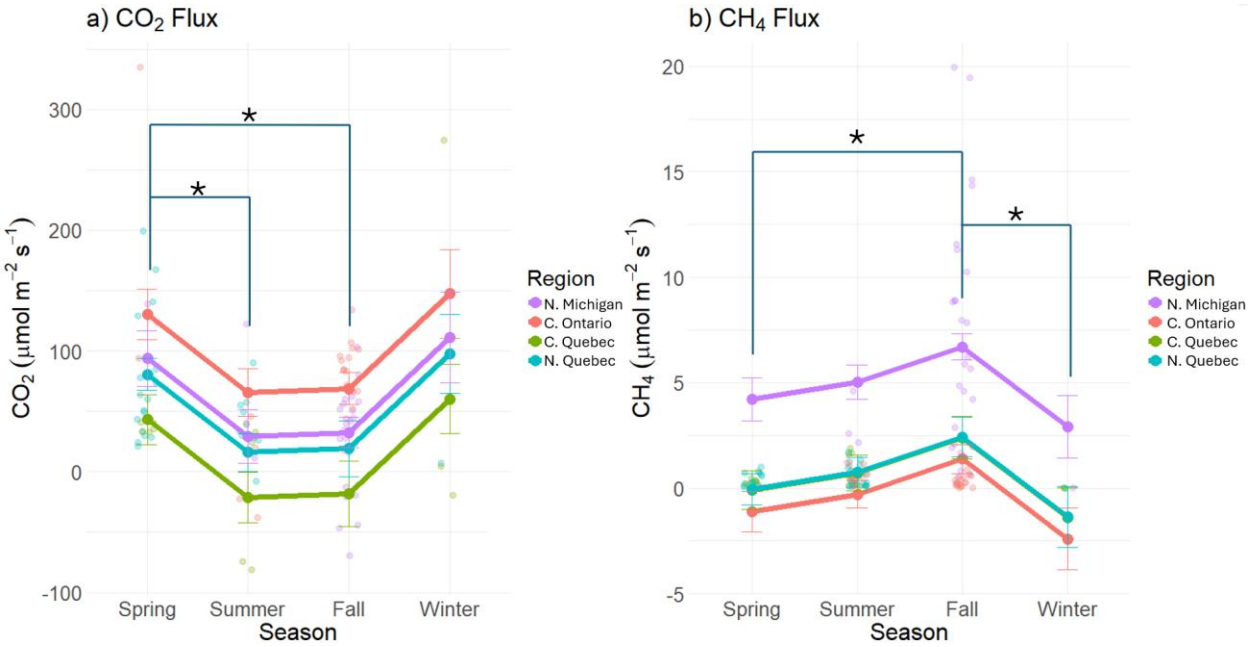

Figure 2: Seasonal variation in modeled greenhouse gas fluxes across the four study regions. (a) CO_2 and (b) CH_4 fluxes (µmol m^{-2} s^{-1}) in central Ontario, central Quebec, northern Quebec, and northern Michigan. Semi-transparent points represent individual chamber-based flux measurements (N = 93 for CO_2 and N = 122 for CH_4). Lines represent marginal means ± standard error estimated from linear mixed-effects models. Square brackets indicate season pairs with statistically significant differences, as determined by Tukey-adjusted pairwise comparisons ($p < 0.05$). CO_2 flux: $R^2_m = 0.23$, $R^2_c = 0.30$ and CH_4 flux: $R^2_m = 0.49$, $R^2_c = 0.61$.

When analyzing regional flux differences, we found that warmer regions tend to, on average, emit the most CO_2 and CH_4. Mean ± SE CO_2 fluxes were highest in central Ontario with 74.8 ± 12.8 µmol m^{-2} s^{-1} (N = 27), followed by northern Quebec (59.6 ± 8.8 µmol m^{-2} s^{-1}, N = 11), northern Michigan (34.0 ± 10.1 µmol m^{-2} s^{-1}, N = 28), and central Quebec (28.7 ± 25.6 µmol m^{-2} s^{-1}, N = 24) (ANOVA: $F_{(3, 83.95)} = 4.90$, $p = 0.003$; Figure 3a). Pairwise comparisons showed that only central Ontario had statistically significant larger CO_2 fluxes than central Quebec ($t = 3.39$, df = 86.0, $p = 0.006$), with no other statistically significant differences ($p > 0.092$). For CH_4, fluxes were highest in northern Michigan (6.2 ± 0.99 µmol CH_4 m^{-2} s^{-1}, N = 31), followed by northern Quebec (0.50 ± 0.08 µmol m^{-2} s^{-1}, N = 32), central Quebec (0.50 ±

0.16 µmol m^{-2} s^{-1}, N = 15), and central Ontario (0.45 ± 0.05 µmol m^{-2} s^{-1}, N = 41) (ANOVA: $F_{(3, 109.16)} = 23.21$, $p < 0.001$; Figure 3b). Pairwise comparisons confirmed that CH_4 fluxes at northern Michigan were higher than all other regions: central Ontario ($t = -8.30$, df = 108, $p < 0.001$), central Quebec ($t = -4.57$, df = 108, $p < 0.001$), and northern Quebec ($t = -5.08$, df = 109, $p < 0.001$). No other pairwise differences were statistically significant (for all, $p > 0.445$).

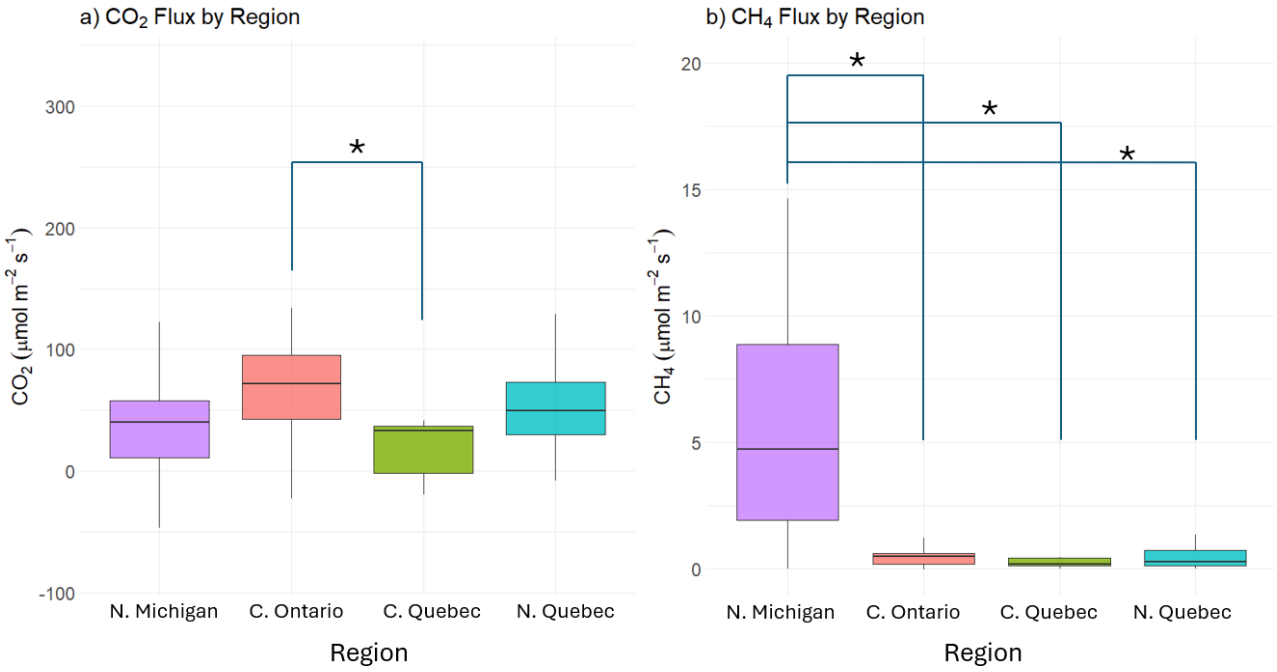

Figure 3: Regional variation in greenhouse gas fluxes across four regions across all seasons show that warmer regions, on average, have higher (a) CO_2 and (b) CH_4 fluxes (µmol m^{-2} s^{-1}). Regions shown are northern Michigan, central Ontario, central Quebec, and northern Quebec. Boxplots show the distribution of chamber-based flux measurements (N = 93 for CO_2 and N = 122 for CH_4). Boxes represent the interquartile range (IQR; 25th to 75th percentiles), the horizontal line indicates the median, and whiskers extend to the most extreme values within 1.5×IQR. Square brackets indicate region pairs with statistically significant differences, as determined by Tukey-adjusted pairwise comparisons ($p < 0.05$). CO_2 flux: $R^2_m = 0.23$, $R^2_c = 0.30$ and CH_4 flux: $R^2_m = 0.49$, $R^2_c = 0.61$.

Seasonal and regional differences in dissolved greenhouse gas concentrations

Dissolved gas concentrations varied across seasons with generally higher GHG concentrations observed in the warmer months. However, CO_2 reached the highest mean ± SE dissolved concentrations in winter (325.6 ± 23.6 μmol L^{-1}, N = 15), only then was it followed by summer (286.6 ± 18.7 μmol L^{-1}, N = 24), spring (270.5 ± 7.4 μmol L^{-1}, N = 30), and fall (256.4 ± 5.6 μmol L^{-1}, N = 17) (ANOVA: $F_{(3, 77.50)} = 4.12$, $p = 0.009$; Figure 4a). Pairwise comparisons indicated only one statistically significant contrast, where dissolved CO_2 in winter was larger than fall ($t = -3.21$, df = 76.5, $p = 0.010$; $p > 0.089$ for all other comparisons). For CH_4, concentrations also varied seasonally (ANOVA: $F_{(3, 77.00)} = 8.16$, $p < 0.001$; Figure 4b). Dissolved CH4 concentrations were highest in summer (129.0 ± 35.4 μmol L^{-1}, N = 25), followed by fall (98.1 ± 22.9 μmol L^{-1}, N = 15), with winter and spring showing similar CH_4 concentrations (26.4 ± 0.7 and 26.1 ± 0.7 μmol L^{-1}, N = 15 and 26 respectively). Pairwise comparisons reveled larger dissolved CH_4 concentrations in summer than in spring ($t = -3.91$, df = 72.0, $p = 0.001$) and than in winter ($t = 4.27$, $df = 72.8$, $p < 0.001$), with other differences not statistically significant (for all, $p > 0.177$).

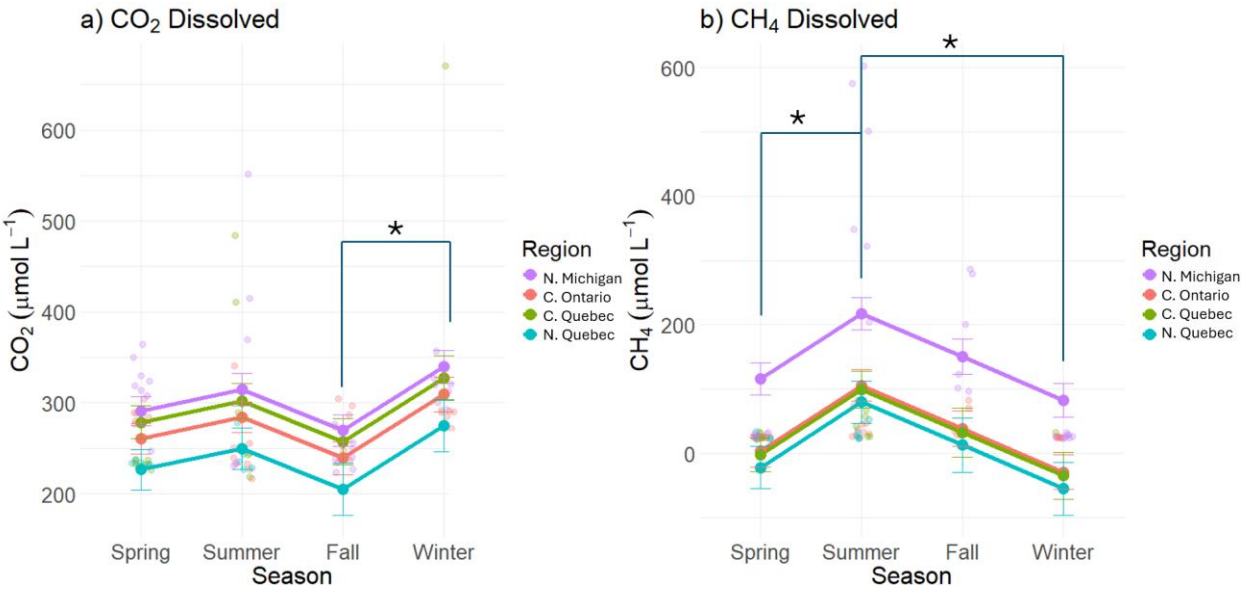

Figure 4: Seasonal variation in dissolved greenhouse gas concentrations across four regions. (a) CO_2 and (b) CH_4 concentrations (µmol L^{-1}) are shown for central Ontario, central Quebec, northern Quebec, and northern Michigan. Semi-transparent points represent individual dissolved measurements (N = 90 for CO_2 and N = 84 for CH_4). Lines represent marginal means ± standard error estimated from linear mixed-effects models. Square brackets indicate season pairs with statistically significant differences, as determined by Tukey-adjusted pairwise comparisons ($p < 0.05$). CO_2 dissolved concentrations: $R^2m = 0.18$, $R^2c = 0.19$; CH_4 dissolved concentrations: $R^2m = 0.38$, $R^2c = 0.38$ (random effect variance was negligible).

Regional analysis of dissolved gas concentration revealed that more southern warmer regions exhibited higher CO_2 and CH_4 concentrations, consistent with the seasonal analysis where the warmer months exhibited the highest GHG concentrations. The mean ± SE dissolved CO_2 concentrations were highest in northern Michigan (300.4 ± 11.2 CO_2 L^{-1}, N = 34), followed by central Quebec (290.7 ± 31.4 µmol L^{-1}, N = 16), central Ontario (270.3 ± 4.7 µmol L^{-1}, N = 29) and then northern Quebec (238.3 ± 4.7 µmol L^{-1}, N = 12) (ANOVA: $F_{(3, 78.04)} = 3.00$, $p = 0.035$; Figure 5a). Pairwise comparisons confirmed that northern Quebec has lower CO_2 concentrations than Michigan ($t = -2.68$, df = 79.7, $p = 0.04$). Northern Michigan also had the highest mean ± SE in CH_4 dissolved gas concentration (139.8 ± 31.8 µmol L^{-1}, N = 30), followed by central Quebec (36.2 ± 4.7 µmol L^{-1}, N = 14), central Ontario (32.1 ± 2.6 µmol L^{-1}, N = 28),

and finally northern Quebec (28.7 ± 2.9 µmol L^{-1}, N = 9). (ANOVA: $F_{(3, 77.00)} = 9.57$, $p < 0.001$; Figure 5b). Pairwise comparisons showed higher CH_4 concentrations in northern Michigan compared to central Ontario ($t = 4.55$, df = 74.0, $p < 0.001$), central Quebec ($t = 3.67$, df = 75.1, $p = 0.003$), and northern Quebec ($t = 3.73$, df = 74.3, $p = 0.002$). No other statistically significant differences were found among other regions for either CO_2 or CH_4 (for all, $p > 0.890$).

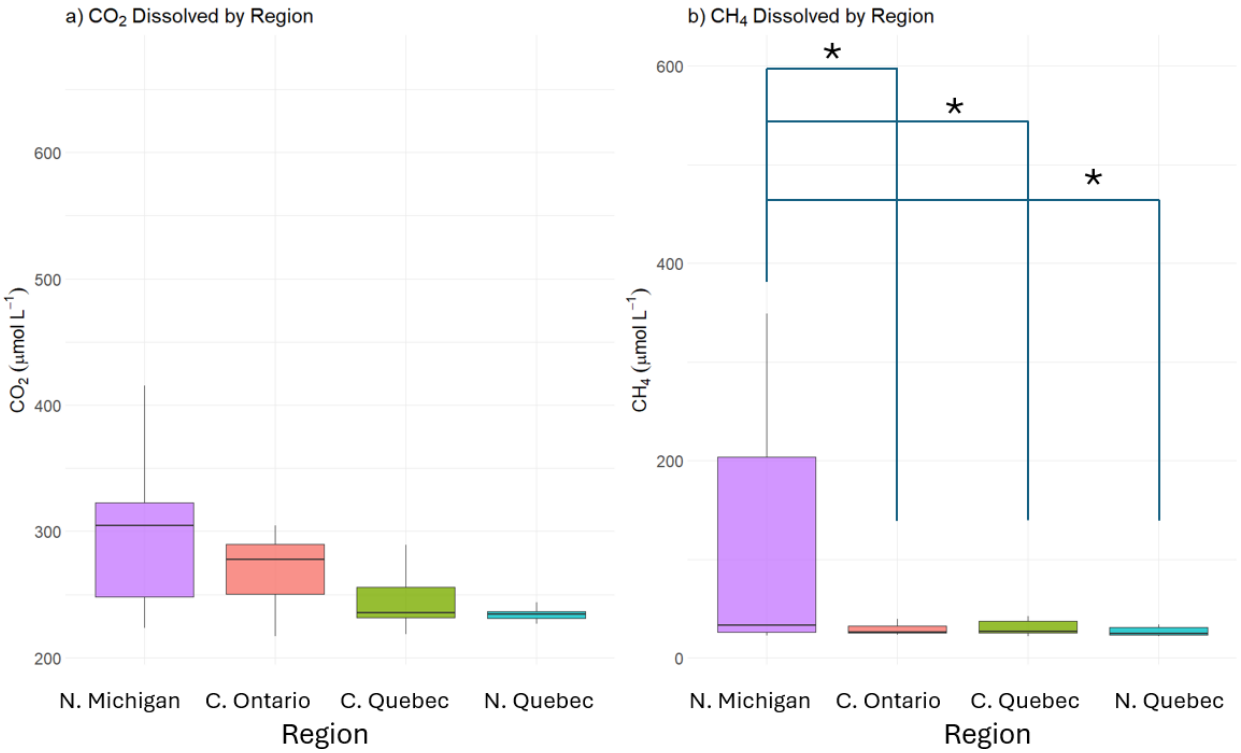

Figure 5: Regional variation in dissolved gas concentrations across four regions across all seasons that show warmer regions have on average, the highest (a) CO_2 and (b) CH_4 dissolved gas concentrations (µmol L^{-1}). Regions shown are for northern Michigan, central Ontario, central Quebec, and northern Quebec. Boxes represent the interquartile range (IQR; 25th to 75th percentiles), the horizontal line indicates the median, and whiskers extend to the most extreme values within 1.5×IQR (N = 90 for CO_2 and N = 84 for CH_4). Square brackets indicate region pairs with statistically significant differences, as determined by Tukey-adjusted pairwise comparisons ($p < 0.05$). CO_2 dissolved concentrations: $R^2m = 0.18$, $R^2c = 0.19$; CH_4 dissolved concentrations: $R^2m = 0.38$, $R^2c = 0.38$ (random effect variance was negligible).

Greenhouse gas concentrations across the water column

Dissolved CO_2 and CH_4 concentrations did not differ significantly between the hypolimnion (N = 24 for CO_2 and 24 for CH_4) and surface (N = 24 for CO_2 and 25 for CH_4) in summer (CO_2: $F_{(1, 36.45)} = 2.80$, $p = 0.103$; CH_4: $F_{(1, 42.60)} = 0.04$, $p = 0.840$) (Figure 6), indicating that vertical stratification during this period did not create strong gradients in gas accumulation.

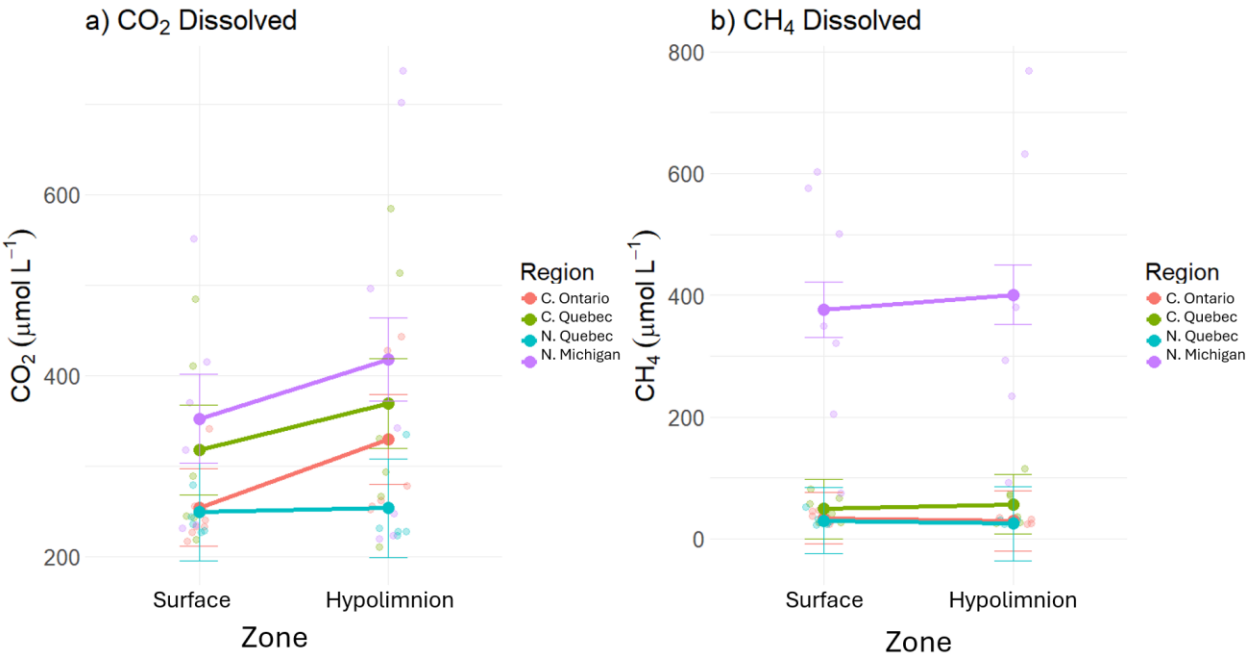

Figure 6: No differences in in dissolved greenhouse gas concentrations between epilimnion and hypolimnion during summer across four regions. Dissolved (a) CO_2 and (b) CH_4 concentrations (µmol L^{-1}) are shown for central Ontario, central Quebec, northern Quebec, and northern Michigan. Semi-transparent points represent individual measurements (N = 49 for CO_2 and N = 48 for CH_4). Lines represent marginal means ± standard error estimated from linear mixed-effects models. Conditional and marginal R^2 for CO_2 were 0.32 and 0.19, respectively, and 0.65 and 0.64, respectively, for CH_4.

Molecular composition of DOM across regions

To understand better the molecular drivers of the greenhouse gas production, we first compared the composition of DOM across the study regions. We observed statistically significant differences among regions in H:C ratios (ANOVA: $F_{(3, 24)} = 11.86$, $p < 0.001$). Pairwise comparisons revealed that central Ontario was 5.7% larger than central Quebec ($t = 4.22$, df = 27, $p = 0.001$), 4.7% larger than northern Quebec ($t = 3.20$, df = 27, $p = 0.017$), and 10.7% smaller than northern Michigan ($t = -3.24$, df = 27, $p = 0.016$). Northern Michigan was also 16.4% larger than central Quebec ($t = -4.97$, df = 27, $p < 0.001$) and 15.4% larger than northern Quebec ($t = -4.60$, df = 27, $p < 0.001$). Other regional comparisons for H:C showed no significance ($p = 0.906$). NOSC was also shown to differ by region ($F_{(3, 24)} = 4.62$, $p = 0.010$). Pairwise comparisons confirmed northern Michigan had 25.6% lower NOSC values than central Quebec ($t = -2.77$, $df = 27$, $p = 0.047$) and 26.3% lower NOSC than northern Quebec ($t = -2.83$, $df = 27$, $p = 0.041$) with other regional NOSC comparisons not statistically significant ($p > 0.110$). Other DOM metrics such as the O:C and AI_{Mod} did not differ significantly amongst the regions. Overall, these results show that warmer, more southern regions, particularly lakes in northern Michigan, are associated with higher H:C ratios, indicative of less aromatic and more aliphatic DOM, and lower NOSC values, reflecting more reduced, labile, energy-rich substrates. Other metrics such as O:C and AI_{Mod} were more consistent across regions.

Relationship between DOM composition and dissolved gas concentrations

Dissolved CO_2 concentrations showed no statistically significant correlations with any DOM metric (Spearman's $\rho = -0.17$ to $+0.38$, $p > 0.087$). In contrast, larger dissolved CH_4

concentrations were associated with DOM of lower oxygen content and higher aromaticity, reflected in significant negative correlations with O:C ($\rho = -0.68$, $p = 0.001$) and positive correlations with AI_{Mod} ($\rho = +0.49$, $p = 0.031$). Correlations between CH_4 and other molecular metrics such as H:C and NOSC were weak and not statistically significant ($\rho = -0.11$ to $+0.14$, $p > 0.542$). Individual molecular formulae followed the bulk DOM metrics where CO_2 was found to not be correlated with any clear composition (Figure 7a) while larger CH_4 concentrations was linked to labile, aliphatic molecules. CH_4 correlated positively with a dense cluster of 293 formulae (red points) concentrated at low O:C (0.2–0.5) and moderate to high H:C (1.0–1.5), which was consistent with its correlations with compounds of lower oxygenation and moderate aromaticity. Negative CH_4 correlations (blue points) are less numerous and more scattered with 13 formulae (Figure 7b).

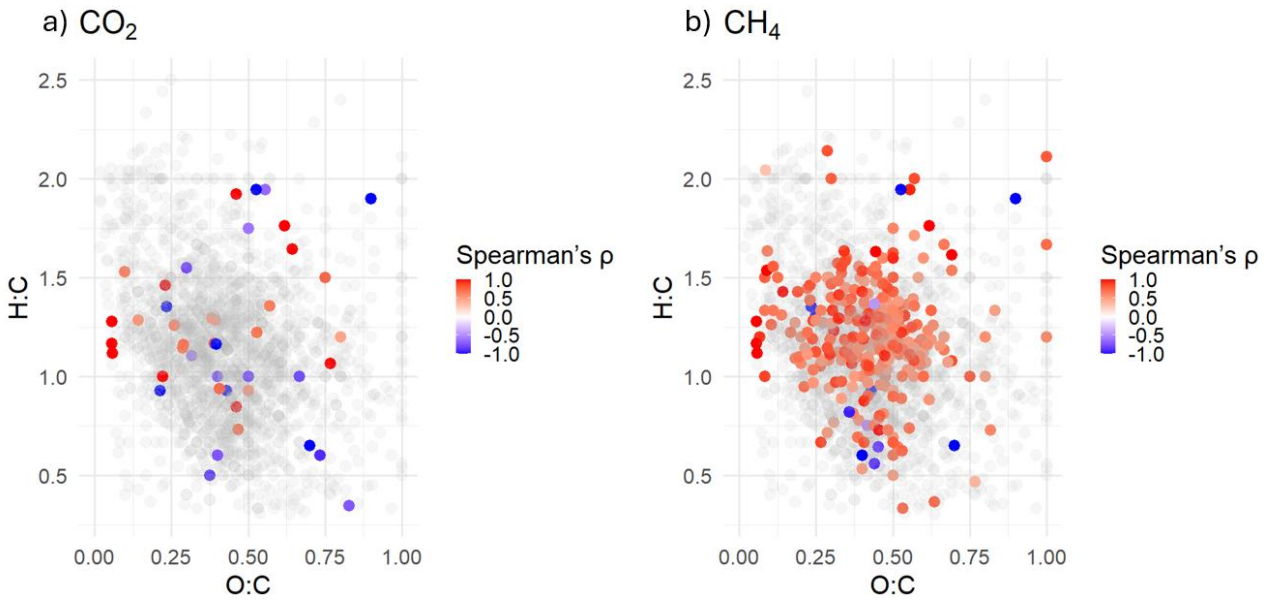

Figure 7: Van Krevelen diagrams show Spearman's rank correlations (ρ) between the relative intensity of individual DOM molecular formulae and dissolved CO_2 and CH_4 across all regions and seasons, revealing that CH_4 was positively correlated with a dense cluster of 293 formulas at low O:C (0.2–0.5) and moderate to high H:C (1.0–1.5). This is consistent with compounds of lower oxygenation and moderate aromaticity, while negative correlations were fewer (13 formulae) and more widely scattered across the Van Krevelen space. Points represent individual

formulae (N = 2013 for CO_2 and 1981 for CH_4), plotted by their atomic H:C and O:C ratios. Statistically significant correlations ($p < 0.05$) are color-coded by direction (red = positive, blue = negative; (N = 43 for CO_2 and 306 for CH_4), while non-statistically significant formulae are shown in grey.

Discussion

Our study examined how greenhouse gas (GHG) emissions vary seasonally across different thermal regimes and how temperature-driven changes in dissolved organic matter (DOM) composition influence these emissions. Warmer seasons and regions, on average, exhibited higher GHG emissions, consistent with the idea that elevated temperatures can accelerate microbial and photochemical processing of DOM (Yvon-Durocher et al., 2012; Gudasz et al., 2010). This process was reflected in regional DOM patterns, where southern lakes showed higher proportions of reduced, aromatic, and labile compounds compared to colder, more northern lakes. While CO_2 concentrations showed no consistent relationship with DOM molecular metrics, CH_4 concentrations were strongly associated with lower oxygen content and moderate aromaticity, consistent in both bulk indices and individual molecular formulae. These patterns show that temperature-driven changes in DOM composition underscore that both DOM quality and seasonal dynamics must be considered to understand and predict lake greenhouse gas emissions under future climate change.

Northern Michigan was shown to have elevated H:C and lower NOSC compared to other regions, which may originate from its enhanced groundwater connectivity. Many northern Michigan lakes are fed by abundant springs and shallow aquifers recharged by precipitation and snowmelt, which may carry organic-rich, reduced DOM derived from wetlands and terrestrial soils (Fienstein et al., 2010; Reeves et al., 2010; Berg et al., 2021). Such groundwater sourced DOM can promote sustained microbial respiration and methanogenesis, especially under

stratified conditions where surface mixing is limited (Saarela et al., 2022). The warmer regional temperatures of Michigan may also accelerate microbial metabolism, enhance the breakdown of organic matter, increase the release of DOM from soils and sediments into connected waters, and support more productive catchments with greater vegetation growth and litter production (Kellerman et al., 2014; Yvon-Durocher et al., 2012). More productive catchments, with greater primary production in aquatic and riparian zones, contribute larger amounts of autochthonous DOM that is typically fresher, more labile, and rich in proteins and carbohydrates (Williamson et al., 1999). At the same time, higher rates of litterfall and runoff from surrounding vegetation increase allochthonous DOM inputs, often enriched in humic and aromatic compounds from soils and wetlands (Fasching et al., 2014; Spencer et al., 2008). Together, Michigan's hydrological connectivity and productive, warm catchments create a diverse and abundant DOM supply that mixes energy-rich, easily degradable substrates with more complex aromatic material that supports high microbial activity and drives elevated GHG emissions (Valiente et al., 2022).

Interestingly, GHG fluxes in our lakes did not follow the expected seasonal peak in summer (Bastviken et al., 2004; DelSontro et al., 2016; Yvon-Durocher et al., 2014), with CO_2 fluxes instead highest in spring and CH_4 fluxes peaking in fall. These patterns are consistent with seasonal buildup of dissolved gases which can accumulate through a mix of biological production and physical trapping (Cole et al., 2010; Prairie & del Giorgio, 2013). In winter, microbial respiration continues beneath the ice, leading to high CO_2 concentrations that are rapidly released at ice melt in spring (Denfeld et al., 2018; López Bellido et al., 2009). In summer, methanogenesis in oxygen-poor hypolimnetic waters steadily produces CH_4, which accumulates until fall turnover mixes the CH_4 back to the surface for rapid release (Borrel et al., 2011; Encinas Fernández et al., 2014). Because flux measurements capture only gas exchange at

the time of sampling and can be influenced by wind, mixing, or temperature changes (DelSontro et al., 2016), they may underestimate emissions linked to seasonal storage and release. In contrast, dissolved gas measurements integrate recent production with storage over weeks to months, which may allow them to predict large flux events. In our study, high under-ice CO_2 concentrations preceded the spring flux peak, and elevated dissolved summer CH_4 concentration set up the large fall emissions. These results highlight the importance of spring and fall in lake carbon budgets and suggest that reliance on summer-only sampling likely underestimates both total GHG fluxes and their seasonal drivers (Davidson et al., 2006; Yvon-Durocher et al., 2014; Rabaey & Cotner, 2024).

The seasonal buildup of dissolved gases may also explain the molecular-level patterns we observed. Because dissolved concentrations reflect both recent production and longer-term storage, their associations with DOM composition may integrate gases that were produced over weeks to months rather than only those occurring at the time of flux measurement (Cole et al., 2007; Prairie & del Giorgio, 2013). In our lakes, CH_4–DOM correlations align with the presence of reduced DOM pools enriched in low O:C compounds, which are generally more labile and can be fermented by anaerobic bacteria into precursor compounds that promote methanogenesis such as acetate, H_2, and CO_2 (Conrad, 2020). These precursors support methanogen activity in anoxic hypolimnetic waters leading to the strong positive CH_4 correlations observed. In contrast, CO_2 showed no clear molecular associations, consistent with its production from a wider range of biological and physical sources, including aerobic respiration, photochemical oxidation, sediment mineralization, and groundwater inflows, that can dilute potential DOM and CO_2 correlations (Raymond et al., 2013). Abiotic influences such as under-ice gas storage, sediment degassing, and groundwater delivery (Denfeld et al., 2018; Bastviken et al., 2008; Encinas

Fernández et al., 2014) further contribute to dissolved gas patterns. Overall, these results support the notion that methane is more tightly connected to DOM chemistry, whereas carbon dioxide arises from a wider range of processes that weaken its direct connection to DOM.

The spatial and temporal patterns observed in this research suggest that climate warming could substantially alter methane emissions by extending warm periods, strengthening stratification, and shifting DOM toward more reduced forms that fuel methanogenesis (Tranvik et al., 2009; Yvon-Durocher et al., 2014). In our dataset, dissolved CH_4 concentrations were consistently higher during summer stratification, while fluxes peaked during fall overturn at more than twice summer averages, underscoring the role of seasonal mixing in driving release (Encinas Fernández et al., 2014; Denfeld et al., 2018). These findings imply that longer and stronger stratification under climate change will allow greater CH_4 accumulation in hypolimnion, with emissions concentrated in large pulses during mixing events. Shorter winters and earlier ice-off may further reduce the duration of under-ice gas buildup, redistribute the timing of fluxes, and amplify the role of fall and spring as flux release windows (Hampton et al., 2017; Rabaey & Cotner, 2024). Although climate warming is predicted to shorten the relative length of spring and fall, our results suggest that these seasons will not diminish in importance and may instead become briefer but more intense release periods by concentrating fluxes that were previously spread across longer intervals. Understanding this reorganization is important for accurately forecasting lake contributions to greenhouse gas budgets under future climate scenarios. Incorporating seasonal and regional dynamics into carbon models may improve predictions of both the timing and magnitude of emissions, while linking them to DOM composition can guide more effective monitoring and mitigation strategies (Raymond et al., 2013; Karlsson et al., 2013). Our results highlight that dissolved gases can act as early indicators of flux events and

including their seasonal buildup and release patterns may better capture the episodic nature of lake carbon emissions and their sensitivity to climate change (Powers & Hampton, 2016).

Appendix B

Table B1: Summary of sampled lake locations and morphometric characteristics, all obtained from the HydroLAKES v10 database (Messager et al., 2016). Latitude and longitude indicate a sampling point, and surface area and maximum depth are as reported in HydroLAKES. Values are *Unavailable* for lakes not included in the database.

Region	Latitude	Longitude	Mean Depth (m)	Lake Area (km^2)
N. Michigan	45.55097	-84.5051	12.3	67.14
N. Michigan	45.26297	-84.9468	16	17.78
N. Michigan	45.58064	-84.6825	7.8	14.66
N. Michigan	45.40923	-84.8302	4.7	9.06
N. Michigan	44.95496	-84.6946	8.3	7.47
N. Michigan	45.3914	-84.7538	4.2	4.2
N. Michigan	45.61659	-84.682	4.7	1.99
N. Michigan	45.19284	-84.7652	10.6	1.95
N. Michigan	45.53492	-84.4008	4.6	1.4
N. Michigan	45.39829	-84.5563	3.9	0.24
C. Ontario	45.22999	-79.028	34	67.66
C. Ontario	45.32961	-79.2715	19.3	15.82
C. Ontario	45.04895	-78.7266	18.4	11.85
C. Ontario	45.34961	-79.1072	13.3	8.43
C. Ontario	45.20861	-78.8693	16.8	5.99
C. Ontario	45.01198	-79.0769	8	3.88
C. Ontario	45.17894	-78.8238	5.4	0.32
C. Ontario	45.21552	-78.9439	9.5	1.57
C. Ontario	45.03792	-79.0163	4.2	1.02
C. Ontario	45.20828	-78.9088	4.8	0.4
C. Quebec	48.48779	-79.241	12.2	47.94
C. Quebec	48.58423	-78.6804	6.5	13.54
C. Quebec	48.43708	-78.9665	8.2	13.51
C. Quebec	48.51263	-79.3794	7.5	7.88
C. Quebec	48.0958	-78.6796	8.9	7.57
C. Quebec	48.67404	-78.6829	4.4	6.6
C. Quebec	48.79315	-79.2785	2.8	2.14
C. Quebec	48.24219	-78.4402	~2.9	*Unavailable*
C. Quebec	48.39053	-79.0171	5.8	1.25
C. Quebec	48.53931	-79.1635	3.4	0.2
N. Quebec	53.29509	-77.4562	8.5	45.37
N. Quebec	53.58773	-77.532	3.7	11.39
N. Quebec	53.86219	-77.472	5	5.48
N. Quebec	53.6488	-77.3535	~2.1	*Unavailable*

N. Quebec	53.76864	-77.5639	4.4	0.25
N. Quebec	53.76178	-77.579	4.6	0.13
N. Quebec	53.70935	-78.8385	1.9	2.11
N. Quebec	53.33172	-77.3998	2.9	1.81
N. Quebec	53.72181	-78.9662	~0.6	*Unavailable*
N. Quebec	53.78057	-77.7801	~8.2	*Unavailable*

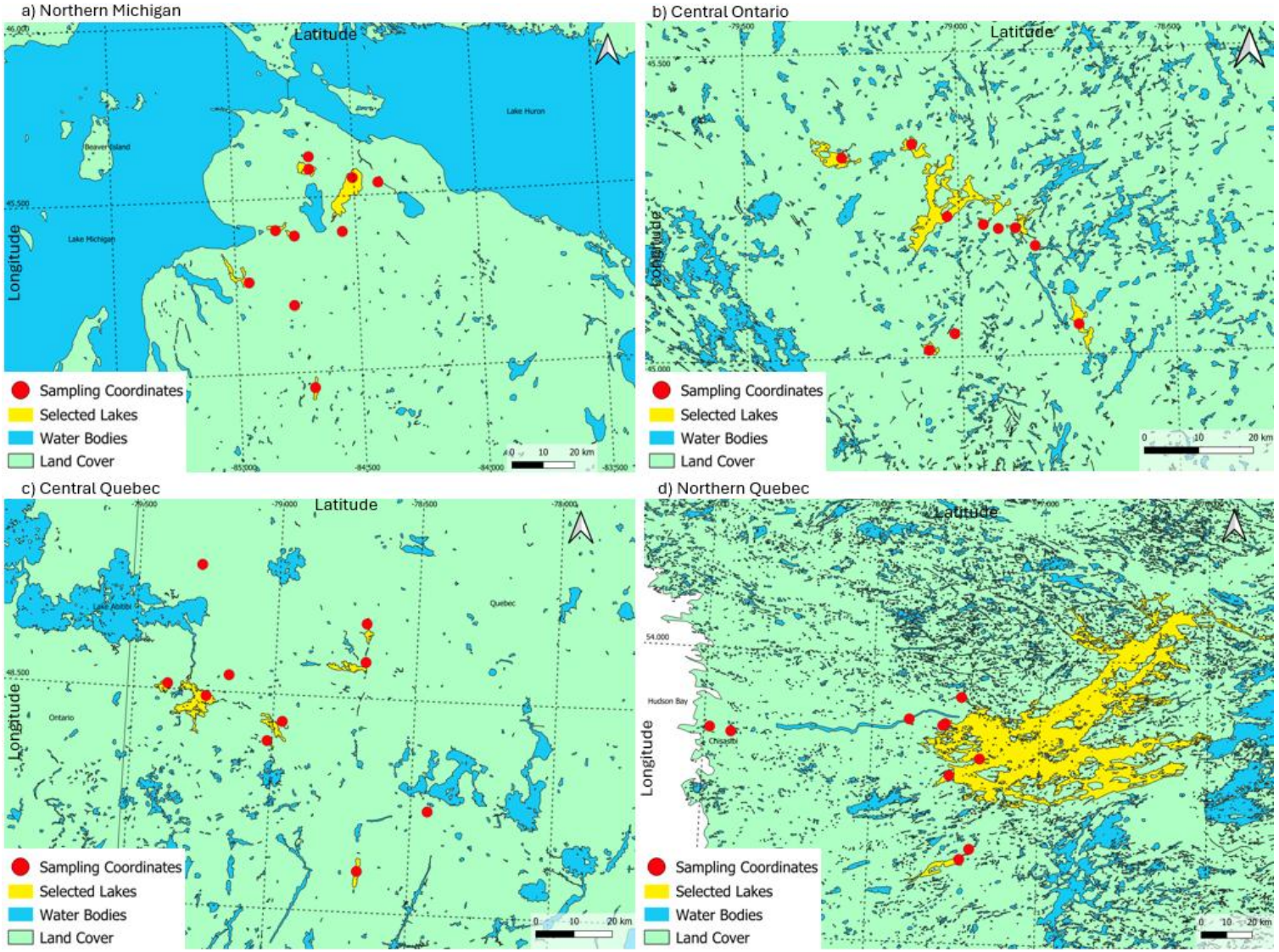

Figure B1: Sampling sites of (a) northern Michigan, (b), central Ontario, (c), central Quebec, and (d) northern Quebec. Red points indicate individual sampling coordinates. Selected lakes are shown in yellow and water bodies are in blue. The map was generated in QGIS using HydroLAKES data (Messager et al., 2016).

References

Bastviken, D., Cole, J., Pace, M., & Tranvik, L. (2004). Methane emissions from lakes: Dependence of lake characteristics, two regional assessments, and a global estimate. *Global Biogeochemical Cycles*, 18(4), 2004GB002238. https://doi.org/10.1029/2004GB002238

Bastviken, D., Cole, J. J., Pace, M. L., & Van De Bogert, M. C. (2008). Fates of methane from different lake habitats: Connecting whole-lake budgets and CH_4 emissions. *Journal of Geophysical Research: Biogeosciences*, *113*(G2), 2007JG000608. https://doi.org/10.1029/2007JG000608

Bastviken, D., Tranvik, L. J., Downing, J. A., Crill, P. M., & Enrich-Prast, A. (2011). Freshwater methane emissions offset the continental carbon sink. *Science*, 331(6013), 50–50. https://doi.org/10.1126/science.1196808

Bates, D., Mächler, M., Bolker, B., & Walker, S. (2015). Fitting linear mixed-effects models using *lme4*. *Journal of Statistical Software, 67*(1), 1–48. https://doi.org/10.18637/jss.v067.i01

Berg, S. M., Mooney, R. J., McConville, M. B., McIntyre, P. B., & Remucal, C. K. (2021). Seasonal and spatial variability of dissolved carbon concentration and composition in lake michigan tributaries. *Journal of Geophysical Research: Biogeosciences*, *126*(10), e2021JG006449. https://doi.org/10.1029/2021JG006449

Berggren, M., Ström, L., Laudon, H., Karlsson, J., Jonsson, A., Giesler, R., Bergström, A. -K., & Jansson, M. (2010). Lake secondary production fueled by rapid transfer of low molecular weight organic carbon from terrestrial sources to aquatic consumers. *Ecology Letters*, *13*(7), 870–880. https://doi.org/10.1111/j.1461-0248.2010.01483.x

Bogard, M. J., del Giorgio, P. A., Boutet, L., Chaves, M. C. G., Prairie, Y. T., Merante, A., & Derry, A. M. (2014). Oxic water column methanogenesis as a major component of aquatic CH4 fluxes. *Nature Communications*, 5(1), 5350. https://doi.org/10.1038/ncomms6350

Borrel, G., Jézéquel, D., Biderre-Petit, C., Morel-Desrosiers, N., Morel, J.-P., Peyret, P., Fonty, G., & Lehours, A.-C. (2011). Production and consumption of methane in freshwater lake ecosystems. *Research in Microbiology*, *162*(9), 832–847. https://doi.org/10.1016/j.resmic.2011.06.004

Bramer L, White A (2025). *ftmsRanalysis: Analysis and visualization tools for FT-MS data*. R package version 1.1.0, https://github.com/EMSL-Computing/ftmsRanalysis.

Brentrup, J. A., Richardson, D. C., Carey, C. C., Ward, N. K., Bruesewitz, D. A., & Weathers, K. C. (2021). Under-ice respiration rates shift the annual carbon cycle in the mixed layer of

an oligotrophic lake from autotrophy to heterotrophy. *Inland Waters*, *11*(1), 114–123. https://doi.org/10.1080/20442041.2020.1805261

Chen, H., Xu, X., Fang, C., Li, B., & Nie, M. (2021). Differences in the temperature dependence of wetland CO2 and CH4 emissions vary with water table depth. *Nature Climate Change*, 11(9), 766–771. https://doi.org/10.1038/s41558-021-01108-4

Cole, J. J., Prairie, Y. T., Caraco, N. F., McDowell, W. H., Tranvik, L. J., Striegl, R. G., Duarte, C. M., Kortelainen, P., Downing, J. A., Middelburg, J. J., & Melack, J. (2007). Plumbing the global carbon cycle: Integrating inland waters into the terrestrial carbon budget. *Ecosystems*, *10*(1), 172–185. https://doi.org/10.1007/s10021-006-9013-8

Conrad, R. (2020). Methane production in soil environments—Anaerobic biogeochemistry and microbial life between flooding and desiccation. *Microorganisms*, *8*(6), 881. https://doi.org/10.3390/microorganisms8060881

Cory, R. M., Ward, C. P., Crump, B. C., & Kling, G. W. (2014). Sunlight controls water column processing of carbon in arctic fresh waters. *Science*, *345*(6199), 925–928. https://doi.org/10.1126/science.1253119

D'Andrilli, J., Cooper, W. T., Foreman, C. M., & Marshall, A. G. (2015). An ultrahigh resolution mass spectrometry index to estimate natural organic matter lability. *Rapid Communications in Mass Spectrometry*, 29(24), 2385–2401. https://doi.org/10.1002/rcm.7400=

D'Andrilli, J., Romero, C. M., Zito, P., Podgorski, D. C., Payn, R. A., Sebestyen, S. D., Zimmerman, A. R., & Rosario-Ortiz, F. L. (2023). Advancing chemical lability assessments of organic matter using a synthesis of FT-ICR MS data across diverse environments and experiments. *Organic Geochemistry*, *184*, 104667. https://doi.org/10.1016/j.orggeochem.2023.104667

Davidson, E. A., Savage, K. E., Trumbore, S. E., & Borken, W. (2006). Vertical partitioning of CO_2 production within a temperate forest soil. *Global Change Biology*, *12*(6), 944–956. https://doi.org/10.1111/j.1365-2486.2005.01142.x

DelSontro, T., Boutet, L., St-Pierre, A., Del Giorgio, P. A., & Prairie, Y. T. (2016). Methane ebullition and diffusion from northern ponds and lakes regulated by the interaction between temperature and system productivity. *Limnology and Oceanography*, *61*(S1). https://doi.org/10.1002/lno.10335

Denfeld, B. A., Baulch, H. M., Del Giorgio, P. A., Hampton, S. E., & Karlsson, J. (2018). A synthesis of carbon dioxide and methane dynamics during the ice-covered period of

northern lakes. *Limnology and Oceanography Letters*, *3*(3), 117–131. https://doi.org/10.1002/lol2.10079

Emerson, J. B., Varner, R. K., Wik, M., Parks, D. H., Neumann, R. B., Johnson, J. E., Singleton, C. M., Woodcroft, B. J., Tollerson, R., Owusu-Dommey, A., Binder, M., Freitas, N. L., Crill, P. M., Saleska, S. R., Tyson, G. W., & Rich, V. I. (2021). Diverse sediment microbiota shape methane emission temperature sensitivity in Arctic lakes. *Nature Communications*, *12*(1), 5815. https://doi.org/10.1038/s41467-021-25983-9

Encinas Fernández, J., Peeters, F., & Hofmann, H. (2014). Importance of the autumn overturn and anoxic conditions in the hypolimnion for the annual methane emissions from a temperate lake. *Environmental Science & Technology*, *48*(13), 7297–7304. https://doi.org/10.1021/es4056164

Fasching, C., Behounek, B., Singer, G. A., & Battin, T. J. (2014). Microbial degradation of terrigenous dissolved organic matter and potential consequences for carbon cycling in brown-water streams. *Scientific Reports*, 4(1), 4981. https://doi.org/10.1038/srep04981

Feinstein, D. T., Hunt, R. J., & Reeves, H. W. (2010). *Regional groundwater-flow model of the Lake Michigan Basin in support of Great Lakes Basin Water Availability and use studies*. U.S. Geological Survey.

Gudasz, C., Bastviken, D., Steger, K., Premke, K., Sobek, S., & Tranvik, L. J. (2010). Temperature-controlled organic carbon mineralization in lake sediments. *Nature*, *466*(7305), 478–481. https://doi.org/10.1038/nature09186

Hampton, S. E., Galloway, A. W. E., Powers, S. M., Ozersky, T., Woo, K. H., Batt, R. D., Labou, S. G., O'Reilly, C. M., Sharma, S., Lottig, N. R., Stanley, E. H., North, R. L., Stockwell, J. D., Adrian, R., Weyhenmeyer, G. A., Arvola, L., Baulch, H. M., Bertani, I., Bowman, L. L., Cary, C. C., Catalan, J., Colom-Montero, W., Domine, L. M., Felip, M., Granados, I., Gries, C., Grossart, H., Haberman, J., Haldna, M., Hayden, B., Higgins, S. N., Jolley, J. C., Kahilainen, K. K., Kaup, E., Kahoe, M. J., Maclntyre, S., Mackay A. W., Mariash, H. L., McKay, R. M., Nixdorf, B., Nõges, P., Nõges, T., Palmer, M., Pierson, D. C., Post, D. M., Pruett, M. J., Rautio, M., Read, J. S., Roberts, S. L., Rücker, J., Sadro, S., Silow, E. A., Smith, D. E., Sterner, R. W., Swann, G. E. A., Timofeyev, M. A., Toro, M., Twiss, M. R., Vogt, R. J., Watson, S. B., Whiteford, E. J., Xenopoulos, M. A. (2017). Ecology under lake ice. *Ecology Letters*, *20*(1), 98–111. https://doi.org/10.1111/ele.12699

Hartnett, H. E. (2017). Dissolved organic matter (DOM). In W. M. White (Ed.), *Encyclopedia of Geochemistry: A Comprehensive Reference Source on the*

Chemistry of the Earth (pp. 1–3). *Springer International Publishing*. https://doi.org/10.1007/978-3-319-39193-9_155-1

Hounshell, A. G., McClure, R. P., Lofton, M. E., & Carey, C. C. (2021). Whole-ecosystem oxygenation experiments reveal substantially greater hypolimnetic methane concentrations in reservoirs during anoxia. *Limnology and Oceanography Letters*, 6(1), 33–42. https://doi.org/10.1002/lol2.10173

Hu, A., Jang, K.-S., Meng, F., Stegen, J., Tanentzap, A. J., Choi, M., Lennon, J. T., Soininen, J., & Wang, J. (2022). Microbial and environmental processes shape the link between organic matter functional traits and composition. *Environmental Science & Technology*, 56(14), 10504–10516. https://doi.org/10.1021/acs.est.2c01432

Jansen, E., Christensen, J. H., Dokken, T., Nisancioglu, K. H., Vinther, B. M., Capron, E., Guo, C., Jensen, M. F., Langen, P. L., Pedersen, R. A., Yang, S., Bentsen, M., Kjær, H. A., Sadatzki, H., Sessford, E., & Stendel, M. (2020). Past perspectives on the present era of abrupt Arctic climate change. *Nature Climate Change*, *10*(8), 714–721. https://doi.org/10.1038/s41558-020-0860-7

Karlsson, J., Giesler, R., Persson, J., & Lundin, E. (2013). High emission of carbon dioxide and methane during ice thaw in high latitude lakes. *Geophysical Research Letters*, 40(6), 1123–1127. https://doi.org/10.1002/grl.50152

Kellerman, A. M., Dittmar, T., Kothawala, D. N., & Tranvik, L. J. (2014). Chemodiversity of dissolved organic matter in lakes driven by climate and Hydrology. *Nature Communications*, 5(1). https://doi.org/10.1038/ncomms4804

Kenward, M. G., & Roger, J. H. (1997). Small sample inference for fixed effects from restricted maximum likelihood. *Biometrics*, *53*(3), 983–997.

Kim, S., Kramer, R. W., & Hatcher, P. G. (2003). Graphical method for analysis of ultrahigh-resolution broadband mass spectra of natural organic matter, the van krevelen diagram. *Analytical Chemistry*, *75*(20), 5336–5344. https://doi.org/10.1021/ac034415p

Koch, B. P., & Dittmar, T. (2006). From mass to structure: An aromaticity index for high-resolution mass data of natural organic matter. *Rapid Communications in Mass Spectrometry*, 20(5), 926–932. https://doi.org/10.1002/rcm.2386

Koehler, B., Landelius, T., Weyhenmeyer, G. A., Machida, N., & Tranvik, L. J. (2014). Sunlight-induced carbon dioxide emissions from inland waters. *Global Biogeochemical Cycles*, *28*(7), 696–711. https://doi.org/10.1002/2014GB004850

Kuhn, M. K. A., Thompson, L. M., Winder, J. C., Braga, L. P., Tanentzap, A. J., Bastviken, D., & Olefeldt, D (2021). Opposing effects of climate and permafrost thaw on CH_4 and CO_2

emissions from Northern Lakes. *AGU Advances*, 2(4). https://doi.org/10.1029/2021av000515

Kuznetsova, A., Brockhoff, P. B., & Christensen, R. H. B. (2017). lmerTest package: Tests in linear mixed effects models. *Journal of Statistical Software, 82*(13), 1–26. https://doi.org/10.18637/jss.v082.i13

LaRowe, D. E., & Van Cappellen, P. (2011). Degradation of natural organic matter: A thermodynamic analysis. *Geochimica et Cosmochimica Acta*, *75*(8), 2030–2042. https://doi.org/10.1016/j.gca.2011.01.020

Lenth, R. (2024). *emmeans: Estimated marginal means, aka least-squares means* (R package version 1.10.0). https://CRAN.R-project.org/package=emmeans

Li, X., Li, Y., Gao, D., Liu, M., & Hou, L. (2022). Methane production linked to organic matter molecule and methanogenic community in estuarine benthic sediments. *Journal of Geophysical Research: Biogeosciences*, *127*(12), e2022JG007236. https://doi.org/10.1029/2022JG007236

López Bellido, J., Tulonen, T., Kankaala, P., & Ojala, A. (2009). CO_2 and CH_4 fluxes during spring and autumn mixing periods in a boreal lake (Pääjärvi, southern Finland). *Journal of Geophysical Research: Biogeosciences*, *114*(G4), 2009JG000923. https://doi.org/10.1029/2009JG000923

Lüdecke, D., Ben-Shachar, M. S., Patil, I., Waggoner, P., & Makowski, D. (2021). performance: An R package for assessment, comparison and testing of statistical models. *Journal of Open Source Software, 6*(60), 3139. https://doi.org/10.21105/joss.03139

Mayumi, D., Mochimaru, H., Tamaki, H., Yamamoto, K., Yoshioka, H., Suzuki, Y., Kamagata, Y., & Sakata, S. (2016). Methane production from coal by a single methanogen. *Science*, 354(6309), 222–225. https://doi.org/10.1126/science.aaf8821

Messager, M. L., Lehner, B., Grill, G., Nedeva, I., & Schmitt, O. (2016). HydroLAKES: Global database of lake volume and catchment attributes. *Scientific Data*, **3**, 160056. https://doi.org/10.1038/sdata.2016.56

Moran, M. A., & Zepp, R. G. (1997). Role of photoreactions in the formation of biologically labile compounds from dissolved organic matter. *Limnology and Oceanography*, *42*(6), 1307–1316. https://doi.org/10.4319/lo.1997.42.6.1307

Nakagawa, S., & Schielzeth, H. (2013). A general and simple method for obtaining R^2 from generalized linear mixed-effects models. *Methods in Ecology and Evolution*, *4*(2), 133–142. https://doi.org/10.1111/j.2041-210x.2012.00261.x

O'Donnell, J. A., Aiken, G. R., Butler, K. D., Guillemette, F., Podgorski, D. C., & Spencer, R. G. (2016). Dom composition and transformation in boreal forest soils:

The effects of temperature and organic-horizon decomposition state. *Journal of Geophysical Research: Biogeosciences*, 121(10), 2727–2744. https://doi.org/10.1002/2016jg003431

Powers, S. M., & Hampton, S. E. (2016). Winter limnology as a new frontier. *Limnology and Oceanography Bulletin*, *25*(4), 103–108. https://doi.org/10.1002/lob.10152

Prairie, Y., & Del Giorgio, P. (2013). A new pathway of freshwater methane emissions and the putative importance of microbubbles. *Inland Waters*, *3*(3), 311–320. https://doi.org/10.5268/IW-3.3.542

Rabaey, J. S., & Cotner, J. B. (2024). The influence of mixing on seasonal carbon dioxide and methane fluxes in ponds. *Biogeochemistry*, *167*(10), 1297–1314. https://doi.org/10.1007/s10533-024-01167-7

Raymond, P. A., Hartmann, J., Lauerwald, R., Sobek, S., McDonald, C., Hoover, M., Butman, D., Striegl, R., Mayorga, E., Humborg, C., Kortelainen, P., Dürr, H., Meybeck, M., Ciais, P., & Guth, P. (2013). Global carbon dioxide emissions from inland waters. *Nature*, *503*(7476), 355–359. https://doi.org/10.1038/nature12760

R Core Team. (2024). *R: A language and environment for statistical computing* (Version 4.4.1) [Computer software]. R Foundation for Statistical Computing. https://www.R-project.org/

Reeves, H. W. (2010). *Water availability and use pilot: A multiscale assessment in the U.S. great lakes basin*. U.S. Geological Survey.

Riedel, T., & Dittmar, T. (2014). A method detection limit for the analysis of natural organic matter via fourier transform ion cyclotron resonance mass spectrometry. *Analytical Chemistry*, *86*(16), 8376–8382. https://doi.org/10.1021/ac501946m

Rosentreter, J. A., Borges, A. V., Deemer, B. R., Holgerson, M. A., Liu, S., Song, C., Melack, J., Raymond, P. A., Duarte, C. M., Allen, G. H., Olefeldt, D., Poulter, B., Battin, T. I., & Eyre, B. D. (2021). Half of global methane emissions come from highly variable aquatic ecosystem sources. *Nature Geoscience*, *14*(4), 225–230. https://doi.org/10.1038/s41561-021-00715-2

Saarela, T., Zhu, X., Jäntti, H., Ohashi, M., Ide, J., Siljanen, H., Pesonen, A., Aaltonen, H., Ojala, A., Nishimura, H., Kekäläinen, T., Jänis, J., Berninger, F., & Pumpanen, J. (2022). *Dissolved organic matter composition regulates microbial degradation and carbon dioxide production in pristine subarctic rivers*. https://doi.org/10.5194/bg-2022-225

Sepulveda-Jauregui, A., Walter Anthony, K. M., Martinez-Cruz, K., Greene, S., & Thalasso, F. (2015). Methane and carbon dioxide emissions from 40 lakes along a north–south

latitudinal transect in Alaska. *Biogeosciences*, *12*(11), 3197–3223. https://doi.org/10.5194/bg-12-3197-2015

Sharma, S., Richardson, D. C., Woolway, R. I., Imrit, M. A., Bouffard, D., Blagrave, K., Daly, J., Filazzola, A., Granin, N., Korhonen, J., Magnuson, J., Marszelewski, W., Matsuzaki, S. S., Perry, W., Robertson, D. M., Rudstam, L. G., Weyhenmeyer, G. A., & Yao, H. (2021). Loss of ice cover, shifting phenology, and more extreme events in northern hemisphere lakes. *Journal of Geophysical Research: Biogeosciences*, *126*(10), e2021JG006348. https://doi.org/10.1029/2021JG006348

Sleighter, R. L., McKee, G. A., Liu, Z., & Hatcher, P. G. (2008). Naturally present fatty acids as internal calibrants for Fourier transform mass spectra of dissolved organic matter. *Limnology and Oceanography: Methods*, *6*(6), 246–253. https://doi.org/10.4319/lom.2008.6.246

Soued, C., & Prairie, Y. T. (2022). Patterns and regulation of hypolimnetic CO_2 and CH_4 in a tropical reservoir using a process-based modeling approach. *Journal of Geophysical Research: Biogeosciences*, *127*(8), e2022JG006897. https://doi.org/10.1029/2022JG006897

Spencer, R. G. M., Aiken, G. R., Wickland, K. P., Striegl, R. G., & Hernes, P. J. (2008). Seasonal and spatial variability in dissolved organic matter quantity and composition from the Yukon River basin, Alaska. *Global Biogeochemical Cycles*, 22(4), 2008GB003231. https://doi.org/10.1029/2008GB003231

Sø, J. S., Martinsen, K. T., Kragh, T., & Sand-Jensen, K. (2024). Hourly methane and carbon dioxide fluxes from temperate ponds. *Biogeochemistry*, *167*(2), 177–195. https://doi.org/10.1007/s10533-024-01124-4

Tanentzap, A. J., Fitch, A., Orland, C., Emilson, E. J., Yakimovich, K. M., Osterholz, H., & Dittmar, T. (2019). Chemical and microbial diversity covary in fresh water to influence ecosystem functioning. *Proceedings of the National Academy of Sciences*, 116(49), 24689–24695. https://doi.org/10.1073/pnas.1904896116

Tranvik, L. J., Downing, J. A., Cotner, J. B., Loiselle, S. A., Striegl, R. G., Ballatore, T. J., Dillon, P., Finlay, K., Fortino, K., Knoll, L. B., Kortelainen, P. L., Kutser, T., Larsen, Soren., Laurion, I., Leech, D. M., McCallister, S. L., McKnight, D. M., Melack, J. M., Overholt, E., Porter, J. A., Prairie, Y., Renwick, W. H., Roland, F., Sherman, B. S., Sobek, S., Tremblay, A., Vanni, M. J., Verschoor, A. M., Von Wachenfeldt, E., Weyhenmeyer, G. A. (2009). Lakes and reservoirs as regulators of carbon cycling and climate. *Limnology and Oceanography*, *54*(6part2), 2298–2314. https://doi.org/10.4319/lo.2009.54.6_part_2.2298

Tukey, J. W. (1949). Comparing individual means in the analysis of variance. *Biometrics*, *5*(2), 99–114.

Valiente, N., Eiler, A., Allesson, L., Andersen, T., Clayer, F., Crapart, C., Dörsch, P., Fontaine, L., Heuschele, J., Vogt, R. D., Wei, J., De Wit, H. A., & Hessen, D. O. (2022). Catchment properties as predictors of greenhouse gas concentrations across a gradient of boreal lakes. *Frontiers in Environmental Science*, *10*, 880619. https://doi.org/10.3389/fenvs.2022.880619

Von Wachenfeldt, E., & Tranvik, L. J. (2008). Sedimentation in boreal lakes—The role of flocculation of allochthonous dissolved organic matter in the water column. *Ecosystems*, *11*(5), 803–814. https://doi.org/10.1007/s10021-008-9162-z

Walter, K. M., Edwards, M. E., Grosse, G., Zimov, S. A., & Chapin, F. S. (2007). Thermokarst lakes as a source of atmospheric ch_4 during the last deglaciation. *Science*, *318*(5850), 633–636. https://doi.org/10.1126/science.1142924

Ward, C. P., & Cory, R. M. (2016). Complete and partial photo-oxidation of dissolved organic matter draining permafrost soils. *Environmental Science & Technology*, 50(7), 3545–3553. https://doi.org/10.1021/acs.est.5b05354

Wik, M., Varner, R. K., Anthony, K. W., MacIntyre, S., & Bastviken, D. (2016). Climate-sensitive northern lakes and ponds are critical components of methane release. *Nature Geoscience*, 9(2), 99–105. https://doi.org/10.1038/ngeo2578

Williamson, C. E., Morris, D. P., Pace, M. L., & Olson, O. G. (1999). Dissolved organic carbon and nutrients as regulators of lake ecosystems: Resurrection of a more integrated paradigm. *Limnology and Oceanography*, *44*(3part2), 795–803. https://doi.org/10.4319/lo.1999.44.3_part_2.0795

Winder, J. C., Braga, L. P. P., Kuhn, M. A., Thompson, L. M., Olefeldt, D., & Tanentzap, A. J. (2023). Climate warming has direct and indirect effects on microbes associated with carbon cycling in northern lakes. *Global Change Biology*, *29*(11), 3039–3053. https://doi.org/10.1111/gcb.16655

Woodcroft, B. J., Singleton, C. M., Boyd, J. A., Evans, P. N., Emerson, J. B., Zayed, A. A. F., Hoelzle, R. D., Lamberton, T. O., McCalley, C. K., Hodgkins, S. B., Wilson, R. M., Purvine, S. O., Nicora, C. D., Li, C., Frolking, S., Chanton, J. P., Crill, P. M., Saleska, S. R., Rich, V. I., & Tyson, G. W. (2018). Genome-centric view of carbon processing in thawing permafrost. *Nature*, *560*(7716), 49–54. https://doi.org/10.1038/s41586-018-0338-1

Yvon-Durocher, G., Allen, A. P., Bastviken, D., Conrad, R., Gudasz, C., St-Pierre, A., Thanh-Duc, N., & del Giorgio, P. A. (2014). Methane fluxes show consistent temperature dependence across microbial to ecosystem scales. *Nature*, 507(7493), 488–491. https://doi.org/10.1038/nature13164

Zhou, Y., Zhou, L., Zhang, Y., Garcia de Souza, J., Podgorski, D. C., Spencer, R. G. M., Jeppesen, E., & Davidson, T. A. (2019). Autochthonous dissolved organic matter potentially fuels methane ebullition from experimental lakes. *Water Research*, *166*, 115048. https://doi.org/10.1016/j.watres.2019.115048

Zuur, A. F., Ieno, E. N., & Smith, G. M. (2007). *Analysing ecological data*. *Springer*. https://doi.org/10.1007/978-0-387-45972-1

Chapter 4 General Discussion

In chapter 1, four questions were laid out that this thesis aimed to answer:

1. How does the composition of DOM differ between thermokarst and lake sources (Chapter 2)?
2. How do microbial communities from lake and thermokarst environments respond to DOM of different origins (Chapter 2)?
3. How do greenhouse gases vary across seasons and regions (Chapter 3)?
4. How does DOM composition relate to the amount and type of GHG produced (Chapter 3)?

This thesis set out to understand how dissolved organic matter (DOM) composition, microbial community identity, and environmental context shape carbon cycling in northern inland waters. By combining a controlled factorial incubation with a seasonal survey of lakes across a broad longitudinal gradient, we were able to link processes occurring at the molecular and microbial scale to GHG patterns observed in the field. This integration reveals how changes in substrate quality, microbial assemblages, and environmental conditions together influence whether carbon is stored, transformed, or released to the atmosphere (Tranvik et al., 2009; Vonk et al., 2015).

This project demonstrated that DOM chemical traits and microbial community identity exert strong and interactive control over degradation pathways (Hu et al., 2022; Wu et al., 2018). Lake microbes preferentially degraded thermokarst DOM but could not use this DOM efficiently, which led to increased CO_2 production and almost no biomass growth. This outcome supports the idea of a “microbial–DOM mismatch” in which communities encounter unfamiliar substrates and respire over biomass growth (Guillemette et al., 2013; Danczak et al., 2020). With permafrost thaw increasing the hydrological mixing of historically isolated waters, such

mismatches may become more frequent, potentially enhancing CO_2 emissions from northern lakes (Vonk et al., 2015).

The seasonal and regional flux patterns observed in the field survey provide a broader environmental context for these mechanisms. CO_2 emissions were highest in spring and winter, while CH_4 emissions peaked in the fall (Wik et al., 2016). Warmer regions consistently produced higher CO_2 and CH_4 fluxes, with northern Michigan being especially high. Although microbial identity was not measured directly, these patterns are consistent with the substrate and redox dynamics observed in the experiment (Bastviken et al., 2004). For example, spring's elevated CO_2 emissions may be driven by the rapid mineralization of fresh, labile DOM from catchment runoff (Fasching et al., 2016), conditions under which generalist microbes are especially active. In contrast, the high CH_4 emissions in fall may reflect enhanced methanogenesis as stratification strengthens, oxygen becomes depleted, and fermentation products accumulate (Segers, 1998).

Across both studies, DOM molecular composition emerged as a consistent driver of biogeochemical fate. In the laboratory, lake DOM was chemically more reduced, saturated, and enriched in lipid-like compounds, traits linked to greater bioavailability (Boye et al., 2017; Kellerman et al., 2015), while thermokarst DOM was more oxidized, aromatic, and structurally complex (Spencer et al., 2015). In the field, summer FT-ICR MS analyses revealed spatial variation in DOM chemistry, with warmer lakes generally containing more labile DOM (Kellerman et al., 2014). These findings align with thermodynamic predictions that reduced, less aromatic compounds are more readily respired, whereas more complex molecules persist longer or are processed via slower anaerobic pathways such as methanogenesis (LaRowe & Van Cappellen, 2011).

Taken together, the results from this thesis highlight three interacting processes likely to shape future carbon cycling in northern lakes: first, that thaw-driven mixing of DOM and microbial communities can enhance CO_2 emissions via inefficient respiration; second, seasonal hydrological and thermal pulses regulate both the magnitude and pathway of DOM mineralization; and third, that regional temperature influence the relative balance of CO_2 and CH_4 production. Each of these processes has the potential to alter the timing and magnitude of GHG release from inland waters under continued climate warming (Raymond et al., 2013; Tranvik et al., 2009). For example, stronger stratification and extended warm periods could allow greater buildup of CH_4 that is then released in large pulses during fall mixing (Encinas Fernández et al., 2014; Denfeld et al., 2018), while shorter winters may reduce under-ice CO_2 accumulation but shift fluxes towards the fall and spring (Powers & Hampton, 2016). Likewise, enhanced DOM–microbe mixing from thaw inputs could increase respiration losses, lower microbial growth efficiency, and reinforce CO_2 dominance over storage (Mostovaya et al., 2017; Guillemette & del Giorgio, 2011). Together, these mechanisms suggest that climate change will not only amplify total GHG emissions but also reorganize when and how those emissions are expressed across the annual cycle.

Limitations of this work should be acknowledged, as they help contextualize the scope of inference and identify priorities for future research. In our first study (Chapter 2), it was conducted under warm, oxic conditions, which may have underestimated the activity of cold-adapted thermokarst microbes more typical of natural systems (Coolen & Orsi, 2015; Mackelprang et al., 2017; Waldrop et al., 2023). The use of 0.2 μm filtration excluded particle-associated microbes and larger eukaryotes, such as protozoa and many phytoplankton, which can exert strong top-down control on bacterial populations and contribute to DOM transformation

through grazing, exudation, and nutrient recycling (Crump et al., 2003; Pernthaler, 2005). The relatively short, three-day duration was chosen to capture early-phase activity while minimizing bottle effects (Hammes et al., 2010), but likely underrepresented slower carbon processing pathways such as syntrophy and methanogenesis (Woodcroft et al., 2018; Winder et al., 2023). In the field survey (Chapter 2), logistical challenges and equipment failures resulted in an unbalanced dataset, with particularly low replication in winter that may have reduced the statistical power to detect seasonal patterns. The field study lacked microbial community data and supplementary chemical metrics such as chromophoric DOM (Helms et al., 2008), limiting the ability to directly link observed GHG fluxes to specific biological or chemical drivers. Across both chapters, the absence of direct dissolved organic carbon (DOC) measurements constrained the ability to track the complete fate of carbon.

Future research should address these limitations to strengthen the mechanistic links between DOM chemistry, microbial processes, and GHG emissions in northern lakes. Laboratory experiments could incorporate colder, seasonally variable temperatures, a broader range of oxygen conditions to better reflect natural thermokarst environments, as well as longer incubations that capture slower carbon processing pathways such as syntrophy and methanogenesis (Coolen & Orsi, 2015; Mackelprang et al., 2011). Including particle-associated microbes, larger microbial eukaryotes, and varying microbial-to-DOM ratios would improve ecological realism. Field surveys should prioritise balanced sampling across all seasons, particularly under ice (Wik et al., 2016), to improve statistical power and capture key transitional periods in carbon cycling. Integrating microbial community profiling with high-resolution DOM characterization, including DOC and chromophoric DOM measurements (Helms et al., 2008), would allow direct attribution of observed fluxes to specific biological and chemical drivers. By

combining these improvements with coordinated laboratory and field approaches, future studies can more accurately constrain the role of northern lakes in carbon cycling and its interactions in different climate scenarios (Vonk et al., 2015).

References

Bastviken, D., Cole, J., Pace, M., & Tranvik, L. (2004). Methane emissions from lakes: Dependence of lake characteristics, two regional assessments, and a global estimate. *Global Biogeochemical Cycles*, 18(4), 2004GB002238. https://doi.org/10.1029/2004GB002238

Boye, K., Noël, V., Tfaily, M. M., Bone, S. E., Williams, K. H., Bargar, J. R., & Fendorf, S. (2017). Thermodynamically controlled preservation of organic carbon in floodplains. *Nature Geoscience*, *10*(6), 415–419. https://doi.org/10.1038/ngeo2940

Coolen, M. J. L., & Orsi, W. D. (2015). The transcriptional response of microbial communities in thawing Alaskan permafrost soils. *Frontiers in Microbiology*, *6*. https://doi.org/10.3389/fmicb.2015.00197

Crump, B. C., Kling, G. W., Bahr, M., & Hobbie, J. E. (2003). Bacterioplankton community shifts in an arctic lake correlate with seasonal changes in organic matter source. *Applied and Environmental Microbiology*, *69*(4), 2253–2268. https://doi.org/10.1128/AEM.69.4.2253-2268.2003

Danczak, R. E., Chu, R. K., Fansler, S. J., Goldman, A. E., Graham, E. B., Tfaily, M. M., Toyoda, J., & Stegen, J. C. (2020). Using metacommunity ecology to understand environmental metabolomes. *Nature Communications*, *11*(1), 6369. https://doi.org/10.1038/s41467-020-19989-y

Denfeld, B. A., Baulch, H. M., Del Giorgio, P. A., Hampton, S. E., & Karlsson, J. (2018). A synthesis of carbon dioxide and methane dynamics during the ice-covered period of northern lakes. *Limnology and Oceanography Letters*, *3*(3), 117–131. https://doi.org/10.1002/lol2.10079

Encinas Fernández, J., Peeters, F., & Hofmann, H. (2014). Importance of the autumn overturn and anoxic conditions in the hypolimnion for the annual methane emissions from a temperate lake. *Environmental Science & Technology*, *48*(13), 7297–7304. https://doi.org/10.1021/es4056164

Fasching, C., Ulseth, A. J., Schelker, J., Steniczka, G., & Battin, T. J. (2016). Hydrology controls dissolved organic matter export and composition in an Alpine stream and its hyporheic zone. *Limnology and Oceanography*, *61*(2), 558–571. https://doi.org/10.1002/lno.10232

Guillemette, F., & Del Giorgio, P. A. (2011). Reconstructing the various facets of dissolved organic carbon bioavailability in freshwater ecosystems. *Limnology and Oceanography*, *56*(2), 734–748. https://doi.org/10.4319/lo.2011.56.2.0734

Guillemette, F., McCallister, S. L., & Del Giorgio, P. A. (2013). Differentiating the degradation dynamics of algal and terrestrial carbon within complex natural dissolved organic carbon

in temperate lakes. *Journal of Geophysical Research: Biogeosciences*, *118*(3), 963–973. https://doi.org/10.1002/jgrg.20077

Hammes, F., Vital, M., & Egli, T. (2010). Critical evaluation of the volumetric "bottle effect" on microbial batch growth. *Applied and Environmental Microbiology*, *76*(4), 1278–1281. https://doi.org/10.1128/AEM.01914-09

Helms, J. R., Stubbins, A., Ritchie, J. D., Minor, E. C., Kieber, D. J., & Mopper, K. (2008). Absorption spectral slopes and slope ratios as indicators of molecular weight, source, and photobleaching of chromophoric dissolved organic matter. *Limnology and Oceanography*, 53(3), 955–969. https://doi.org/10.4319/lo.2008.53.3.0955

Hu, A., Choi, M., Tanentzap, A. J., Liu, J., Jang, K.-S., Lennon, J. T., Liu, Y., Soininen, J., Lu, X., Zhang, Y., Shen, J., & Wang, J. (2022). Ecological networks of dissolved organic matter and microorganisms under global change. *Nature Communications*, *13*(1), 3600. https://doi.org/10.1038/s41467-022-31251-1

Kellerman, A. M., Dittmar, T., Kothawala, D. N., & Tranvik, L. J. (2014). Chemodiversity of dissolved organic matter in lakes driven by climate and hydrology. *Nature Communications*, 5(1). https://doi.org/10.1038/ncomms4804

Kellerman, A. M., Kothawala, D. N., Dittmar, T., & Tranvik, L. J. (2015). Molecular dissolved organic matter composition in lakes across Sweden as relative intensities of FT-ICR-MS peaks and PARAFAC components and optical indices. 2 datasets. https://doi.org/10.1594/PANGAEA.844884

LaRowe, D. E., & Van Cappellen, P. (2011). Degradation of natural organic matter: A thermodynamic analysis. *Geochimica et Cosmochimica Acta*, 75(8), 2030–2042. https://doi.org/10.1016/j.gca.2011.01.020

Mackelprang, R., Waldrop, M. P., DeAngelis, K. M., David, M. M., Chavarria, K. L., Blazewicz, S. J., Rubin, E. M., & Jansson, J. K. (2011). Metagenomic analysis of a permafrost microbial community reveals a rapid response to thaw. *Nature*, 480 (7377), 368–371. https://doi.org/10.1038/nature10576

Mostovaya, A., Hawkes, J. A., Koehler, B., Dittmar, T., & Tranvik, L. J. (2017). Emergence of the reactivity continuum of organic matter from kinetics of a multitude of individual molecular constituents. *Environmental Science & Technology*, *51*(20), 11571–11579. https://doi.org/10.1021/acs.est.7b02876

Pernthaler, J. (2005). Predation on prokaryotes in the water column and its ecological implications. *Nature Reviews Microbiology*, *3*(7), 537–546. https://doi.org/10.1038/nrmicro1180

Powers, S. M., & Hampton, S. E. (2016). Winter limnology as a new frontier. *Limnology and Oceanography Bulletin*, *25*(4), 103–108. https://doi.org/10.1002/lob.10152

Prairie, Y., & Del Giorgio, P. (2013). A new pathway of freshwater methane emissions and the putative importance of microbubbles. *Inland Waters*, *3*(3), 311–320. https://doi.org/10.5268/IW-3.3.542

Raymond, P. A., Hartmann, J., Lauerwald, R., Sobek, S., McDonald, C., Hoover, M., Butman, D., Striegl, R., Mayorga, E., Humborg, C., Kortelainen, P., Dürr, H., Meybeck, M., Ciais, P., & Guth, P. (2013). Global carbon dioxide emissions from inland waters. *Nature*, *503*(7476), 355–359. https://doi.org/10.1038/nature12760

Segers, R. (1998). Methane production and methane consumption: A review of processes underlying wetland methane fluxes. *Biogeochemistry*, *41*(1), 23–51. https://doi.org/10.1023/A:1005929032764\

Spencer, R. G. M., Mann, P. J., Dittmar, T., Eglinton, T. I., McIntyre, C., Holmes, R. M., Zimov, N., & Stubbins, A. (2015). Detecting the signature of permafrost thaw in Arctic rivers. *Geophysical Research Letters*, *42*(8), 2830–2835. https://doi.org/10.1002/2015GL063498

Tranvik, L. J., Downing, J. A., Cotner, J. B., Loiselle, S. A., Striegl, R. G., Ballatore, T. J., Dillon, P., Finlay, K., Fortino, K., Knoll, L. B., Kortelainen, P. L., Kutser, T., Larsen, Soren., Laurion, I., Leech, D. M., McCallister, S. L., McKnight, D. M., Melack, J. M., Overholt, E., Porter, J. A., Prairie, Y., Renwick, W. H., Roland, F., Sherman, B. S., Sobek, S., Tremblay, A., Vanni, M. J., Verschoor, A. M., Von Wachenfeldt, E., Weyhenmeyer, G. A. (2009). Lakes and reservoirs as regulators of carbon cycling and climate. *Limnology and Oceanography*, *54*(6part2), 2298–2314. https://doi.org/10.4319/lo.2009.54.6_part_2.2298

Vonk, J. E., Tank, S. E., Mann, P. J., Spencer, R. G. M., Treat, C. C., Striegl, R. G., Abbott, B. W., & Wickland, K. P. (2015). Biodegradability of dissolved organic carbon in permafrost soils and aquatic systems: A meta-analysis. *Biogeosciences*, *12*(23), 6915–6930. https://doi.org/10.5194/bg-12-6915-2015

Waldrop, M. P., Chabot, C. L., Liebner, S., Holm, S., Snyder, M. W., Dillon, M., Dudgeon, S. R., Douglas, T. A., Leewis, M.-C., Walter Anthony, K. M., McFarland, J. W., Arp, C. D., Bondurant, A. C., Taş, N., & Mackelprang, R. (2023). Permafrost microbial communities and functional genes are structured by latitudinal and soil geochemical gradients. *The ISME Journal*, 17(8), 1224-1235. https://doi.org/10.1038/s41396-023-01429-6

Wik, M., Varner, R. K., Anthony, K. W., MacIntyre, S., & Bastviken, D. (2016). Climate-sensitive northern lakes and ponds are critical components of methane release. *Nature Geoscience*, 9(2), 99–105. https://doi.org/10.1038/ngeo2578

Winder, J. C., Braga, L. P. P., Kuhn, M. A., Thompson, L. M., Olefeldt, D., & Tanentzap, A. J. (2023). Climate warming has direct and indirect effects on microbes associated with carbon cycling in northern lakes. *Global Change Biology*, 29(11), 3039–3053. https://doi.org/10.1111/gcb.16655

Woodcroft, B. J., Singleton, C. M., Boyd, J. A., Evans, P. N., Emerson, J. B., Zayed, A. A. F., Hoelzle, R. D., Lamberton, T. O., McCalley, C. K., Hodgkins, S. B., Wilson, R. M., Purvine, S. O., Nicora, C. D., Li, C., Frolking, S., Chanton, J. P., Crill, P. M., Saleska, S. R., Rich, V. I., & Tyson, G. W. (2018). Genome-centric view of carbon processing in thawing permafrost. *Nature*, 560(7716), 49–54. https://doi.org/10.1038/s41586-018-0338-1

Wu, X., Wu, L., Liu, Y., Zhang, P., Li, Q., Zhou, J., Hess, N. J., Hazen, T. C., Yang, W., & Chakraborty, R. (2018). Microbial interactions with dissolved organic matter drive carbon dynamics and community succession. *Frontiers in Microbiology*, *9*, 1234. https://doi.org/10.3389/fmicb.2018.01234